

# Quantifying changes in the Distribution of Atlantic Cod and Yellowtail Flounder on Georges Bank

David M. Keith<sup>1</sup>, Jessica A. Sameoto<sup>1</sup>, Freya M. Keyser<sup>1</sup>, and Irene Andrushchenko<sup>2</sup>

## Abstract

Sustainably managing marine fisheries has long been recognized as a global priority which has proven difficult to achieve. The reasons sustainable fisheries management goals have not been achieved include various socio-economic, political, and scientific factors. Scientifically, one of the major challenges has been understanding how spatial and temporal heterogeneity in processes impact the populations dynamics of a stock. Fisheries science has spent a great deal of effort collecting data, both biological and environmental, which are inherently spatial and temporal in nature. Computational and statistical limitations have resulted in science products which do not fully utilize the spatio-temporal information contained in these data and tend to treat stocks as homogeneous entities. Fortunately, computational advances coupled with more accessible statistical methods have resulted in new methodologies which can harness the spatio-temporal information contained in these fisheries data. Here we develop temporally variable species distribution models for yellowtail flounder (*Limanda ferruginea*) and Atlantic cod (*Gadus morhua*) on Georges Bank (GB) using a suite of static environmental covariates and presence-absence information from groundfish trawl surveys in Canada and the United States. These models indicate there are both seasonal and long term shifts in the distribution of both species. The average sea surface temperature (SST; average from 1997-2008) and depth were significant predictors of the distribution of both species throughout the year. Significant shifts in the distribution of both species occurs relatively frequently, with the distribution of cod observed to differ approximately every 5 years, while the Yellowtail distribution appears to fluctuate at least every 3 years. The core areas for both species shifts to the north and east throughout the study period. Much of this shift is due to the loss of the species from southern and western portions of GB. The seasonal distribution of cod and yellowtail are relatively consistent throughout the late winter and spring, while in the fall the distribution of cod shifts towards the edge of the bank. For cod there has been a substainal decline in core area within the United States waters on Georges Bank while there has been little change in Canadian waters. In U.S. waters the yellowtail core area declined rapidly in the late 1970s and early 1980s, but rebounded rapidly in the 1990s and early 2000s, while the core area was unchanged or slowly increased in Canadian waters over this time. These trends have resulted in an increase in the proportion of both stocks in Canadian waters in recent years. The models for both stocks were also relatively successful at predicting the likely location of the stock up to 3 years into the future, in addtion the simplified models which use only the random field for prediction performed as well as the models that included environmental covariates. Here we show how these models are able to provide novel insights into both seasonal and inter-annual variability in species distributions even without the use of environmental covariates. The incorporation of spatial information into science advice will improve our ability to sustainably manage these stocks.

## INTRODUCTION

Sustainable management of marine fisheries has been recognized as a critical challenge facing society in the 21<sup>st</sup> century (CBD 2018). The challenges facing sustainable fisheries management are multifaceted and include interactions between complex ecological, socio-economic, and political factors (CITE). For example, fisheries management regions were often delineated as a result of political or geographic considerations rather than biological or ecological rationale. As a result, the management region can vary from situations in which it encompasses only a small subset of the total population of a species, to situations in which the majority of the stock is manged across a region with significant heterogeneity in the processes that drive the population dynamics. (CITE).

Accounting for spatial and temporal heterogeneity in the processes that drive a stocks population dynamics has long been recognized as a challenge in fisheries science Ricker (1944). Many of the traditional fisheries methods developed, and still currently used to assess fisheries, require assumptions about the underlying spatial processes, these assumptions generally result in models that treat stocks as spatially homogeneous entities. (Beverton and Holt 1957; Ricker 1975; Hilborn and Walters 1992). Many of these assumptions were required because of computational and statistical limitations and has lead to science products that do not fully utilize the spatio-temporal information contained in the underlying data. Techniques, such as survey stratification, have been utilized in an effort to account for spatial heterogeneity and reduce uncertainty in the indices feeding these models [CITE]. Other methods have been developed to quantify changes in spatial patterns over time (CITE Gini, D50, etc). These methods generally measure how evenly a population is distributed across some domain with data that is aggregated at some scale (often at the scale of the strata). These indices are an additional source of information providing a synoptic view of whether the distribution of parameters of interest (e.g. survey abundance or biomass) has changed over time, but they are unable to provide a detailed understanding of the spatial changes in these distributions.

Species distribution models (SDMs) were one of the earliest modelling frameworks developed to better understand spatial distributions and the processes that influence the observed patterns in species distributions (Grinnell 1904; Box 1981; Booth et al. 2014). These models use environmental data and species ecological information to map the occurrence probability (OP; or some measure of abundance) of a species across some land(sea)-scape; quantitative SDMs originated with attempts to predict terrestrial plant distributions (Box 1981). In the marine realm, the use of SDMs has increased rapidly in recent years; SDMs have been used in the development of Marine Protect Areas (MPAs) and MPA networks, to better understand the distribution of Species at Risk (SAR), and to predict the impact of climate change (Cheung et al. 2008; Robinson et al. 2011; Sundblad et al. 2011; Domisch et al. 2019; McHenry et al. 2019).

Historically, SDMs often did not explicitly consider temporal changes in the relationship between the environment and the response of the species; these SDMs therefore provide a snapshot in time based on available data (Elith and Leathwick 2009). However, more sophisticated SDM frameworks have been developed in which the underlying relationships can vary in time and space, this has lead to more dynamic models which can provide improved predictions and more completely utilize the information contained within these data (Merow et al. 2011; Thorson et al. 2016; Martínez-Minaya et al. 2018). The development of these new spatio-temporal SDM models have been made possible by a number of recent statistical and computational advances such as the implementation of the Laplace approximation (LA), Automatic Differentiation (AD), Stochastic Partial Differential Equations (SPDE), and Gaussian Markov Random Fields (GMRFs) in commonly used programming languages (Kristensen et al. 2016; Rue et al. 2016; Thorson 2019). This has enabled the complex spatio-temporal analytical problems associated with these advanced SDM models to be solved in a fraction of the time required by traditional methods.

**So we could have short intro and jump right to the objectives here and put at least some of this in the methods and/or discussion?**

Georges Bank (GB) has been home to some of the most productive fisheries in the world for centuries and is home to a wealth of natural resources (Backus and Bourne 1987). In the 1960s and 1970s numerous countries had large unsustainable fisheries in the region, but with the expansion of territorial seas to 200 miles offshore in 1977, control of resource exploitation (e.g. fisheries) on GB fell under the jurisdiction of the United States (U.S.) and Canada (Halliday and Pinhorn 1996; Anderson 1997). The final demarcation of the Canadian and U.S. territorial waters on GB was implemented with an International Court of Justice (ICJ) decision in 1984. Within three years of this decision both countries had independent groundfish surveys and each of these surveys covered the entirety of GB at different times of the year.

Historically, GB supported substantial groundfish fisheries including Atlantic Cod (*Gadus morhua*), Atlantic Haddock (*Melanogrammus aeglefinus*), Yellowtail Flounder (*Limanda ferruginea*) and numerous other species (Anderson 1997). As observed throughout the northwest Atlantic, the biomass of Atlantic Cod on GB declined significantly in the early 1990s and there has been little evidence for recovery of this stock since this collapse (Andrushchenko et al. 2018). Between the 1970s and the 1990s, the biomass of Yellowtail Flounder on GB was low, but evidence for a rapid recovery of this stock in the early 2000s resulted in directed fisheries for several

years. However, this recovery was short lived and the biomass of this stock has been near historical lows for the last decade (Legault and McCurdy 2018). While the biomass of Atlantic Cod and Yellowtail Flounder remains low, both Atlantic Haddock and Sea Scallop (*Placopecten magellanicus*), the latter being one of the most lucrative fisheries on GB over the last two decades, have experienced unprecedented productivity during this time (Stokesbury 2002; Hart et al. 2013; Finley et al. 2019; DFO 2020).

Here we use a recently developed statistical framework (R-INLA) ; (INLA); Lindgren and Rue (2015); Rue et al. (2016); Bakka et al. (2018)] to develop spatio-temporal species distribution models for two depleted groundfish stocks on GB (Atlantic cod and Yellowtail flounder). Our objectives were to use data from 3 groundfish surveys in the region to; 1) develop temporally variable species distribution models for these two species and explore whether these distributions were influenced by a suite of static environmental layers, 2) identify any long-term shifts in the distribution of these stocks, 3) identify any seasonal changes in the SDMs using survey data collected in the winter, spring and fall, and 4) use the SDMs to quantify any observed shifts in core area within Canadian and U.S. waters.

## Methods

### Study area

Georges Bank, located in the northwest Atlantic straddling the U.S.-Canada maritime border, is a 3-150 m deep plateau that covers approximately 40,000 km<sup>2</sup> and is characterized by high primary productivity, and historically high fish abundance (Townsend and Pettigrew 1997). It is an eroding bank with no sediment recharge and covered with coarse gravel and sand that provides habitat for many species (Valentine and Lough 1991). Since the establishment of the ICJ decision in 1984, the Canadian and U.S. portions of GB have been largely managed separately by the two countries, though some collaborative management exists (Figure 1).

### Data

Survey data were obtained from the Fisheries and Oceans Canada (DFO) “Winter” Research Vessel (RV) survey from 1987-2019 and the National Marine Fisheries Service (NMFS) “Spring” and “Fall” groundfish surveys from 1972-2019. The Winter survey on GB typically occurs in February and early March, the Spring survey typically occurs in April and May, while the Fall survey generally takes place between September and November. For all surveys only tows deemed *successful* (Class 1 data) were used in this analysis. This resulted in 2590 tows from the Winter survey, 2393 tows from the Spring survey, and 2506 tows from the Fall survey.

### Environmental covariates

A suite of 21 spatial environmental and oceanographic datasets were obtained for this analysis (Table 1). To eliminate redundant variables, Variance Inflation Factors (VIFs) were calculated for all variables and any variables with VIF scores > 3 were removed. This procedure was repeated until no variables remained with a VIF score > 3 (Zuur et al. 2010). A Principal Component Analysis (PCA) was undertaken using the data from the associated station locations for each survey with variables excluded from the PCA if they showed no evidence for correlation with other variables or if they had very non-linear correlation patterns (Table 1). The top 4 PCA components, accounting for at least 80% of the variability in the data for a given survey, were retained and included as covariates for the models in addition to the retained environmental covariates (Figure ??).

### Statistical Analysis

A Bayesian hierarchical methodology was implemented using the INLA approach available within the R Statistical Programming software R-INLA (Lindgren and Rue 2015; Bakka et al. 2018; R Core Team 2020). In recent years, R-INLA has seen a rapid increase in use to model species distributions in both the terrestrial and marine realms (e.g. Cosandey-Godin et al. 2015; Leach et al. 2016; Boudreau et al. 2017). This methodology

solves stochastic partial differential equations on a spatial triangulated mesh; the mesh is typically based on the available data (Rue et al. 2016). The mesh used in this study included 6610 vertices and was extended beyond the boundaries of the data to avoid edge effects (Figure 2). Default priors were used for the analysis, except for the range and standard deviation hyperparameters used to generate the random fields, which were Penalized Complexity (PC) priors (Zuur et al. 2017; Fuglstad et al. 2019). The range PC prior had a median of 50 km with a probability of 0.05 that the range was smaller than 50 km. The standard deviation of the PC prior had a median of 0.5 with a probability of 0.05 that the marginal standard deviation was larger than 0.5.

For the INLA models, survey data up to 2016 were used (*Winter* survey from 1987-2016, *Spring* and *Fall* surveys from 1972-2016). Survey data from 2017-2019 were excluded from the main analysis and used only as a testing dataset. For all analyses, the response variable was the probability of the survey detecting the stock of interest (Occurrence Probability,  $OP_{it}$ ) and a *Bernoulli* GLM was utilized within R-INLA. Cells with an estimated  $OP \geq 0.75$  were considered the *core area*. A dashboard has been developed that can be used to explore the effect of defining different OPs as *core area* and is available at [https://github.com/Dave-Keith/Paper\\_2\\_SDMs/tree/master/Dashboard](https://github.com/Dave-Keith/Paper_2_SDMs/tree/master/Dashboard).

$$OP_{it} \sim Bernoulli(\pi_{it})$$

$$E(OP_{it}) = \pi_{it} \quad \text{and} \quad var(OP_{it}) = \pi_{it} \times (1 - \pi_{it}) \quad (1)$$

$$\text{logit}(\pi_{it}) = \alpha + f(Cov_i) + u_{it}$$

$$u_{it} \sim GMRF(0, \Sigma)$$

Each variable retained after the VIF analysis, along with each of the 4 PCA components, was added to the model individually. All continuous covariates were modelled using the INLA random walk '*rw2*' smoother, which allows for non-linear relationships between the response and each covariate (Zuur et al. 2017; Zuur and Leno 2018). The continuous covariates were centred at their mean value and scaled by their standard deviation. Covariates that were highly skewed (e.g. depth) were log transformed before being standardized. Due to low sample size of several of the levels the Sediment type (Sed ; data obtained from McMullen et al. 2014) these infrequent categories were amalgamated into one factor level that was represented by an *Other* term, resulting in three levels for the Sediment covariate (*Other*, *Sand*, and *Gravel-Sand*). Across the three surveys approximately 93% of the survey tows were on the *Sand* or *Gravel-Sand* bottoms and 7% were in the amalgamated *Other* category.

Four spatial random field ( $u_{it}$ ) models with differing temporal components were compared for each stock and each survey, these were a) a static random field ( $t = 1$ ), b) independent random fields every 10 years, c) independent random fields every 5 years, and d) independent random fields every 3 years. The independent random fields (options b through d) were set retroactively from the most recent year resulting in a shorter duration random field at the beginning of the time series whenever the field time period was not a multiple of the whole time series length (e.g. the 10 year random fields for the Spring models were 2007-2016, 1997-2006, 1987-1996, 1977-1986, and 1972-1976). Models with the same covariate structure but different random fields were compared using WAIC, CPO, and DIC; the results for each of these metrics were similar and only the WAIC results are discussed further. In all cases, the static random field was an inferior model when compared to models with multiple random fields and the results discussed here are largely limited to the comparison of the 10/5/3 year random fields. For brevity we refer to the results from each random field as an *era* (e.g. the *core area* estimated when using the 2012-2016 random field is the *core area* during the 2012-2016 *era*).

## Model Selection Overview

Stage 1 model selection for the different covariate models was undertaken using the static random field by adding individual covariates. For this first analysis, covariates were retained if low WAIC scores were obtained. CPO and DIC results were similar to WAIC so only WAIC is discussed further; the model selection results are available in the supplement and the complete results can be found in the Model Output and Model Diagnostics sections of the interactive dashboard ([https://github.com/Dave-Keith/Paper\\_2\\_SDMS/tree/master/Dashboard](https://github.com/Dave-Keith/Paper_2_SDMS/tree/master/Dashboard)). For Atlantic Cod this analysis identified depth (DEP) and the average sea surface temperature between 1997 and 2008 (SST) as having low WAIC scores in 2 of the 3 surveys (data obtained from Greenlaw et al. 2010). For Yellowtail Flounder, DEP was identified as an informative covariate in all 3 surveys. In addition, SED, and the average chlorophyll concentration between 1997 and 2008 (CHL) were retained based on their low WAIC scores in the Fall survey. Given the low number of informative covariates DEP, SST, and CHL were all retained for both species in Stage 2 of model selection. In Stage 2 of model selection, these variables were added pairwise (e.g. models included SST + DEP, DEP + CHL, and SST + CHL) for both stocks and again compared using WAIC using the 10-year random fields. In Stage 3 of covariate model selection, models with 3 covariates were tested based on the Stage 2 results. For Atlantic Cod a three term model that included additive terms for SST, DEP, and CHL was the most complex model tested. For Yellowtail Flounder, the most complex model included SST, DEP, and SED. In Stage 3, additional covariates were retained if the WAIC for that model resulted in an improvement of the WAIC of more than 2, as compared to the lowest WAIC for the more parsimonious model.

Model selection on the temporal random fields was done while holding the environmental covariate terms the same. Initial model selection for the random fields (10 and 5-year fields) was done using the Dep + SST model for both species in all seasons given the general support for the Dep + SST model identified in Stage 2 of covariate model selection. For both species this indicated that the 10-year field was inferior to the more flexible 5-year random fields. For Atlantic Cod, the 3 and 5-year random fields were compared using the Dep + SST (which was the covariate model with the lowest WAIC). For Yellowtail, the final step of the random field model selection used the Dep + SST + Sed model (which was the covariate model with the lowest WAIC) for the 3-year and 5-year random field comparison. Note that for Yellowtail Flounder the Dep + SST + Sed covariate model was not run with the 10 year random field and the Dep + SST covariate model was not run using the 3-year random fields in all three seasons, thus there were no results to show for these *potential* models. The key model selection results are provided in the supplement and the full results can be found in the dashboard. For Atlantic Cod the *Full Model* chosen included additive *Dep* and *SST* covariates and used a random field which changed every 5 years. For Yellowtail Flounder, the *Full Model* chosen included additive *Dep*, *SST*, and *Sed* covariates, the *Winter* and *Spring* models used a 3-year random field, while the *Fall* used a 5-year random field.

## Model Prediction

A predictive grid with cells having an area of approximately 9.1 km<sup>2</sup> was developed (Figure ??). The models were developed using data up to and including 2016 To obtain the predictions of the *OP* for Cod, the *Full Model* included additive *Dep* and *SST* terms and used the 5-year random field. For Yellowtail *OP* predictions, the *Full Model* included additive *Dep*, *SST*, and *Sed* covariates, the models for the Winter and Spring used the 3-year random field, while the model for the Fall used the 5-year random field (see either the interactive dashboard or the Supplemental Figures S1-S4 for model selection results). Each cell was intersected with average *SST*, *DEP*, and *Sed* fields (see Supplemental Figure S5 for the distribution of these environmental covariates) and the *OP* was estimated for each grid cell in each *era* for Atlantic Cod and Yellowtail Flounder in the Winter, Spring, and Fall. The results using the predictive grid were used to calculate the *core area* for each *era*.

This predictive grid was used to calculate the centre of gravity (COG) of the *core area* for each *era*. The COG was calculated in the UTM coordinate system (EPSG Zone: 32619) using the easting (*X*) and northing (*Y*) for each cell identified as *core area* (*i*) in each *era* (*t*) and weighted by the *OP* at each of these locations.

$$x_t^{cog} = \frac{\sum_{i=1}^n (X_{i,t} \times OP_{i,t})}{\sum_{i=1}^n OP_{i,t}} \quad (2)$$

$$y_t^{cog} = \frac{\sum_{i=1}^n (Y_{i,t} \times OP_{i,t})}{\sum_{i=1}^n OP_{i,t}} \quad (3)$$

The standard deviation around the mean COG in the X and Y direction was calculated as:

$$\sigma_{cog,t}^x = \sqrt{\frac{\sum_{i=1}^n OP_{i,t}}{[(\sum_{i=1}^n OP_{i,t})^2 - \sum_{i=1}^n OP_{i,t}^2] \times \sum_{i=1}^n (OP_{i,t} \times (X_{i,t} - x_t^{cog})^2)}} \quad (4)$$

$$\sigma_{cog,t}^y = \sqrt{\frac{\sum_{i=1}^n OP_{i,t}}{[(\sum_{i=1}^n OP_{i,t})^2 - \sum_{i=1}^n OP_{i,t}^2] \times \sum_{i=1}^n (OP_{i,t} \times (Y_{i,t} - y_t^{cog})^2)}} \quad (5)$$

To quantify the ability of these models to predict future spawning aggregations, data from the 2017-2019 surveys were used as a testing dataset. This analysis utilized the *Full Models* to predict the *OP* 1, 2, and 3 years into the future. In addition to the full models, an *Intercept Model* which used only the temporally varying random field for prediction (i.e. the model excluded all environmental covariates) was compared to the predictions from the *Full Models* for 2017-2019. Both the model residual and the 2017-2019 predictive error were calculated for each year using RMSE, MAE, and SD. Given the similarity of the results only the RMSE is presented (full results are available in the dashboard).

## Model Validation

Five fold cross validation was used to compare the out-of-sample predictive performance for a subset of the 5-year random field models: intercept only, SST (Atlantic Cod), DEP (Yellowtail Flounder), and DEP + SST. The Atlantic Cod model validation was performed using the Winter survey data, the Yellowtail Flounder validation used the Spring survey data. The data were *randomly* divided into 5 subsets and trained using 4 of the subsets; the 5th dataset was treated as a testing dataset to determine how well the model was able to predict out-of-sample data. Model performance was measured by comparing the model residuals from the training data to the prediction error from the testing data. The metrics used for this comparison were Root Mean Squared Error (RMSE), Mean Average Error (MAE), and the standard deviation (SD), given the similarity of the results only the RMSE is presented (full results are available in the dashboard). A subset of models were chosen because of the computational demands of this validation procedure.

# RESULTS

## Inter-annual and Seasonal Variability

For both stocks their core areas shifted towards the north and east throughout the study period, this was most noticeable when focusing on the core area ( $OP \geq 0.75$ ) regions (Figure 3). For Atlantic Cod the shift in distribution of the core area regions occurred relatively rapidly in the 1990s and the centre of gravity (COG) has been relatively stable since this period (Figure 3). In the 1970s and 1980s, core area was observed across the bank, however since the mid-1990s there is a clear shift in distribution with core area concentrated along the north-east of the bank mainly in Canadian waters (Figures S7 -S9). In addition, in the Fall, Atlantic Cod has tended to be distributed along the northern edge of GB and the distribution of Atlantic Cod during this time likely includes the northern slope of the bank where there is limited survey coverage. The size of

the core area has followed a similar temporal pattern as the distribution, with a rapid decline in the core area for Atlantic Cod occurring in the 1990s in the Winter and Spring (Figure 4). In the Fall the decline in the size of the core area was observed approximately a decade earlier than in the Winter or Spring and the core area has been much smaller in the Fall (Figure 4). Given the location of the stock along the edge of the bank during the Fall it is likely that a substantial portion of the stock is located along the slope where survey coverage is limited (Figure 1).

The Yellowtail Flounder shift in core area has, in large part, resulted from a reduction in the core area along the southern flanks of GB. The core area has been consolidated in a central region of GB that straddles the ICJ line dividing Canada and the U.S (Figure 3). The COG of Yellowtail Flounder has been relatively stable both seasonally and between eras since the 1990s despite large changes in the size of the core area during this time. The trends in, and size of, the core area during the Spring and Fall have been very similar since the 1980s. In both seasons there were large increases in core area in the 1990s followed by a variable, yet generally increasing, size of core area more recently (Figure 4). In the Winter an area of similar location and size is observed, but the size of the core area in the Winter has been in decline since a period of increase in the 1990s (Figure 4).

For both stocks the changes in the size of the core area were larger in the U.S. than in Canadian waters (Figure 5). In the U.S. the declines in the size of core area of Atlantic Cod occurred rapidly in the early 1990s in the Winter and Spring. In the Fall the loss of core area occurred approximately a decade earlier, although the size of the core area in the U.S. during the Fall was always substantially lower than in the Winter or Spring. In Canada there has been minimal change in the size of the core area in any of the seasons through time; the size of the core area in the Fall has tended to be lower than observed in the Winter or Spring (Figure 5). The size of the core area of Yellowtail Flounder in the U.S. declined steadily throughout the 1970s and 1980s, this was followed by an increase in the 1990s and early 2000s (Figure 5). In the last decade the size of the core area in the U.S. appeared to stabilize. In Canada the size of core area for Yellowtail Flounder throughout the 1970s and 1980s was variable and relatively low, but in the mid-1990s the size of the core area increased and has been relatively stable since the late 1990s (Figure 5).

## Environmental Variables

The spatial fields for the three environmental variables retained by model selection are shown in Figure S5. The average SST between 1997 and 2008 had the largest effect on the OP of Atlantic Cod; they were more likely to be found in regions of the bank with a lower SST (Figure 6). For all 3 surveys the OP of Atlantic Cod declined rapidly in regions of the bank where the SST was above approximately 10°C (Figure 6). Although the Dep relationship was also retained in the final Atlantic Cod model the effect of Dep on OP was substantially smaller than the SST effect. During the Winter and Spring the OP peaked between 70-82 m and declined slowly in shallower and deeper waters (Figure 6). There was no clear relationship with Dep in the Winter.

For Yellowtail Flounder, Dep had the largest effect on OP, with Yellowtail Flounder most likely to be observed between depths of 66-75 m in each of the 3 surveys and the Dep effect on OP was highest during the Spring (Figure 7). The average SST between 1997 and 2008 was also included in the final model for all three seasons, with Yellowtail Flounder OP generally declining as SST increased. The effect of SST was least pronounced in the Fall. The sediment type also had a significant influence on the OP for Yellowtail Flounder in the Winter and Fall, with Sand and Gravel-Sand having higher OPs than the Other sediment category, this difference is most notable during the Winter (Figures S3 and 7).

## Range and Variability of Random Fields

The decorrelation range for Atlantic Cod was above 100 km throughout the year and was generally higher than that observed for Yellowtail Flounder (Figure 8). The range was highest for Atlantic Cod in the Spring with an estimate of 218 (95% CI:131-346) km while the range during the Winter spawning period was the lowest at 154 (95% CI:99-227) km. In the Fall the estimate declined from the Spring; the range in this period may be influenced by a portion of the stock being located outside of the survey domain and the stock being more concentrated in one area (Figure 8). For Yellowtail Flounder, the lowest range was estimated in the

Winter at 86 (95% CI:63-109) km with the Spring and Fall range estimates being higher and somewhat more variable than the Winter range estimate. The range estimates of Yellowtail Flounder throughout the year were smaller and less variable than that observed with Atlantic Cod (Figure 8). The uncertainty of these estimates precludes any statistical differences being observed between the seasons.

The standard deviation of the random field was lower for Atlantic Cod in the Winter and Spring than during the Fall (Figure 9). The significant increase in the standard deviation in the Fall was related to the increased influence of the random field (i.e. the relatively small effect of the environmental covariates) during this season for Atlantic Cod. The standard deviation of the random field is highest for Yellowtail Flounder in the Winter and the seasonal differences for Yellowtail Flounder are smaller than those observed with Atlantic Cod (Figure 9). The standard deviation of the Yellowtail Flounder field is higher than Atlantic Cod in the Winter and Spring, but lower in the Fall (Figure 9). The posteriors of other hyperparameters for both stocks in the Winter, Spring, and Fall are provided in Figures S33 - S38.

## Validation and Prediction

The 5-fold cross validation indicated that each of the models used for 5-fold cross validation (intercept only, SST (Atlantic Cod), DEP (Yellowtail Flounder), and DEP + SST) were able to predict the distribution for both stocks without an increase in bias or a loss of accuracy (Figure 10). The mean error of the residuals for the validation training set predictions were similar to the error from the predicted test data and while the mean error of the test data was generally more variable, the estimates were centred on 0 and thus there was no evidence of bias in these predictions (Figure 10). The RMSE from the test and training data showed similar patterns for both stocks and most of the models, although for Yellowtail Flounder the RMSE for both the training and test data from the intercept only model was slightly lower than either of the models with covariates indicating that the inclusion of the environmental covariates may result in a small loss of out-of-sample prediction (Figure 10).

The models resulted in a slight loss of accuracy when predicting the spawning distributions of each stock 1, 2, and 3 years into the future (Figure 11), but the predictions were well below the RMSE associated with a model with no predictive ability (dashed line; Figure 11). For both stocks the 2018 data consistently had the lowest prediction accuracy with the models tending to predict individuals where none were observed. This is in agreement with observations of the survey biomass indices being near historic lows for both stocks in 2018 (Andrushchenko et al. 2018; Legault and McCurdy 2018). Generally, the predictive error from these models were at the high end of the range of the model error estimates when data were available, this indicates that the predictions from these models could be used to inform the spatial OP for both stocks up to 3 years into the future (Figure 11).

## DISCUSSION

### Implications from the closure framework (excludes anything about closures)

The core area for Atlantic Cod collapsed rapidly in the early 1990s in unison with the collapse of Atlantic Cod (and other groundfish) stocks throughout the Northwest Atlantic (Bundy et al. 2009). Since the collapse, the size of the core area has remained relatively consistent but has continued to slowly shift to the northeast with this shift more pronounced in the Fall. The Fall distribution of Atlantic Cod is likely now located on the northeastern slope of the bank outside of the core survey domains of any of these surveys. This northeastern shift of the stock over the course of this study suggests that the surveys may no longer be sampling the entirety of this stock throughout the course of the year (i.e. a higher proportion of the stock may now be located outside of the survey domain in the Fall than in the past). Each of the survey indices had been used as inputs to the Atlantic Cod stock assessment model for eastern GB Atlantic Cod (Andrushchenko et al. 2018). However, this assessment model suffered from such significant retrospective patterns that the model was recently rejected; the results of this study are in agreement with the suggestion that the observed shift in the distribution of Atlantic Cod outside of the survey domain was a contributing factor to the model retrospective problems (Andrushchenko et al. 2018). In addition, because the management of this stock is shared between Canada and the U.S., the observed shift in the core distribution to Canadian waters suggests

that shared management policies, such as quota sharing agreements between the two jurisdictions, may require regular review (e.g. TMGC 2002).

Yellowtail Flounder was unlikely to be found on bottom types which did not include sand and was more frequently found at depths between 66-75 meters which is consistent with the known life history for this species (Johnson et al. 1999). In historically lower SST regions of the bank most of the remaining habitat on GB which meet these criteria straddle the ICJ line on GB. In addition, there was a consistent increased likelihood of encountering Yellowtail Flounder in this area which was not explained by the environmental covariates. This suggests this region has some unexplained ecological or environmental significance to Yellowtail Flounder.

The shift in the distribution of Yellowtail Flounder away from more southern and western parts of GB combined with the declines in biomass of Yellowtail Flounder throughout the U.S. supports the view that the environmental change which has been observed throughout U.S. waters has been a factor in the recent decline of Yellowtail Flounder both on GB and throughout the region (NFSC 2012; Pershing et al. 2015; Legault and McCurdy 2018; NOAA 2020). Given the loss of Yellowtail Flounder from the warmer portions of the bank observed in this study it is possible that the remaining core area straddling the ICJ line represents the most northern suitable habitat on GB for this species. If temperatures continue to increase, as projected with climate change, the suitability of this habitat may decline which would increase the risk of extirpation of Yellowtail Flounder from GB irrespective of any fisheries management action (Allyn et al. 2020).

The influence of the average SST layer as an environmental covariate in the models was somewhat surprising given this layer was derived from monthly SST composites from the Advanced Very High Resolution Radiometer (AVHRR) satellite from 1997 to 2008 (Greenlaw et al. 2010) and thus represents an aggregate, static layer from only a temporal subset of the time period covered by the groundfish survey data. However, the importance of this SST layer may be due to it capturing general widespread oceanographic features across the bank domain. Further, the observed variability of the effect between seasons is likely a reflection of the connection between surface waters and the benthos given that the degree of vertical mixing and stratification varies with season and spatially across the bank (Kavanaugh et al. 2017). It is acknowledged that the interpretation of the static SST layer used in these analyses as a thermal effect is likely somewhat unrealistic as it assumes that the relative temperature patterns and the species reaction to these patterns have remained static over the study period. Therefore, more advanced models using either dynamic SST or modelled bottom temperature layer could lead to further insights into how changes in the thermal environment have influenced the distribution of both stocks (Pershing et al. 2015; Greenan et al. 2019).

Here we have shown how models which incorporate environmental, spatial, and multi-scale temporal information can be used to partition static environmental relationships from dynamic changes which occur both inter and intra-annually. This framework enables a better understanding of the magnitude of dynamical shifts along with identifying regions of consistently high and low probability of encounter throughout the study region. The results indicate that few of the static environmental covariates related to groundfish distribution with only a static SST layer, depth, and sediment type having any consistent relationship to the likelihood of encountering either species throughout the duration of this study. A general shift in the distribution of both species towards the east and north was identified, in both cases this shift was in large part due to the loss of high EP areas in the southern and western portion of GB (primarily in US waters). In addition, the analysis of surveys from different times of the year provided a snapshot of the seasonal changes in the distributions of the species; we observed that the yellowtail distribution is relatively stable throughout the year, while cod move towards the slope of GB during the fall. The models were able to predict the location of cod and yellowtail during spawning up to 3 years in the future with only a modest loss of predictive ability.

\*\*\* ADD THIS SOMEWHERE??\*\* Using spatial only models performs as well as the available static environmental data in terms of prediction for these species. If environmental data aren't available or are expensive to collect, these spatial models on their own seem to have some utility in prediction of species location.

The incorporation of dynamic environmental covariates either from remote sensing or oceanographic models would be a logical next step to determine if changes in, for example bottom temperature, have driven the patterns observed for these species.

While using a simple aggregation index does indicate that the spatial distribution of these stocks has changed over time, it does not provide information to understand how the spatial distributions have shifted (e.g. Gini index S6)

The flexibility of the random fields alone (intercept models) indicated that from a predictive standpoint the random fields were often able to predict the OP without a substantial loss of predictive ability when compared to the more complex models including the static environmental data (e.g. Figure 10). This occurred because the random fields are flexible enough to capture the variability inherent in the data in each era, while the environmental covariate relationships were constrained to be invariant throughout the entire time series. Recent research suggests that using a static random field in conjunction with a spatio-temporal random field may provide less biased and more accurate estimates than models that rely on environmental covariates (Yin et al. n.d.).

#### \*\*\* THE OLD DISCUSSION \*\*\* #### Yellowtail

The depth, static SST, and sediment type were generally the most influential variables for yellowtail for all the models tested. Yellowtail was unlikely to be found on bottom types which did not include sand and was more frequently found at depths between XXX and XXX meters (Johnson et al. 1999) and in historically lower SST regions of the bank; most of the remaining habitat which meet these criteria are found straddling the border between Canada and the U.S.A and in Canadian waters on GB. The random fields in each season (see supplemental material) also indicated a consistent increased likelihood of encountering yellowtail in the region straddling the Canadian and U.S. border and this suggests there is some unexplained ecological or environmental significance in this region. The shift in the distribution of yellowtail away from more southern and western parts of GB combined with the declines in biomass of yellowtail throughout the U.S. supports the view that the environmental change that has been observed throughout U.S. waters has been a factor in the recent decline of yellowtail both on GB and throughout the region (NFSC 2012; Pershing et al. 2015; Legault and McCurdy 2018; NOAA 2020). Given the loss of Yellowtail from the warmer portions of the bank observed in this study it is possible that the remaining core area around CA II and in Canada represents the most northern suitable habitat on GB for this species. If temperatures continue to increase as projected the suitability of this habitat may decline which would increase the risk of extirpation of yellowtail from GB irrespective of any fisheries management action (Allyn et al. 2020).

#### Cod

For cod the static SST layer and depth were the most influential covariates and indicated that cod preferred the colder portions of the bank throughout the year. The distribution of cod has steadily shifted throughout the duration of the study period. While the depth preference of cod is more variable than yellowtail (Fahay et al. 1999; Johnson et al. 1999), as observed with yellowtail, the loss of high EP areas in the more southern and western reaches of the bank have primarily been the reason for the apparent shift in the distribution of cod into Canadian waters. More advanced models using either a dynamic SST or modelled bottom temperature layer would lead to further insights into how changes in the thermal environment have influenced the distribution of cod over time (Pershing et al. 2015; Greenan et al. 2019). The interpretation of the static SST layer used in these analyses as thermal effect is likely somewhat unrealistic as it assumes that the relative temperature patterns and the species reaction to these patterns have remained static over the study period.

The high EP area for cod collapsed rapidly in the early 1990's in unison with the collapse of cod (and other groundfish) stocks throughout the Northwest Atlantic (Bundy et al. 2009). Since the collapse the core area has remained relatively consistent but has continued to slowly shift to the north and east, though the shift is more pronounced in the fall. The fall distribution of cod is likely now located on the northeastern slope of the bank outside of the core Georges Bank survey domain. This northeastern shift of the population over the course of this study suggests that this population is found outside the Georges Bank survey domain throughout the course of the year (i.e. a higher proportion of the stock is now located outside of this area). Each of the survey indices area used as inputs to the cod stock assessment model for eastern GB cod (Andrushchenko et al. 2018). This assessment model suffered from such significant retrospective patterns that this stock assessment model was eventually rejected; it is possible that the observed shift in the distribution of cod outside of the survey domain was a contributing factor to the model retrospective problems which was not accounted for in

the model (Andrushchenko et al. 2018). In addition, because the management of this stock is shared between Canada and the U.S., the observed shift in the core distribution to Canadian waters suggests that shared management policies, such as quota sharing agreements between the two jurisdictions, may require regular review (e.g. TMGC 2002).

In the U.S. portion of GB closures were put in place in 1994 to assist with the rebuilding of stocks in the region, these closures have been considered as instrumental in the rebuilding of several stocks in the late 1990s (Murawski et al. 2000; Link et al. 2005). On the Canadian side of GB the primary source of fishery mortality for these species comes from bycatch in the Canadian groundfish and offshore scallop fisheries. In an effort to protect spawning aggregations on Georges Bank from bycatch the Canadian groundfish fishery is excluded from GB from early February until the end of May while the COSF is excluded from fishing inside smaller time-area closures in February, March and June. The temporal shifts in the distribution of these stocks will result in changes in the efficacy of these closed areas over time in terms of protection of the species they were originally designed to protect. In general, the shifts in both stocks to the northeast suggests that closures towards the west of Georges Bank will be less effective in protecting these two stocks than they were when the closures were first implemented while closures towards the north-east portion of Georges Bank may have more influence on these stocks than they did in the past. Additionally, recent work has found little evidence for an effect of the smaller time-area closures in reducing bycatch from the Canadian Offshore Scallop Fishery (CITE PLOS-One). Spatio-temporal models such as these enables the development of metrics which can quantify the overlap between closed areas and the species they are designed to protect, which can lead to insights into the effectiveness of these closures and how the overlap has changes over time and throughout the year (CITE SOMEONE??).

These models provide insight into how the distribution of both species changes both seasonally and inter-annually and how simple static environmental covariates generally have minimal ability to predict these patterns. The only static environmental data which had a significant effect on the species distributions were the average sea surface temperature (1997-2008), depth, and bottom type (yellowtail only). The inter-annual shifts in species distribution indicate the increasing importance of Canadian waters for both species on GB which is likely due to the long-term environmental shifts observed in the region. Given the habitat constraints faced by both species the continuation of directed environmental change will likely put both species at increased risk of extirpation from U.S. portion of Georges Bank and, in the longer term, all of GB irrespective of any fisheries management action. The utilization of the spatio-temporal information contained in these models provides novel insights which can be used to improve science advice (e.g. accounting for shifting distributions in stock assessments or choosing the location of protected areas) and lead to more informed fisheries management decisions.

## ACKNOWLEDGEMENTS

Thanks to Yanjun Wang, Dheeraj Busawon, Monica Finley, Phil Politis, and Nancy Shackell for help with data, questions, and the development and exploration of various parts of this project. Thanks to the CSASdown team for the development of the tools used to craft this manuscript. Thanks to Trish Pearo Drew, Jamie Raper, and Brittany Wilson for general support. Finally, thanks to Dan Ricard and Joanna Mills Flemming for their helpful reviews. This project was made possible by funding from DFOs Strategic Program for Ecosystem-based Research and Advice (SPERA).

## REFERENCES

- Allyn, A.J., Alexander, M.A., Franklin, B.S., Massiot-Granier, F., Pershing, A.J., Scott, J.D., and Mills, K.E. 2020. Comparing and synthesizing quantitative distribution models and qualitative vulnerability assessments to project marine species distributions under climate change. PLOS ONE **15**(4): e0231595. Public Library of Science. doi:10.1371/journal.pone.0231595.
- Anderson, E.D. 1997. The history of fisheries management and scientific advice – the ICNAF/NAFO history from the end of World War II to the present. J. Northw. Atl. Fish. Sci.
- Andrushchenko, I., Legault, C.M., Martin, R., Brooks, E.N., Wang, Y., and Andrews, S. 2018. Assessment of Eastern Georges Bank Atlantic Cod for 2018. TRAC. Ref. Doc **2018/01**: 97.
- Backus, R.H., and Bourne, D.W. 1987. Georges Bank. MIT, Cambridge, Mass.
- Bakka, H., Rue, H., Fuglstad, G.-A., Riebler, A., Bolin, D., Krainski, E., Simpson, D., and Lindgren, F. 2018. Spatial modelling with R-INLA: A review. Available from <https://arxiv.org/abs/1802.06350v2> [accessed 22 September 2020].
- Beverton, R., and Holt, S. 1957. On the dynamics of exploited Fish Populations. UK Ministry of Agriculture, Fisheries and Food.
- Booth, T.H., Nix, H.A., Busby, J.R., and Hutchinson, M.F. 2014. Bioclim: The first species distribution modelling package, its early applications and relevance to most current MaxEnt studies. Diversity and Distributions **20**(1): 1–9. doi:10.1111/ddi.12144.
- Boudreau, S.A., Shackell, N.L., Carson, S., and Heyer, C.E. den. 2017. Connectivity, persistence, and loss of high abundance areas of a recovering marine fish population in the Northwest Atlantic Ocean. Ecology and Evolution **7**(22): 9739–9749. doi:10.1002/ece3.3495.
- Box, E.O. 1981. Predicting Physiognomic Vegetation Types with Climate Variables. Vegetatio **45**(2): 127–139. Springer. Available from <http://www.jstor.org/stable/20037033>.
- Bundy, A., Heymans, J.J., Morissette, L., and Savenkoff, C. 2009. Seals, cod and forage fish: A comparative exploration of variations in the theme of stock collapse and ecosystem change in four Northwest Atlantic ecosystems. Progress in Oceanography **81**(1): 188–206. doi:10.1016/j.pocean.2009.04.010.
- CBD. 2018, May 11. Aichi Biodiversity Targets. Available from <https://www.cbd.int/sp/targets/> [accessed 11 March 2020].
- Cheung, W.W.L., Close, C., Lam, V., Watson, R., and Pauly, D. 2008. Application of macroecological theory to predict effects of climate change on global fisheries potential. Marine Ecology Progress Series **365**: 187–197. doi:10.3354/meps07414.
- Cosandey-Godin, A., Krainski, E.T., Worm, B., and Flemming, J.M. 2015. Applying Bayesian spatiotemporal models to fisheries bycatch in the Canadian Arctic. Can. J. Fish. Aquat. Sci. **72**(2): 186–197. doi:10.1139/cjfas-2014-0159.
- DFO. 2020. Stock Status Update of Georges Bank ‘a’ Scallops (*Placopecten magellanicus*) in Scallop Fishing Area 27.
- Domisch, S., Friedrichs, M., Hein, T., Borgwardt, F., Wetzig, A., Jähnig, S.C., and Langhans, S.D. 2019. Spatially explicit species distribution models: A missed opportunity in conservation planning? Diversity and Distributions **25**(5): 758–769. doi:10.1111/ddi.12891.
- Elith, J., and Leathwick, J.R. 2009. Species Distribution Models: Ecological Explanation and Prediction Across Space and Time. Annu. Rev. Ecol. Evol. Syst. **40**(1): 677–697. doi:10.1146/annurev.ecolsys.110308.120159.
- Fahay, M.P., Berrien, P.L., Johnson, D.L., and Morse, W.W. 1999. Atlantic Cod, *\*Gadus morhua\**, Life History and Habitat Characteristics. NOAA Technical Memorandum.
- Finley, M., Brooks, E.N., McCurdy, Q., Barrett, M.A., and Wang, Y. 2019. Assessment of Haddock on Eastern Georges Bank for 2019. TRAC. Ref. Doc **2019/xx**: 92.

- Fuglstad, G.-A., Simpson, D., Lindgren, F., and Rue, H. 2019. Constructing Priors that Penalize the Complexity of Gaussian Random Fields. *null* **114**(525): 445–452. Taylor & Francis. doi:10.1080/01621459.2017.1415907.
- Greenan, B.J.W., Shackell, N.L., Ferguson, K., Greyson, P., Cogswell, A., Brickman, D., Wang, Z., Cook, A., Brennan, C.E., and Saba, V.S. 2019. Climate Change Vulnerability of American Lobster Fishing Communities in Atlantic Canada. *Front. Mar. Sci.* **6**. Frontiers. doi:10.3389/fmars.2019.00579.
- Greenlaw, M.E., Sameoto, J.A., Lawton, P., Wolff, N.H., Incze, L.S., Pitcher, C.R., Smith, S.J., and Drozdowski, A. 2010. A geodatabase of historical and contemporary oceanographic datasets for investigating the role of the physical environment in shaping patterns of seabed biodiversity in the Gulf of Maine. Available from <http://waves-vagues.dfo-mpo.gc.ca/Library/342505.pdf>.
- Grinnell, J. 1904. The Origin and Distribution of the Chest-Nut-Backed Chickadee. *The Auk* **21**(3): 364–382. American Ornithological Society. doi:10.2307/4070199.
- Halliday, R.G., and Pinhorn, A.T. 1996. North Atlantic Fishery Management Systems: A Comparison of Management Methods and Resource Trends. *Journal of Northwest Atlantic Fishery Science*; Dartmouth **20**. Northwest Atlantic Fisheries Org, Dartmouth, Canada, Dartmouth. Available from <http://search.proquest.com/docview/2377266062/abstract/B0E1653EF6254974PQ/1> [accessed 22 September 2020].
- Hart, D.R., Jacobson, L.D., and Tang, J. 2013. To split or not to split: Assessment of Georges Bank sea scallops in the presence of marine protected areas. *Fisheries Research* **144**: 74–83. doi:10.1016/j.fishres.2012.11.004.
- Hilborn, R., and Walters, C.J. 1992. Quantitative fisheries stock assessment: Choice, dynamics and uncertainty.
- Johnson, D.L., Morse, W.W., Berrien, P.L., and Vitaliano, J.J. 1999. Yellowtail Flounder, *Limanda ferruginea*, Life History and Habitat Characteristics. NOAA Technical Memorandum.
- Kavanaugh, M.T., Rheuban, J.E., Luis, K.M.A., and Doney, S.C. 2017. Thirty-Three Years of Ocean Benthic Warming Along the U.S. Northeast Continental Shelf and Slope: Patterns, Drivers, and Ecological Consequences. *Journal of Geophysical Research: Oceans* **122**(12): 9399–9414. doi:10.1002/2017JC012953.
- Kristensen, K., Nielsen, A., Berg, C.W., Skaug, H., and Bell, B.M. 2016. TMB: Automatic Differentiation and Laplace Approximation. *Journal of Statistical Software* **70**(1): 1–21. doi:10.18637/jss.v070.i05.
- Leach, K., Montgomery, W.I., and Reid, N. 2016. Modelling the influence of biotic factors on species distribution patterns. *Ecological Modelling* **337**: 96–106. doi:10.1016/j.ecolmodel.2016.06.008.
- Legault, C.M., and McCurdy, Q.M. 2018. Stock Assessment of Georges Bank Yellowtail Flounder for 2018. TRAC. Ref. Doc **2018/03**: 64.
- Lindgren, F., and Rue, H. 2015. Bayesian Spatial Modelling with R-INLA. *Journal of Statistical Software* **63**(1, 1): 1–25. doi:10.18637/jss.v063.i19.
- Link, J., Almeida, F.P., Valentine, P., Auster, P., Reid, R.N., and Vitaliano, J. 2005. The Effects of Area Closures on Georges Bank. In *Benthic Habitats and the Effects of Fishing* (American Fisheries Society, Symposium 41, Bethesda, Maryland, 12–14 November, 2002). (Eds P.W.Barnes and J.P. Thomas). pp. 345–368.
- Martínez-Minaya, J., Cameletti, M., Conesa, D., and Pennino, M.G. 2018. Species distribution modeling: A statistical review with focus in spatio-temporal issues. *Stoch Environ Res Risk Assess* **32**(11): 3227–3244. doi:10.1007/s00477-018-1548-7.
- McHenry, J., Welch, H., Lester, S.E., and Saba, V. 2019. Projecting marine species range shifts from only temperature can mask climate vulnerability. *Global Change Biology* **0**(0). doi:10.1111/gcb.14828.
- McMullen, K.Y., Paskevich, V.F., and Poppe, L.J. 2014. 2014, GIS data catalog, in Poppe, L.J., McMullen, K.Y., Williams, S.J., And Paskevich, V.F., Eds., 2014, USGS east-coast sediment analysis: Procedures, database, and GIS data (ver. 3.0, November 2014). Available from <http://pubs.usgs.gov/of/2005/1001/>.

- Merow, C., LaFleur, N., Silander Jr., J.A., Wilson, A.M., and Rubega, M. 2011. Developing Dynamic Mechanistic Species Distribution Models: Predicting Bird-Mediated Spread of Invasive Plants across Northeastern North America. *The American Naturalist* **178**(1): 30–43. The University of Chicago Press. doi:10.1086/660295.
- Murawski, S.A., Brown, R., Lai, H.-L., Rago, P.J., and Hendrickson, L. 2000. Large-scale closed areas as a fishery-management tool in temperate marine systems: The Georges Bank experience. *Bull. US Fish Comm* **66**: 775–798. Available from <https://www.ingentaconnect.com/content/umrsmas/bullmar/2000/00000066/00000003/art00020> [accessed 24 July 2019].
- NFSC. 2012. 54th Northeast Regional Stock Assessment Workshop (54th SAW), assessment summary report. Available from <https://repository.library.noaa.gov/view/noaa/4184> [accessed 1 September 2020].
- NOAA. 2020. NOAA Yellowtail Flounder Overview. Accessed September 1, 2020. <https://www.fisheries.noaa.gov/species/yellowtail-flounder#overview>. NOAA Yellowtail Flounder Overview. Available from <https://www.fisheries.noaa.gov/species/yellowtail-flounder#overview> [accessed 1 September 2020].
- Pershing, A.J., Alexander, M.A., Hernandez, C.M., Kerr, L.A., Bris, A.L., Mills, K.E., Nye, J.A., Record, N.R., Scannell, H.A., Scott, J.D., Sherwood, G.D., and Thomas, A.C. 2015. Slow adaptation in the face of rapid warming leads to collapse of the Gulf of Maine cod fishery. *Science* **350**(6262): 809–812. American Association for the Advancement of Science. doi:10.1126/science.aac9819.
- R Core Team. 2020. R: A language and environment for statistical computing. R Foundation for Statistical Computing, Vienna, Austria. Available from <https://www.R-project.org/>.
- Ricker, W.E. 1944. Further Notes on Fishing Mortality and Effort. *Copeia* **1944**(1): 23–44. doi:10.2307/1438245.
- Ricker, W.E. 1975. Computation and Interpretation of Biological Statistics of Fish Populaions. Environment Canada, Ottawa.
- Robinson, L.M., Elith, J., Hobday, A.J., Pearson, R.G., Kendall, B.E., Possingham, H.P., and Richardson, A.J. 2011. Pushing the limits in marine species distribution modelling: Lessons from the land present challenges and opportunities. *Global Ecology and Biogeography* **20**(6): 789–802. doi:10.1111/j.1466-8238.2010.00636.x.
- Rue, H., Riebler, A., Sørbye, S.H., Illian, J.B., Simpson, D.P., and Lindgren, F.K. 2016. Bayesian Computing with INLA: A Review. Available from <https://arxiv.org/abs/1604.00860v2> [accessed 22 September 2020].
- Stokesbury, K.D.E. 2002. Estimation of Sea Scallop Abundance in Closed Areas of Georges Bank, USA. *Transactions of the American Fisheries Society* **131**(6): 1081–1092. doi:10.1577/1548-8659(2002)131<1081:EOSSAI>2.0.CO;2.
- Sundblad, G., Bergström, U., and Sandström, A. 2011. Ecological coherence of marine protected area networks: A spatial assessment using species distribution models. *Journal of Applied Ecology* **48**(1): 112–120. doi:10.1111/j.1365-2664.2010.01892.x.
- Thorson, J.T. 2019. Guidance for decisions using the Vector Autoregressive Spatio-Temporal (VAST) package in stock, ecosystem, habitat and climate assessments. *Fisheries Research* **210**: 143–161. doi:10.1016/j.fishres.2018.10.013.
- Thorson, J.T., Ianelli, J.N., Larsen, E.A., Ries, L., Scheuerell, M.D., Szuwalski, C., and Zipkin, E.F. 2016. Joint dynamic species distribution models: A tool for community ordination and spatio-temporal monitoring. *Global Ecology and Biogeography* **25**(9): 1144–1158. doi:10.1111/geb.12464.
- TMGC. 2002. Development of a Sharing Allocation Proposal for Transboundary Resources of Cod, Haddock and Yellowtail Flounder on Georges Bank. *Fisheries Management Regional Report*.
- Townsend, D.W., and Pettigrew, N.R. 1997. Nitrogen limitation of secondary production on Georges Bank. *J Plankton Res* **19**(2): 221–235. doi:10.1093/plankt/19.2.221.

- Valentine, P., and Lough, R.G. 1991. The Sea Floor Environment and the Fishery of Eastern Georges Bank - The Influence of Geological and Oceanographic Environmental Factors on the Abundance and Distribution of Fisheries Resources of the Northeast United States Continental Shelf. Open- File Rep: 91-439.
- Yin, Y., Sameoto, J.A., Keith, D.M., and Mills Flemming, J. (n.d.). (In Review) A Spatiotemporal Model of the Meat Weight - Shell Height Relationship for Sea Scallops in the Bay of Fundy.
- Zuur, A.F., Ieno, E.N., and Elphick, C.S. 2010. A protocol for data exploration to avoid common statistical problems: Data exploration. *Methods in Ecology and Evolution* **1**(1): 3–14. doi:10.1111/j.2041-210X.2009.00001.x.
- Zuur, A.F., and Leno, E.N. 2018. Beginner's guide to spatial, temporal, and spatial-temporal ecological data analysis with R-INLA /. Highland Statistics Ltd, Newburgh, United Kingdom.
- Zuur, A.F., Leno, E.N., and Saveliev, A.A. 2017. Beginner's guide to spatial, temporal, and spatial-temporal ecological data analysis with R-INLA /. Highland Statistics Ltd, Newburgh, United Kingdom.

## TABLES

Table 1: Environmental variables used in the analysis. Variables in **bold** were retained after Variance Inflation Factor (VIF) analyses and were included in the linear models. Variables in **italics** were used for the Principal Component Analysis (PCA)

Data	Variable	Source	Resolution(m)	Units
USGS Yearly median Bottom Shear Stress <i>Stratification from 1996-2007</i>	Year.median <i>strat</i>	USGS(SFS – SMD) <sup>3</sup> CoML <sup>1</sup>	3500 <b>2500</b>	Pa <b>none</b>
Seasonal Range of SST <i>Average SST</i>	sst.rg <i>sst.avg</i>	CoML <sup>1</sup>	<b>972</b>	°C
Benthic Silicate	<i>sil</i>	CoML <sup>1</sup>	<b>6000</b>	µM
Sediment Grain size (CONMAP)	Sed	USGS(CONMAP) <sup>2</sup>	-	<b>none</b>
Sand	<i>sand</i>	CoML <sup>1</sup>	<b>6000</b>	%
<i>Seasonal Range of Benthic Salinity 1996-2007</i>	<i>sal.rg</i>	CoML <sup>1</sup>	<b>6000</b>	psu
<i>Benthic Salinity 1996-2007</i>	<i>sal.avg</i>	CoML <sup>1</sup>	<b>6000</b>	psu
<i>Benthic Phosphate 1996-2007</i>	<i>phos.avg</i>	CoML <sup>1</sup>	<b>6000</b>	µM
<i>Benthic Nitrate 1996-2007</i>	<i>nit.avg</i>	CoML <sup>1</sup>	40000	µM
<i>Mud</i>	<i>Mud</i>	CoML <sup>1</sup>	<b>6000</b>	%
Average K490	k490.avg	CoML <sup>1</sup>	8000	none
<i>USGS Median of Bottom Shear Stress</i>	<i>gmaine</i>	USGS(SFS – SMD) <sup>3</sup>	<b>3500</b>	Pa
Benthic Complexity	<i>complexity</i>	CoML <sup>1</sup>	<b>397</b>	°
Slope	<i>slope</i>	CoML <sup>1</sup>	<b>397</b>	°
<i>Depth</i>	<i>Dep</i>	CoML <sup>1</sup>	<b>397</b>	m
<i>Aspect</i>	<i>comlaspect</i>	CoML <sup>1</sup>	<b>397</b>	°
Seasonal Range of Sea Surface Chlorophyll	<i>chl.rg</i>	CoML <sup>1</sup>	1119	mg × m <sup>-3</sup>
<i>Average Sea Surface Chlorophyll</i>	<i>Chl</i>	CoML <sup>1</sup>	<b>855</b>	mg × m <sup>-3</sup>
Benthic Current Stress with Wind and Tidal Influences	botstr.wt	CoML <sup>1</sup>	952	N × m <sup>-2</sup>
Benthic Current Stress with only tidal influence	botstr.t	CoML <sup>1</sup>	3800	N × m <sup>-2</sup>

<sup>1</sup> CoML obtained from <http://waves-vagues.dfo-mpo.gc.ca/Library/342505.pdf>

<sup>2</sup> USGS(CONMAP) obtained from <https://woodshole.er.usgs.gov/openfile/of2005-1001/htmldocs/datacatalog.htm>

<sup>3</sup> USGS(SFS-SMD) obtained from <https://woodshole.er.usgs.gov/project-pages/mobility/gmaine.html>

## **FIGURES**

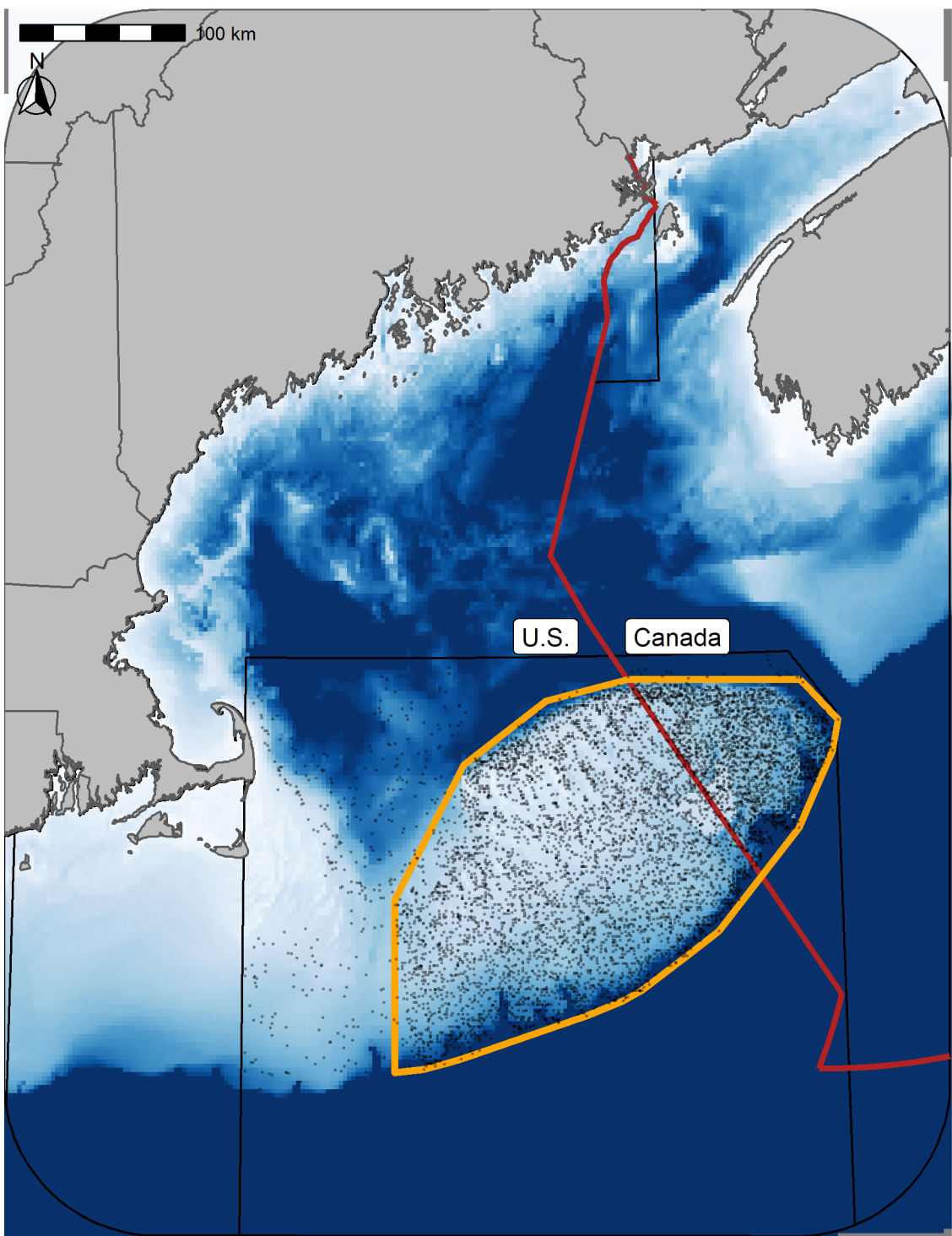


Figure 1: Georges Bank (GB) study area. Points represent the sample locations for each of the three surveys and the orange outline represents the core region of GB included in these analyses ( $42,000 \text{ km}^2$ ). In the U.S. the blue polygon is Closed Area I (CA I) and the white polygon is Closed Area II (CA II). In Canada the small gold bordered cells (each cell covers an area of approximately  $42.7 \text{ km}^2$ ) represent areas which have been included in either the cod or yellowtail closures at least once. Some of the cells have been part of both closures and not all cells are closed each year; darker fill indicates cells which have been closed more frequently. The red line indicates the Canadian exclusive economic zone (EEZ).

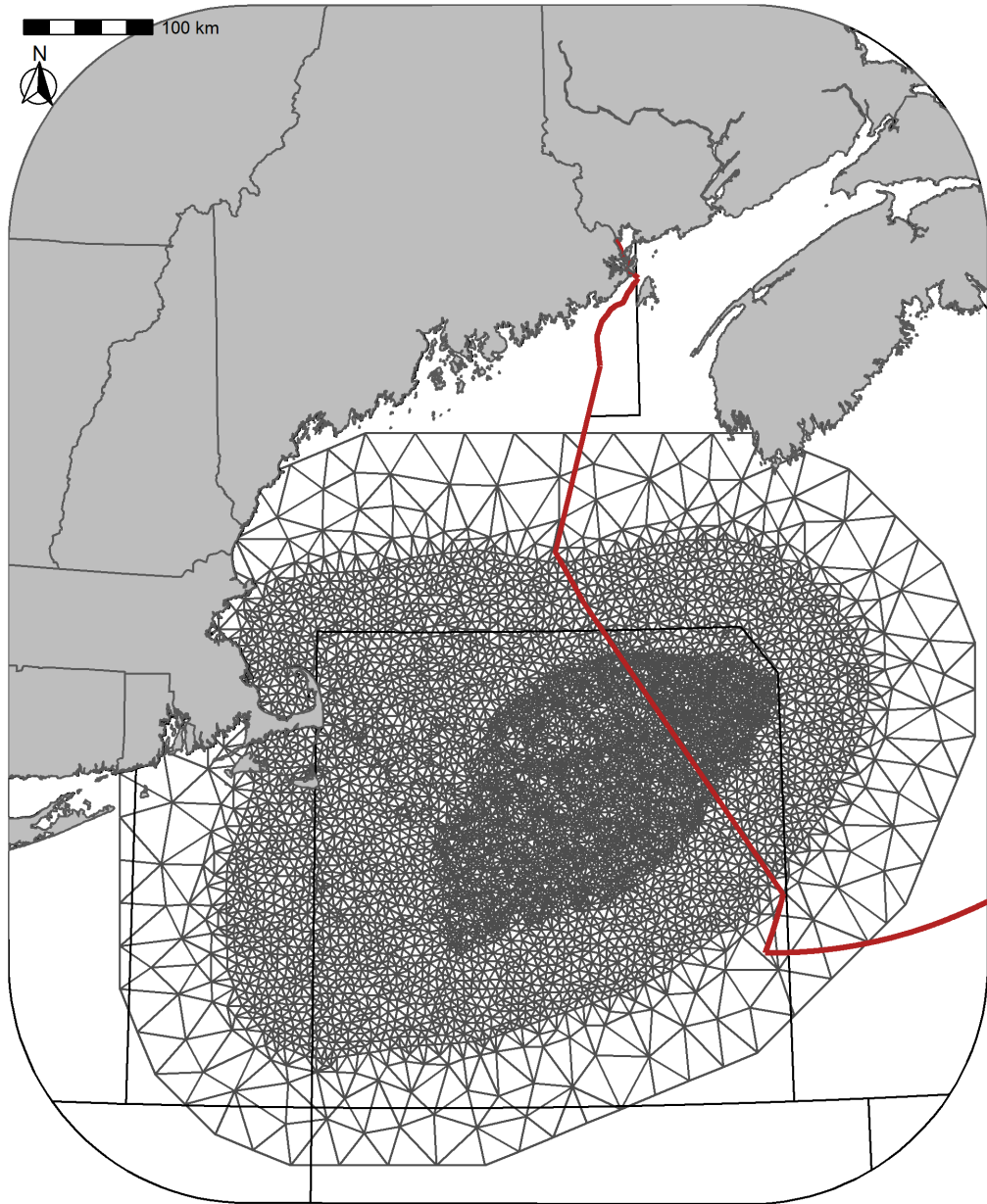


Figure 2: Delaunay triangular mesh used for the spatial fields mesh. The mesh contains 6610 vertices.

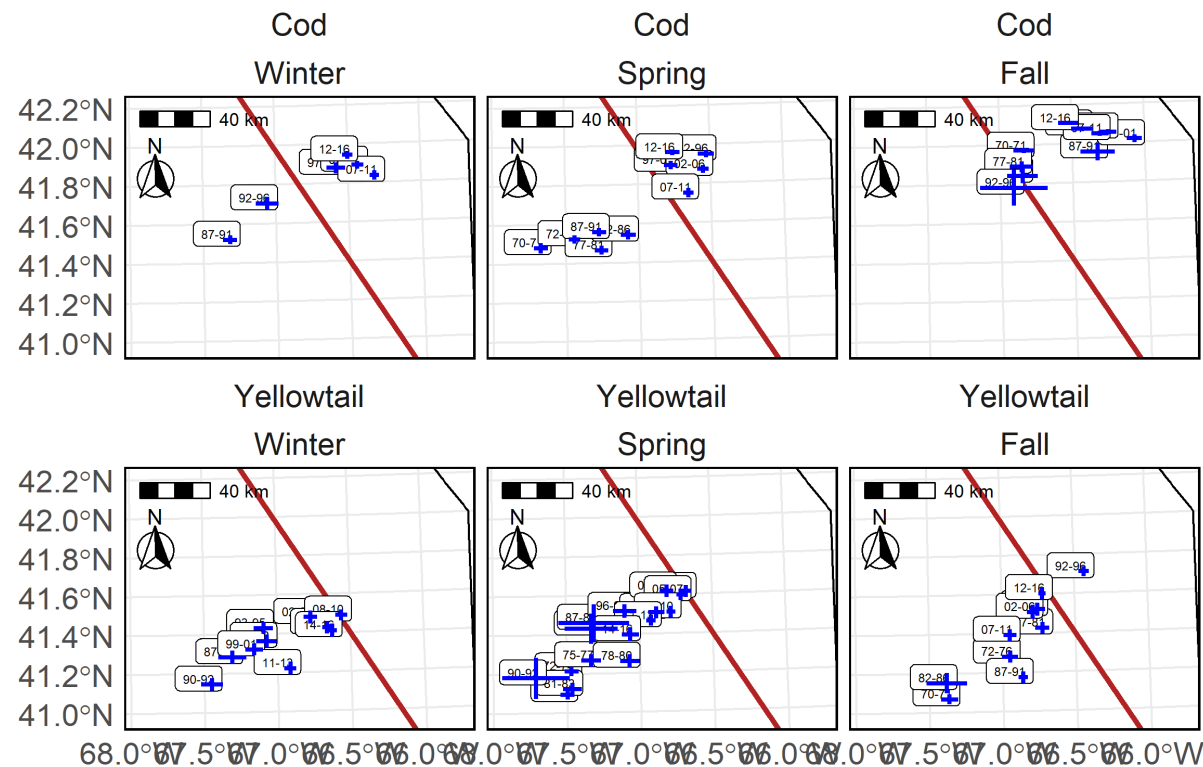


Figure 3: Center of Gravity (COG) for the high EP areas for cod (top panel) and yellowtail (bottom panels) in the Winter (left), Spring (center), and Fall (right) using the preferred models. Blue lines indicate  $\pm 3$  standard deviation units from the mean COG. Labels indicate the years associated with each era and the red line is border between the U.S. and Canada.

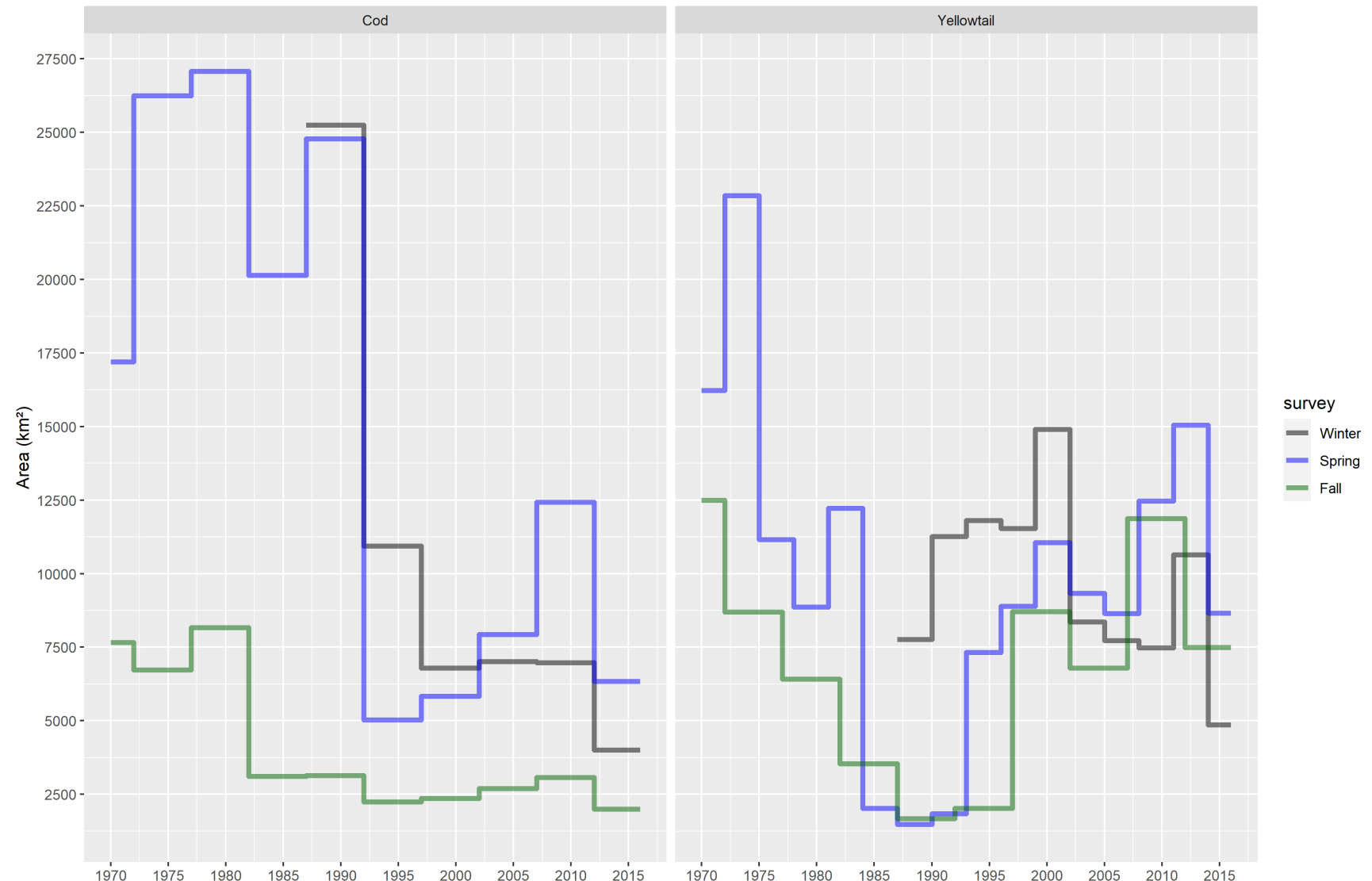


Figure 4: Time series of the total area on GB classified as high EP for each of the three surveys using the preferred models. The cod time series is on the left and the yellowtail on the right. The black line represents the Winter trend, the Blue line is the Spring trend and the red line is the Fall trend.

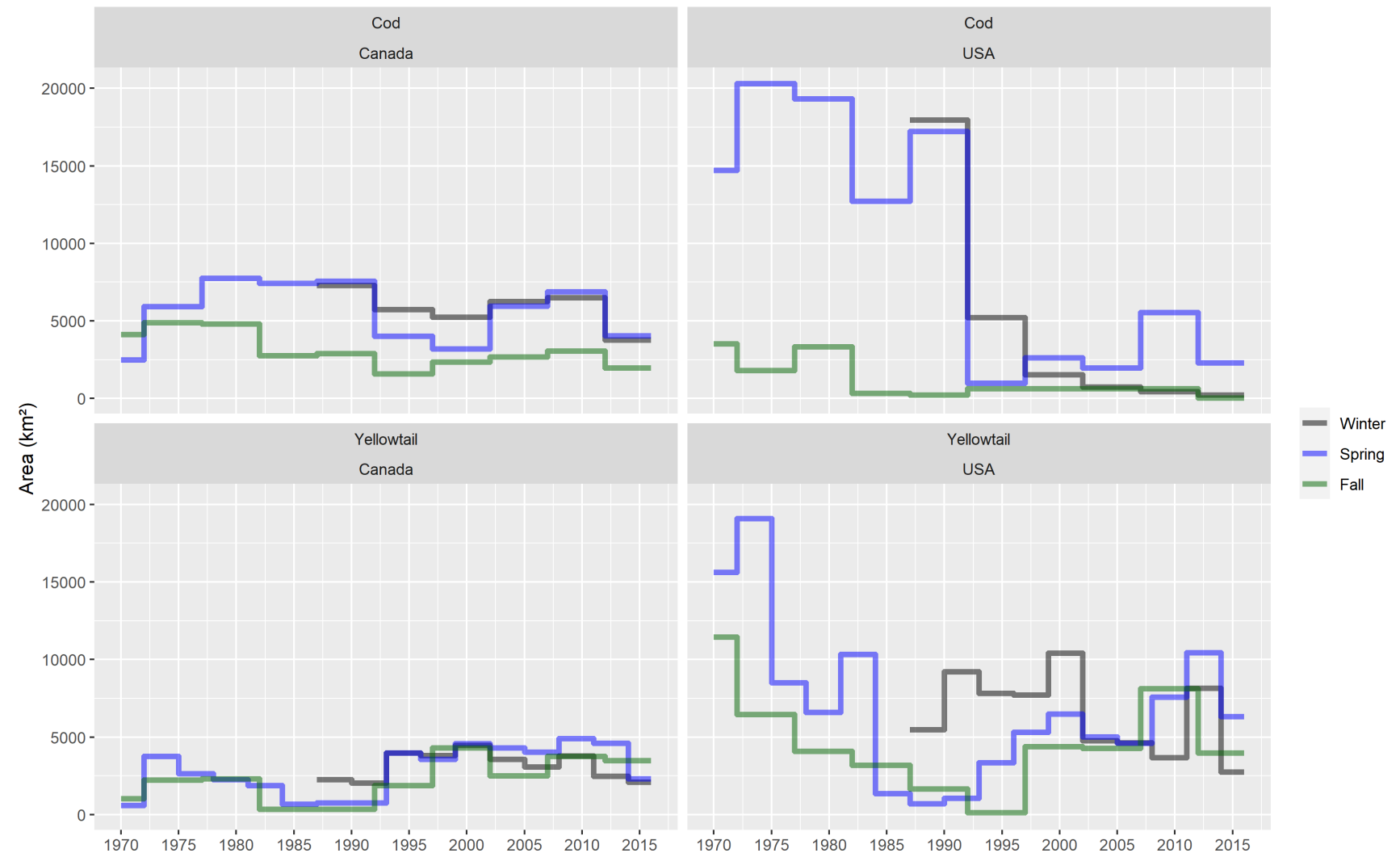


Figure 5: Time series of the total area on GB classified as core area for each of the three seasons in Canada and the U.S.. The Atlantic Cod time series is in the top row and Yellowtail Flounder in the bottom row, Canada is on the left and U.S. is on the right. The black line represents the Winter trend, the Blue line is the Spring trend and the Green line is the Fall trend.

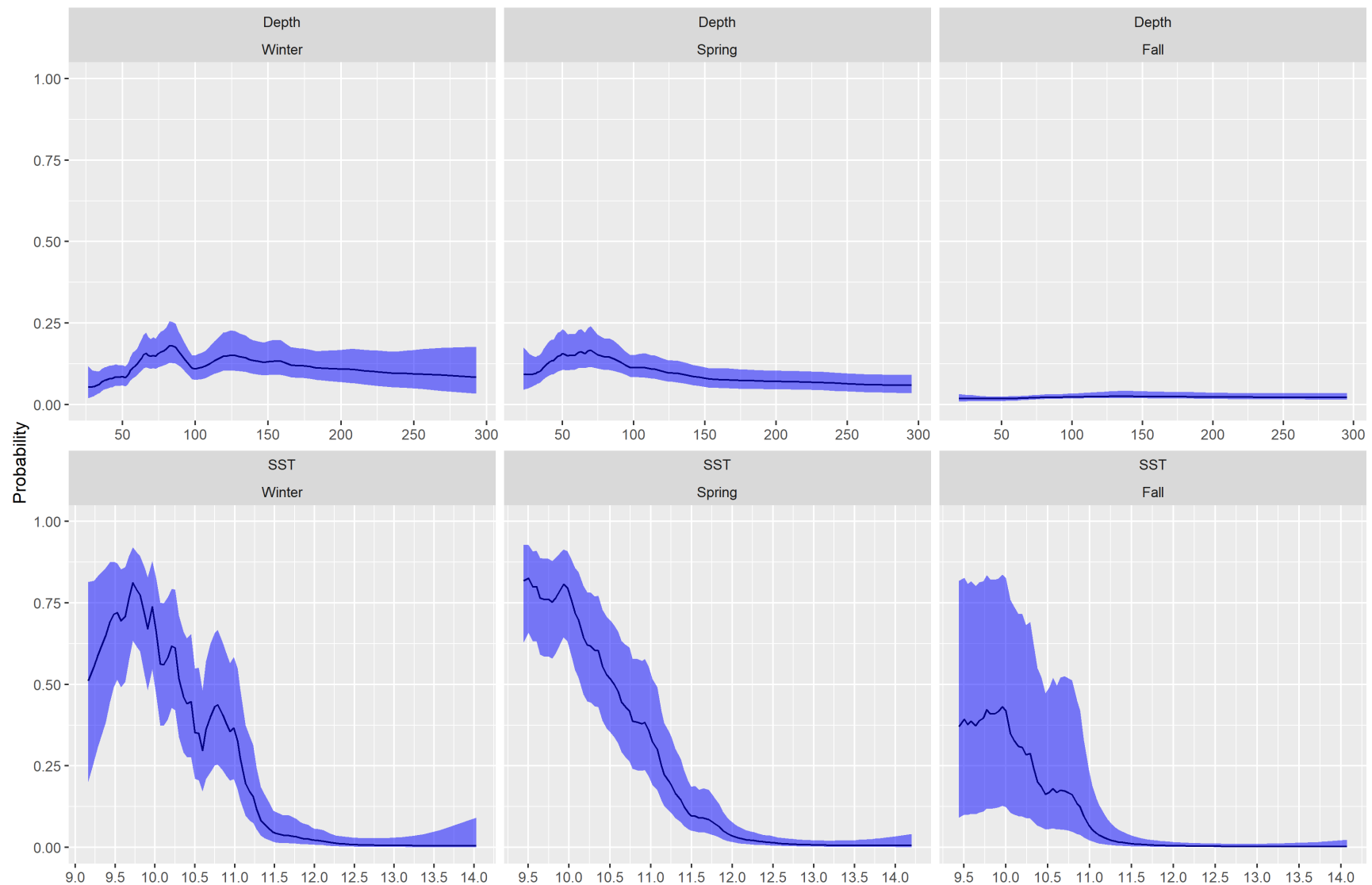


Figure 6: Fixed effects for cod from each survey, top row is the depth covariate effect, bottom row is the SST effect. Results transformed to the probability scale and the blue shaded region represents the 95% credible interval.

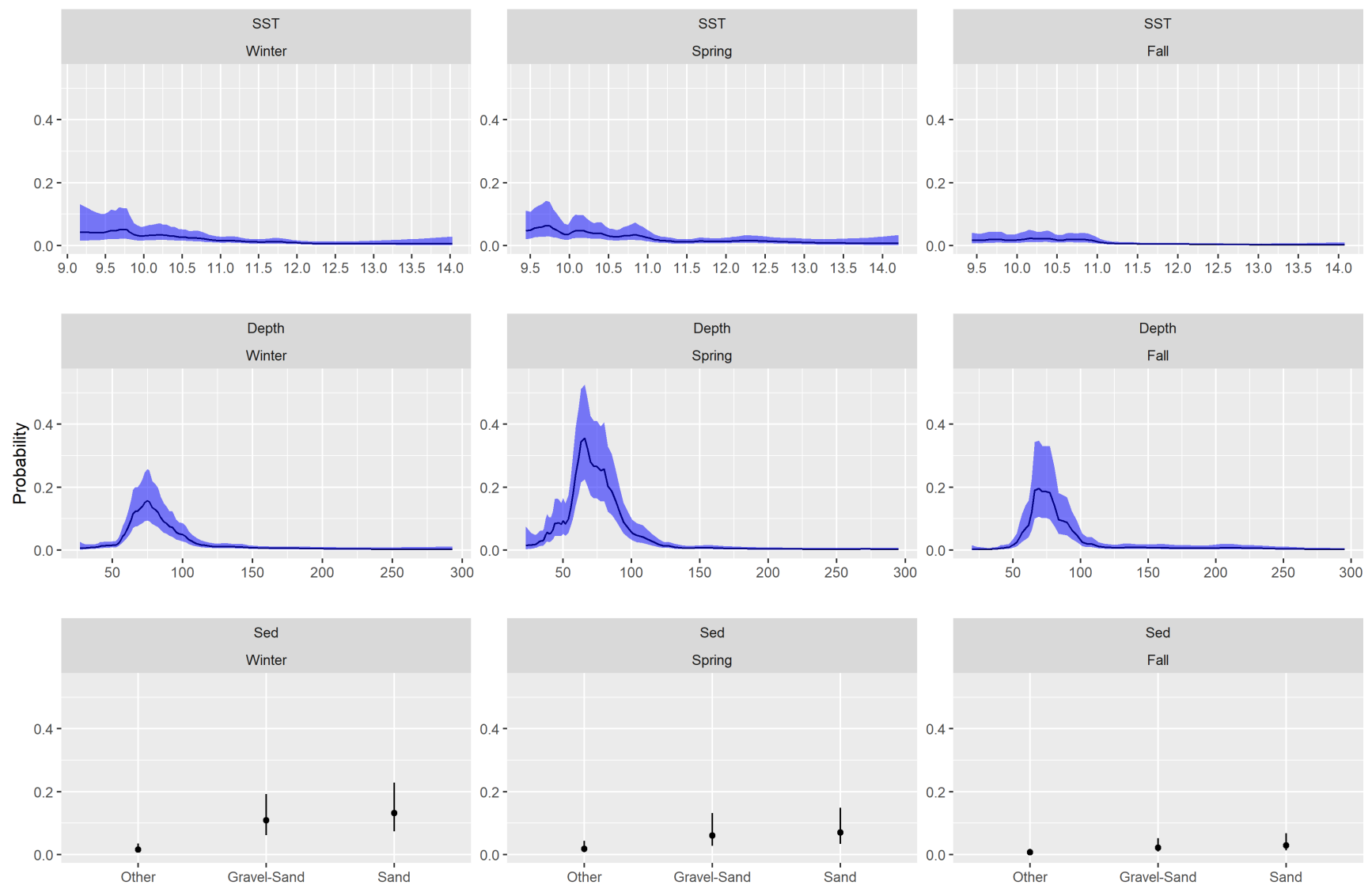


Figure 7: Fixed effects for yellowtail from each survey, the top row is the depth covariate effect, middle row is the SST effect and the bottom row is the effect of sediment type. Results transformed to the probability scale, and the blue shaded region and the error bars represent the 95% credible intervals. The winter and spring results use a 3 year random field while the fall results are for the preferred 5 year random field model.

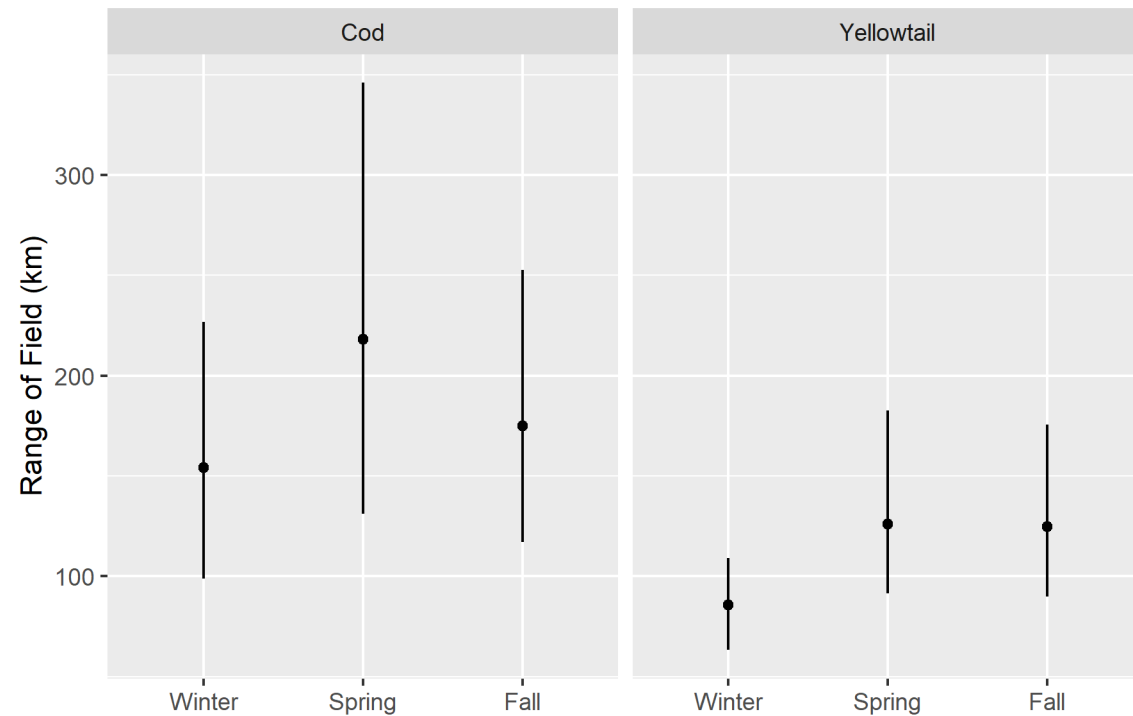


Figure 8: Decorrelation range estimate with 95%CI's for each season.

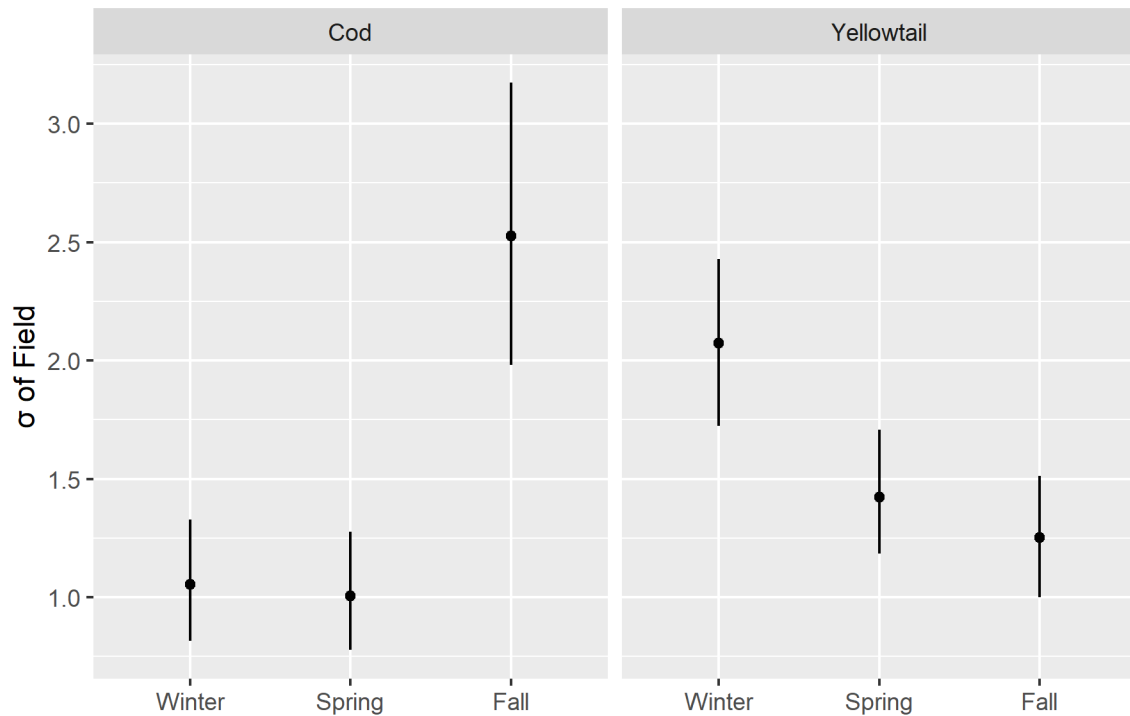


Figure 9: Standard Deviation of the field with 95%CI's for each season.

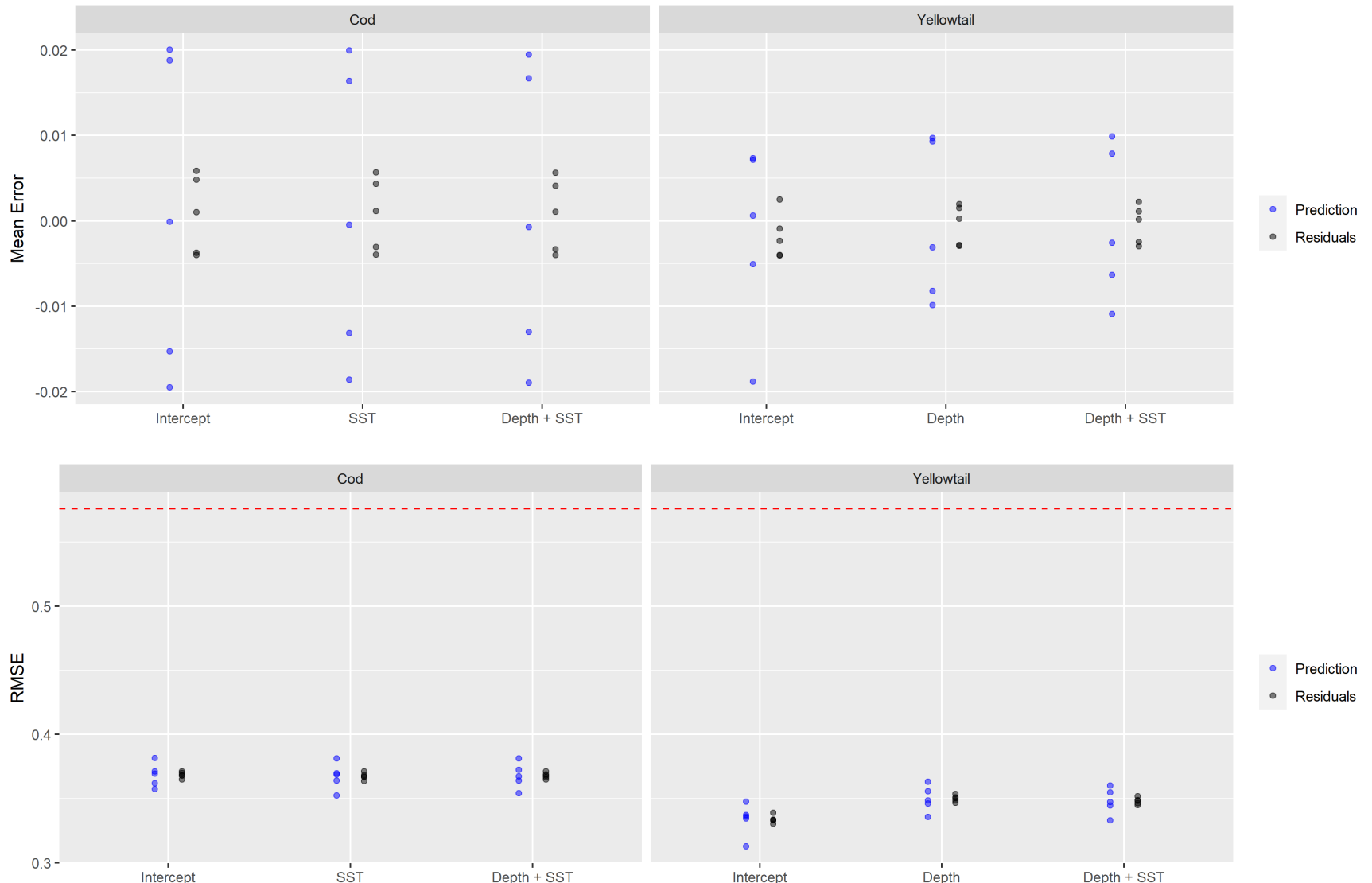


Figure 10: Results of 5 fold cross validation analyses. Top panels represents the mean error for each of the three covariate models tested for cod and yellowtail. Blue points represent the prediction error from the testing dataset, while the black points are the residuals from the training dataset. The bottom panels are the Root Mean Squared Error (RMSE) for these models. The dashed line represents the RMSE for randomly generated data and represents the RMSE for a model with no predictive ability. All models use the 5 year random field due to computational constraints.

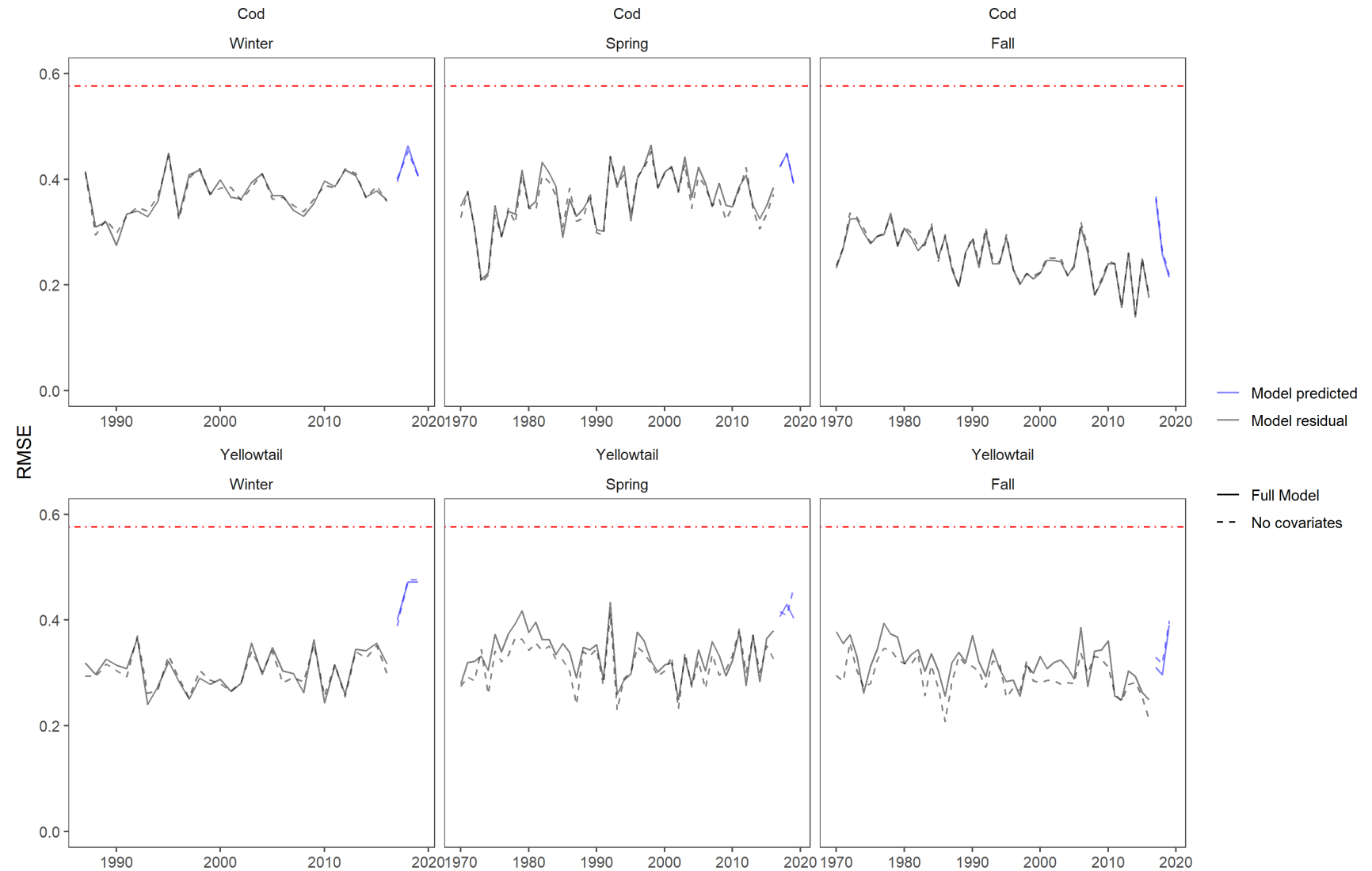


Figure 11: The residual Root Mean Squared Error for the model is shown in black, while the blue lines represent the prediction RMSE for data in years 2017, 2018, and 2019. The models compared were a model with no covariates (intercept + random field) represented with a dashed line and a model which includes the additive SST and Depth covariates along with the random field represented with the solid line. The cod results are in the top row and use a 5 year random field. The yellowtail results are in the bottom row and use a 3 year random field for the Winter and Spring and the 5 year random field for the Fall. The red dot-dash line represents the RMSE for randomly generated data and represents the RMSE for a model with no predictive ability.

## SUPPLEMENT 1

### Model Selection

Stage 1 of model selection resulted in a significant reduction in the number of covariates. For Atlantic Cod, sea surface temperature (*SST*) was identified as a significant covariate in the Winter and Spring, in addition depth (*Dep*) and stratification were also significant predictors in the Spring. In the Fall no covariates had a WAIC that were a significant improvement from the intercept only model (Figure S1). Further model selection indicated that an additive *Dep + SST* model was the preferred model in all 3 seasons for Atlantic Cod (Figures S2 and S3). When exploring the effect of temporal variability on the random fields, the models using the 5-year random field had the lowest WAIC in all seasons (Figure S4).

For Yellowtail Flounder, stage 1 of model selection indicated that the inclusion of *Dep* significantly improved the models in all 3 seasons (surveys), while Sediment type (*Sed*) and chlorophyll concentration (*Chl*) in the Fall had a similar impact on the model WAIC as *Dep*. As a result *SST*, *Dep*, *Chl*, and *Sed* were used to explore the development of more complex covariate models. For Yellowtail Flounder the best models in stage 2 of model selection included 2 covariates with a combination of *Dep*, *SST*, and *Sed* (Figure S2). Further model selection indicated that the preferred model for Yellowtail Flounder in all 3 seasons was an additive model including *Dep*, *SST*, and *Sed* (Figure S3). When exploring the effect of temporal variability on the random fields, the 3-year field had the lowest WAIC in the Winter and Spring, while the 5-year field had the lowest WAIC in the Fall (Figure S4). Additional model selection results are available in the Model Output and Model Diagnostics sections of the interactive dashboard ([https://github.com/Dave-Keith/Paper\\_2\\_SDMS/tree/master/Dashboard](https://github.com/Dave-Keith/Paper_2_SDMS/tree/master/Dashboard)).

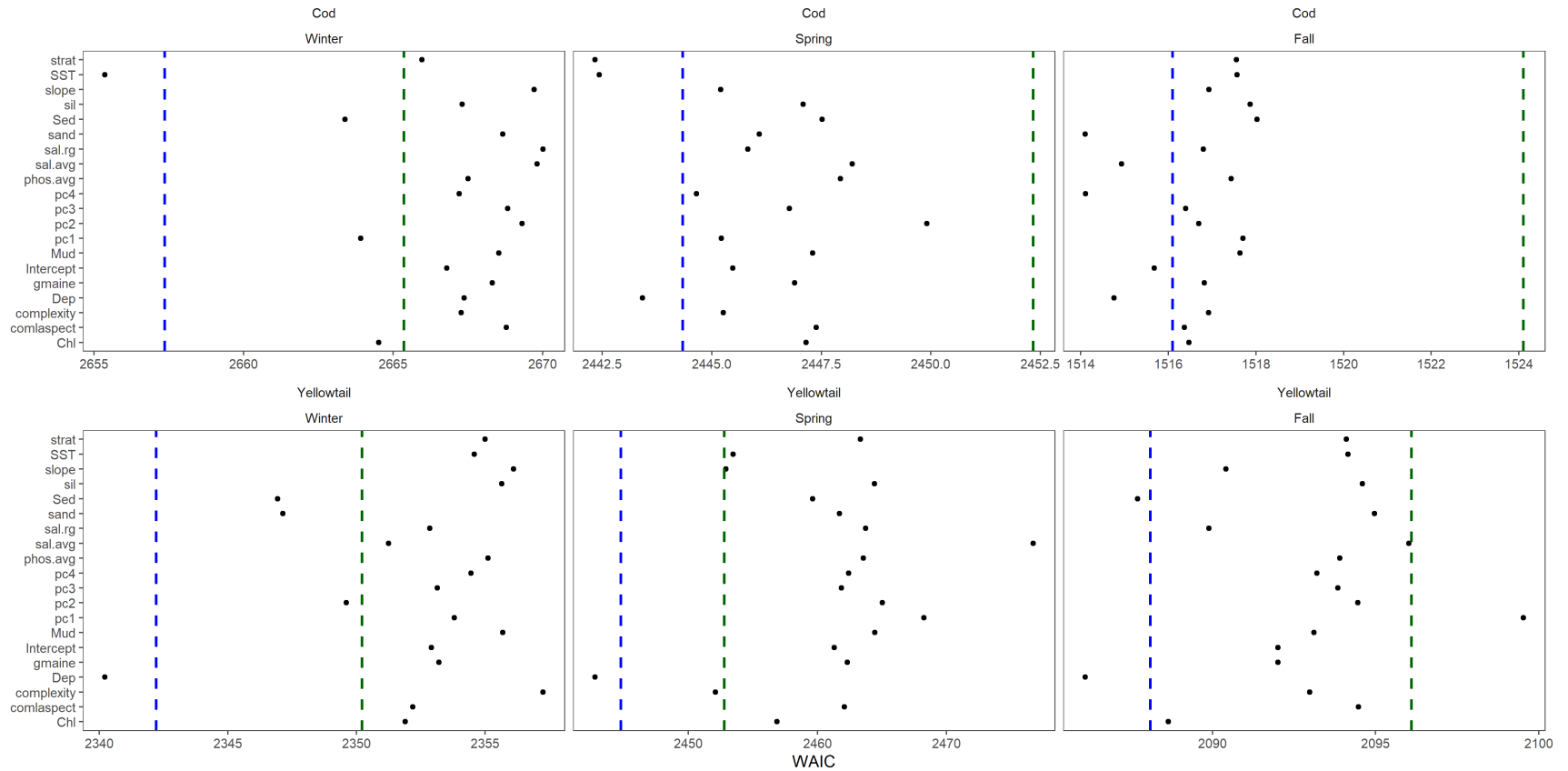


Figure S1: Initial stage of forward model selection using each of the environmental covariates individually. This model selection was done using a static random field. Blue dashed line represents 2 WAIC units larger than the preferred model, the red dashed line is 10 WAIC units larger than the preferred model WAIC.

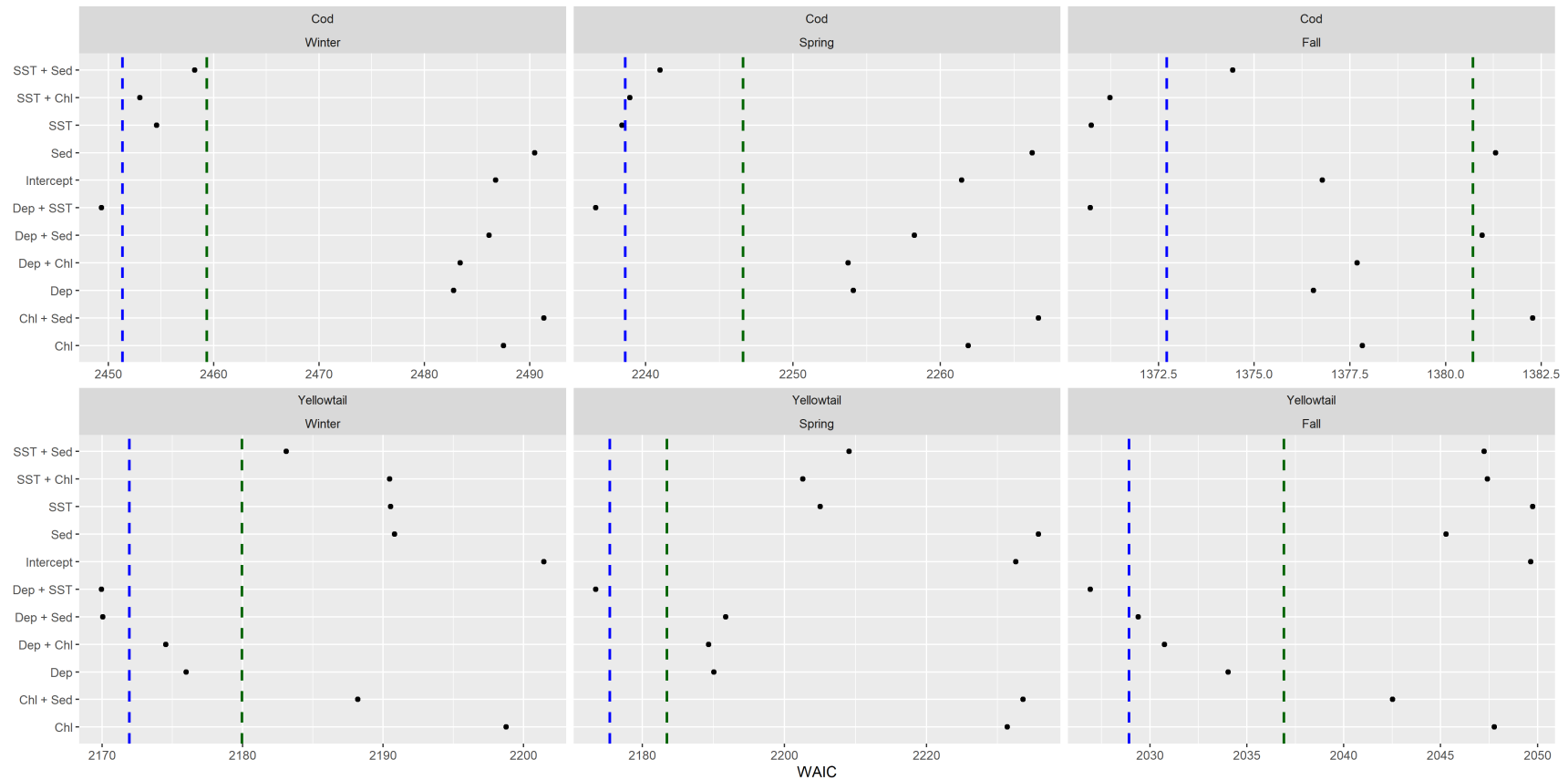


Figure S2: Stage 2 of model selection including additive models with 2 covariates based on the covariates identified in the initial model selection stage. These models were compared using the 10-year random field models. Blue dashed line represents 2 WAIC units larger than the preferred model, the red dashed line is 10 WAIC units larger than the preferred model WAIC.

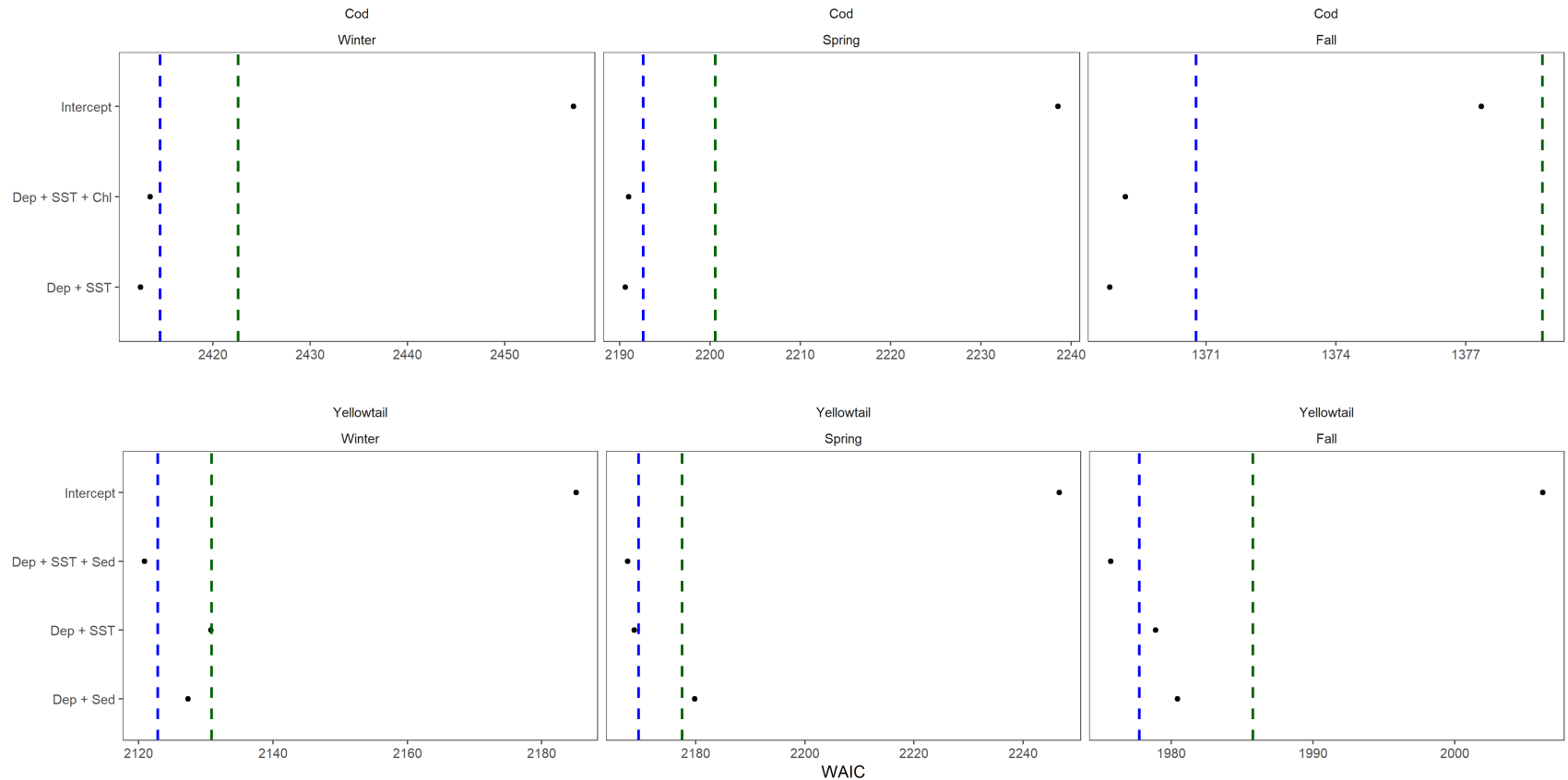


Figure S3: Final stage of covariate model selection which includes model with up to 3 covariate terms based on models selected at stage 2. Blue dashed line represents 2 WAIC units larger than the preferred model, the red dashed line is 10 WAIC units larger than the preferred model WAIC.

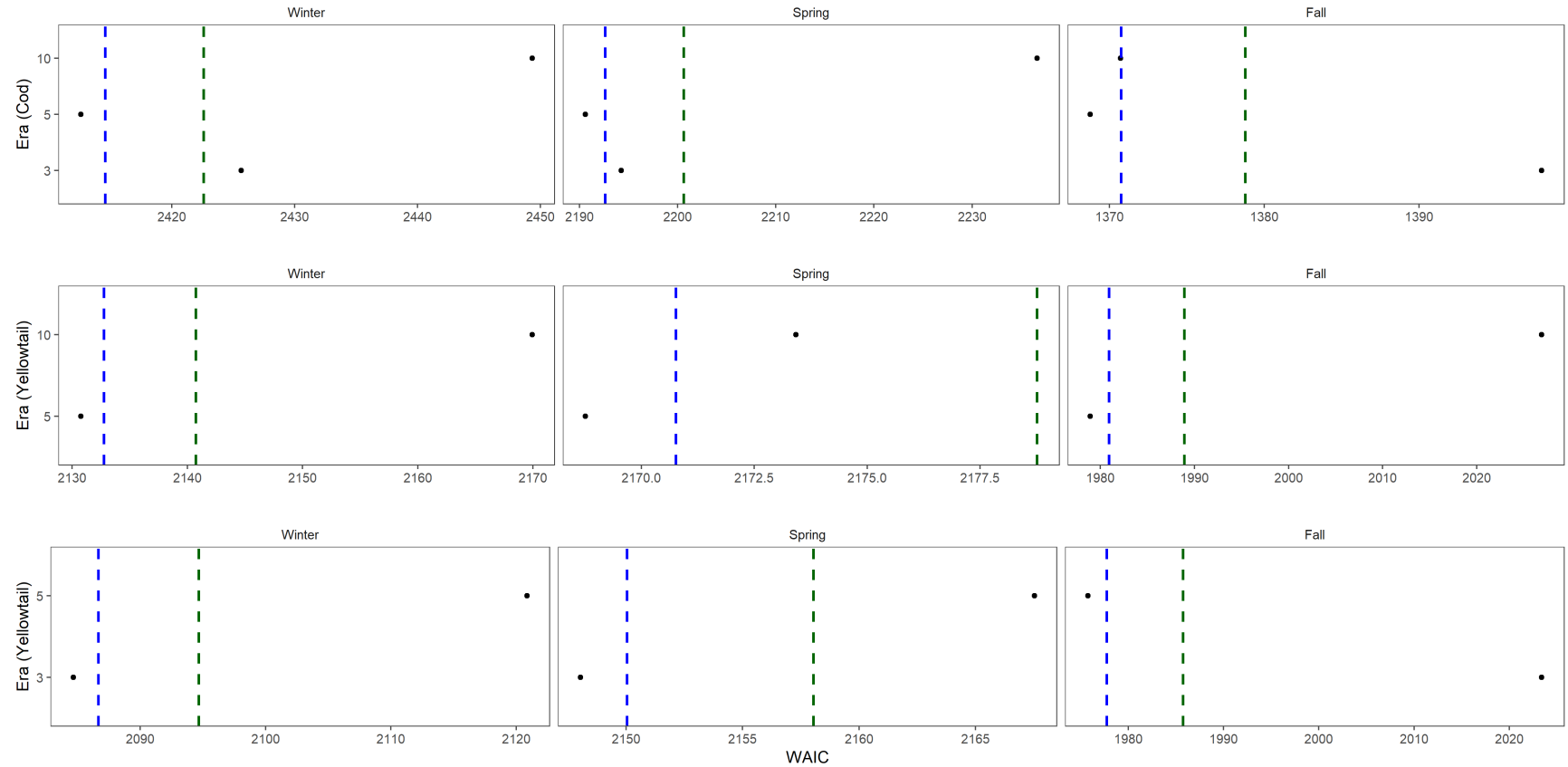


Figure S4: Model selection comparing the random fields models. For cod the model used is Dep + SST for all of the random fields. For Yellowtail the 5 and 10 year random fields were compared using the Dep + SST model, while the 5 and 3 fields were compared using the slightly preferred Dep + SST + Sed model. Blue dashed line represents 2 WAIC units larger than the preferred model, the red dashed line is 10 WAIC units larger than the preferred model WAIC.

## Predicted Occurance Probability

The modelled OP for Atlantic Cod in the Winter and Spring was elevated on all but the most southern portion of GB in the 1970s and 1980s, in the early 1990s there was an abrupt decline in the OP throughout much of the U.S. portion of GB, while OP remained elevated in Canadian waters and in the area straddling the ICJ line (Figures S7 - S8). In the Fall the core areas were isolated to the north of GB. An area on the northwest of GB had some core area until the early 1980s but the OP in this area declined steadily after this time and has had a low OP in the Fall for over 20 years, the highest OP areas remaining during the Fall are along the northern edge of the bank and mostly in Canadian waters (Figure S9).

The modelled OP patterns for Yellowtail Flounder on GB are similar in Winter, Spring, and Fall with core area consistently observed in the region straddling the ICJ line in each season and throughout the study period (Figures S10 - S12). A second region along the western border of the bank also has an elevated OP and appears to be connected via a narrow band of varying width to the core area straddling the ICJ line. The core area of Yellowtail Flounder declined in the late 1980s and early 1990s and was relatively stable until 2016 (Figure S12).

The SD of the Atlantic Cod prediction field in the Winter and Spring tended to be elevated in the central portion of the bank, and lowest in the south and along the edges of the prediction domain. In the Fall the Atlantic Cod prediction field SD was lowest in the south, with the low SD area expanding to central regions later in the study period (Figures S13 - S15). For Yellowtail Flounder, the SD was consistently low in the part of the region with a core area that straddled the ICJ line in the Winter, Spring and Fall (Figures S16 - S18). Areas surrounding this region displayed an increase in the SD, while a region in the north and along the southern flank of GB had relatively low SDs; these regions also had relatively low OPs (Figures S10 - S12 and S16 - S18).

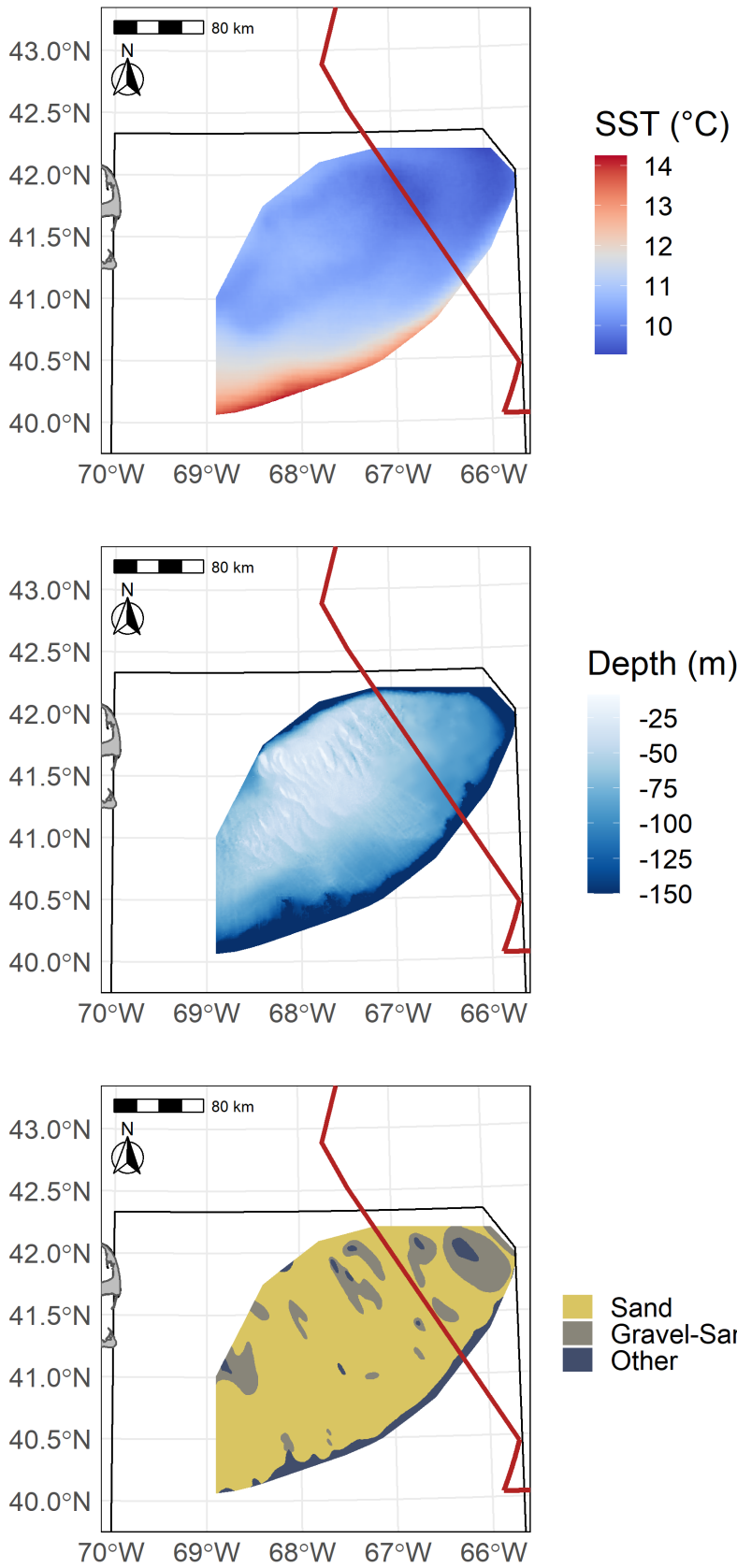
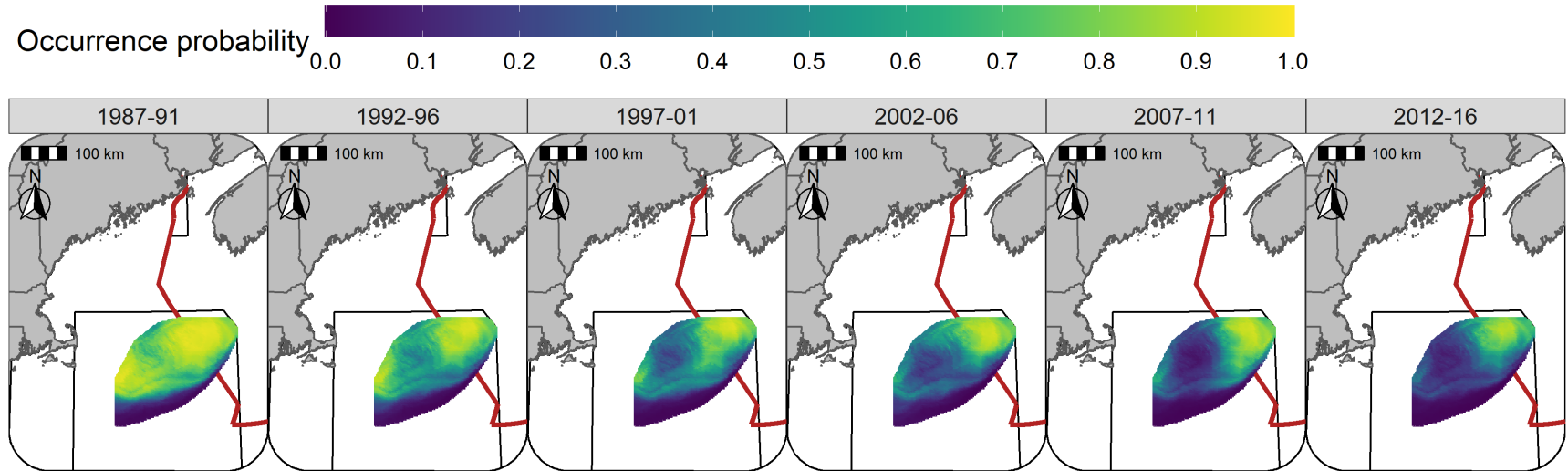


Figure S5: Average Sea Surface Temperature on Georges Bank (GB) from 1997-2008 (SST in °C) in the top panel, GB bathymetry (depth in meters) in the center panel, and GB sediment type in the bottom panel.



Figure S6: Gini Index



88

Figure S7: Predicted occurrence probability for Atlantic Cod in each era during the Winter (RV survey) using the SST + Depth model and 5 year random field.

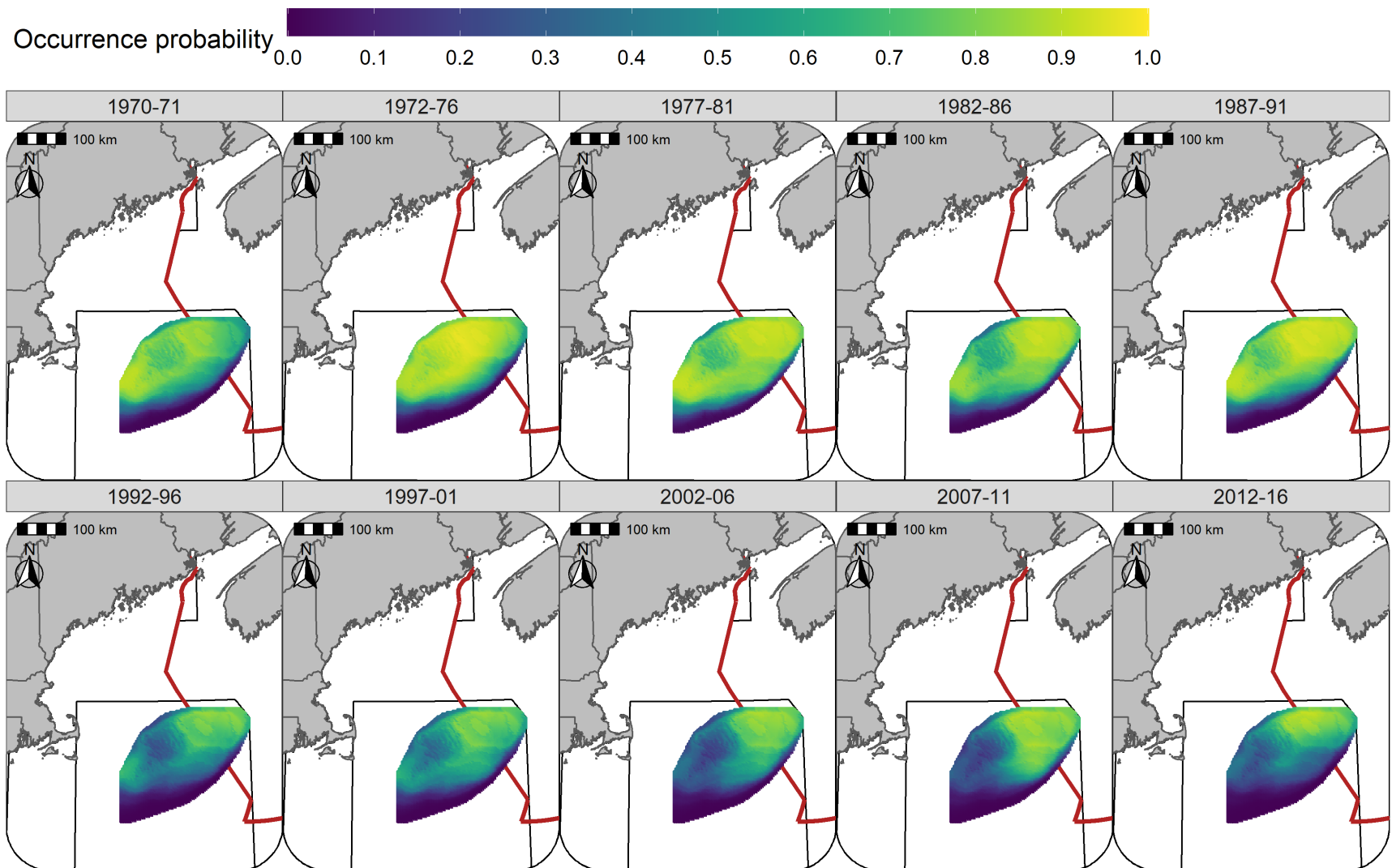


Figure S8: Predicted occurrence probability for Atlantic Cod in each era during the Spring (NMFS-spring survey) using the SST + Depth model and 5 year random field.

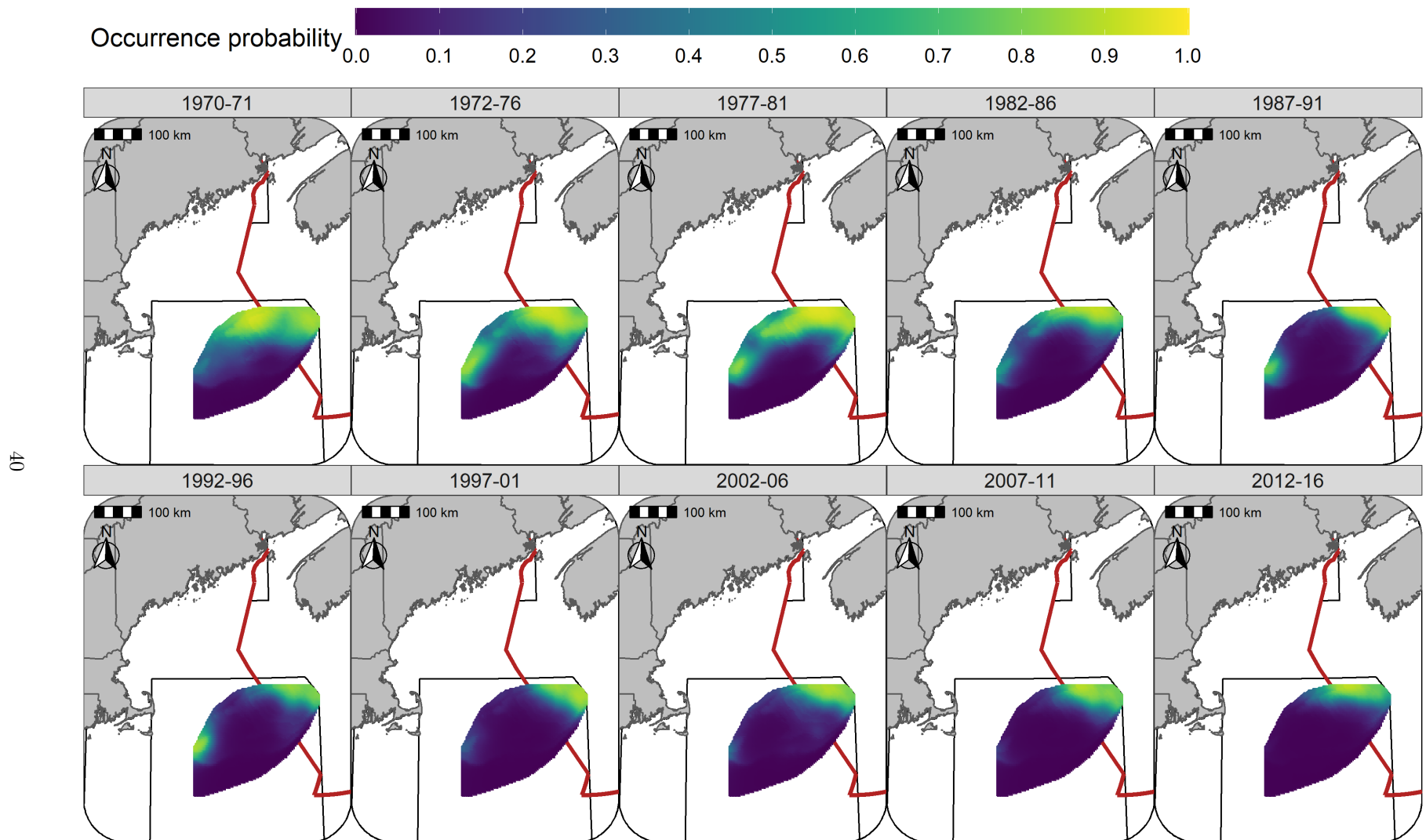


Figure S9: Predicted occurrence probability for Atlantic Cod in each era during the Fall (NMFS-fall survey) using the SST + Depth model and 5 year random field.

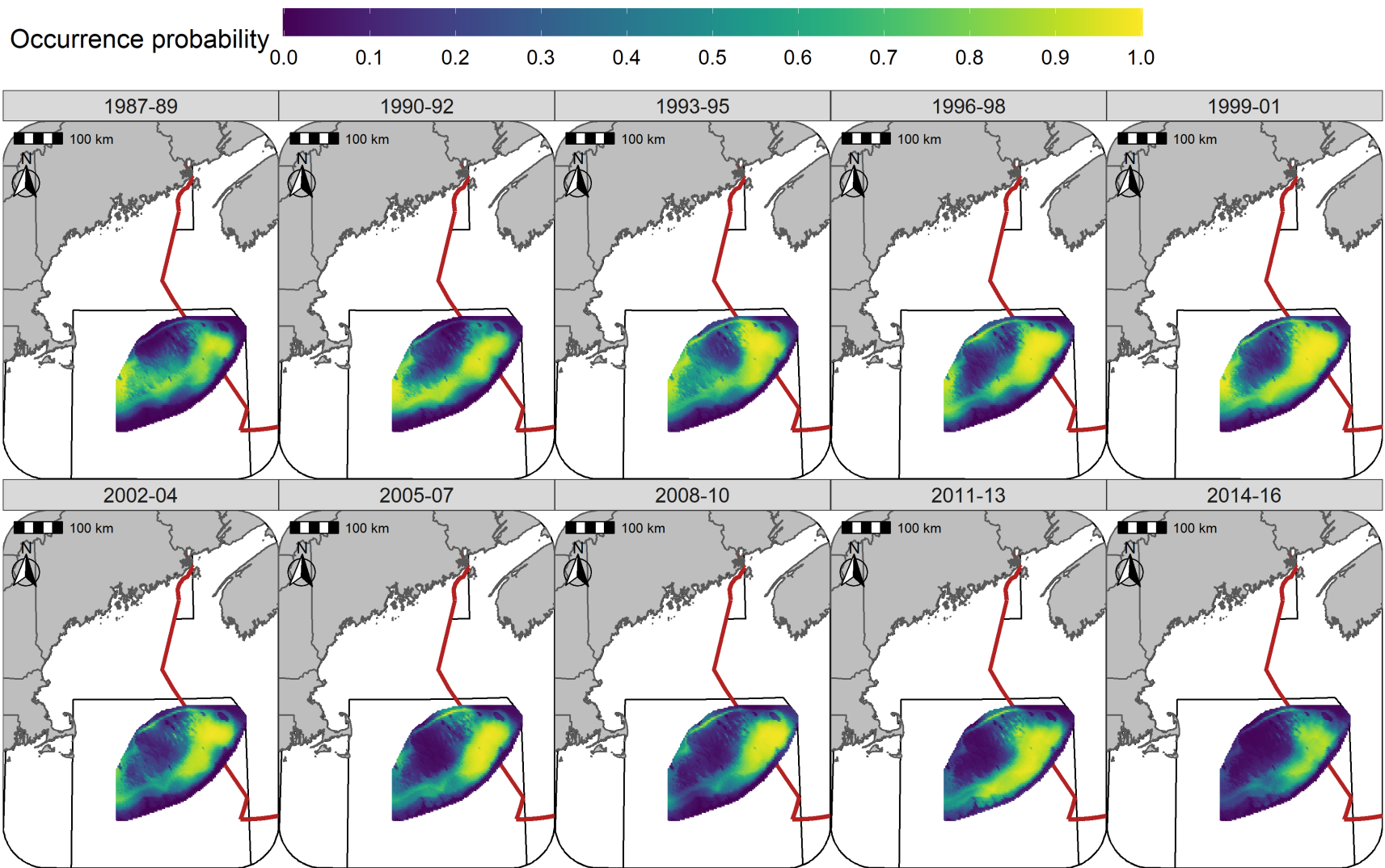


Figure S10: Predicted occurrence probability for Yellowtail Flounder in each era during the Winter (RV survey) using the SST + Depth +Sed model and 3 year random field.

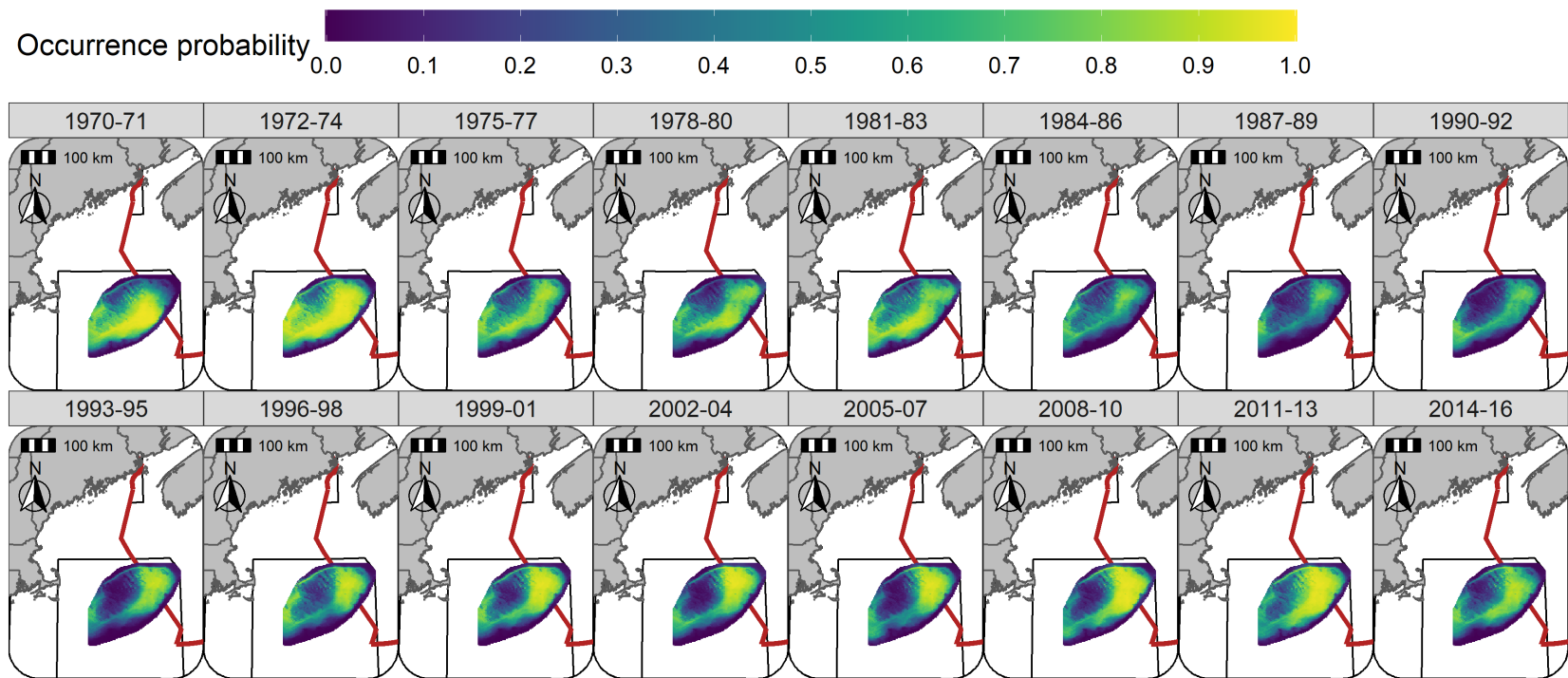


Figure S11: Predicted occurrence probability for Yellowtail Flounder in each era during the Spring (NMFS-spring survey) using the SST + Depth + Sed model and 3 year random field.

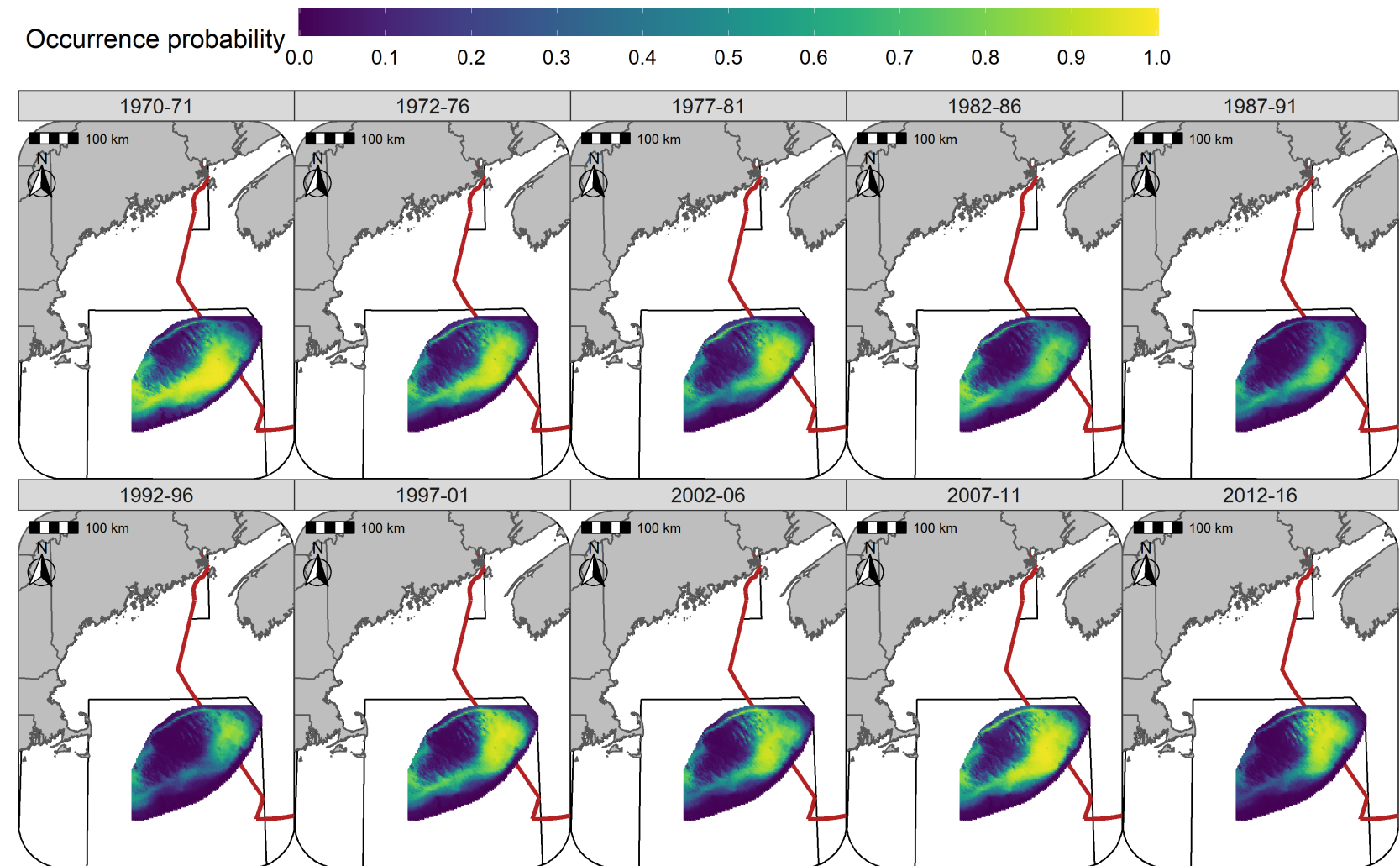


Figure S12: Predicted occurrence probability for Yellowtail Flounder in each era during the Fall (NMFS-fall survey) using the SST + Depth + Sed model and 5 year random field.

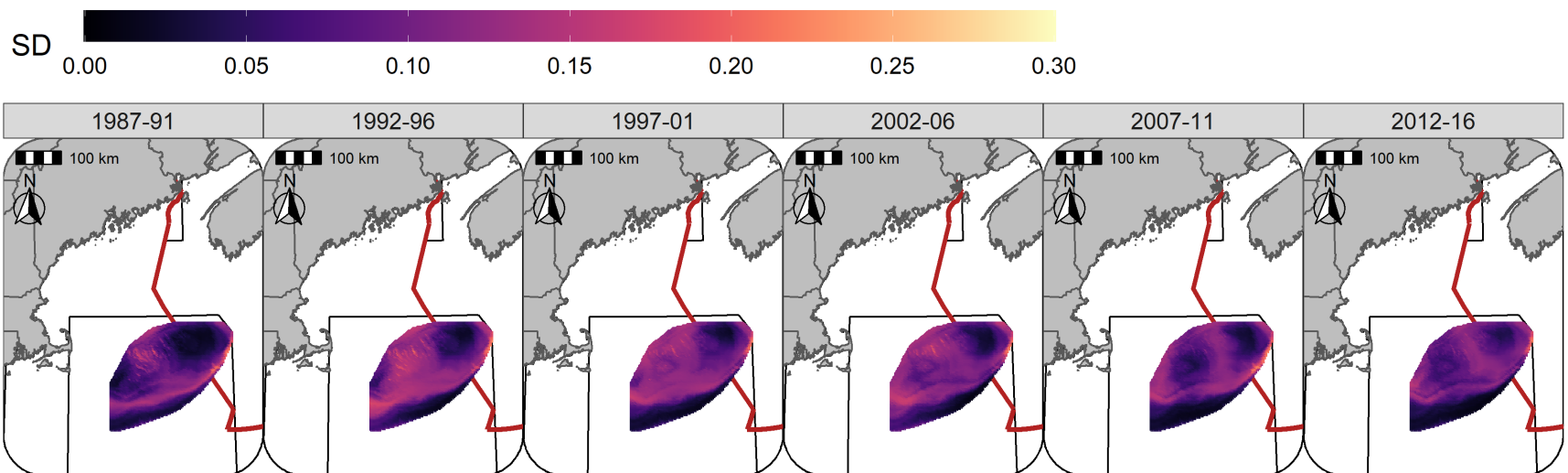


Figure S13: Standard deviation (logit scale) of predicted occurrence probability for Atlantic Cod in each era during the Winter (RV survey) using the SST + Depth model and 5 year random field.

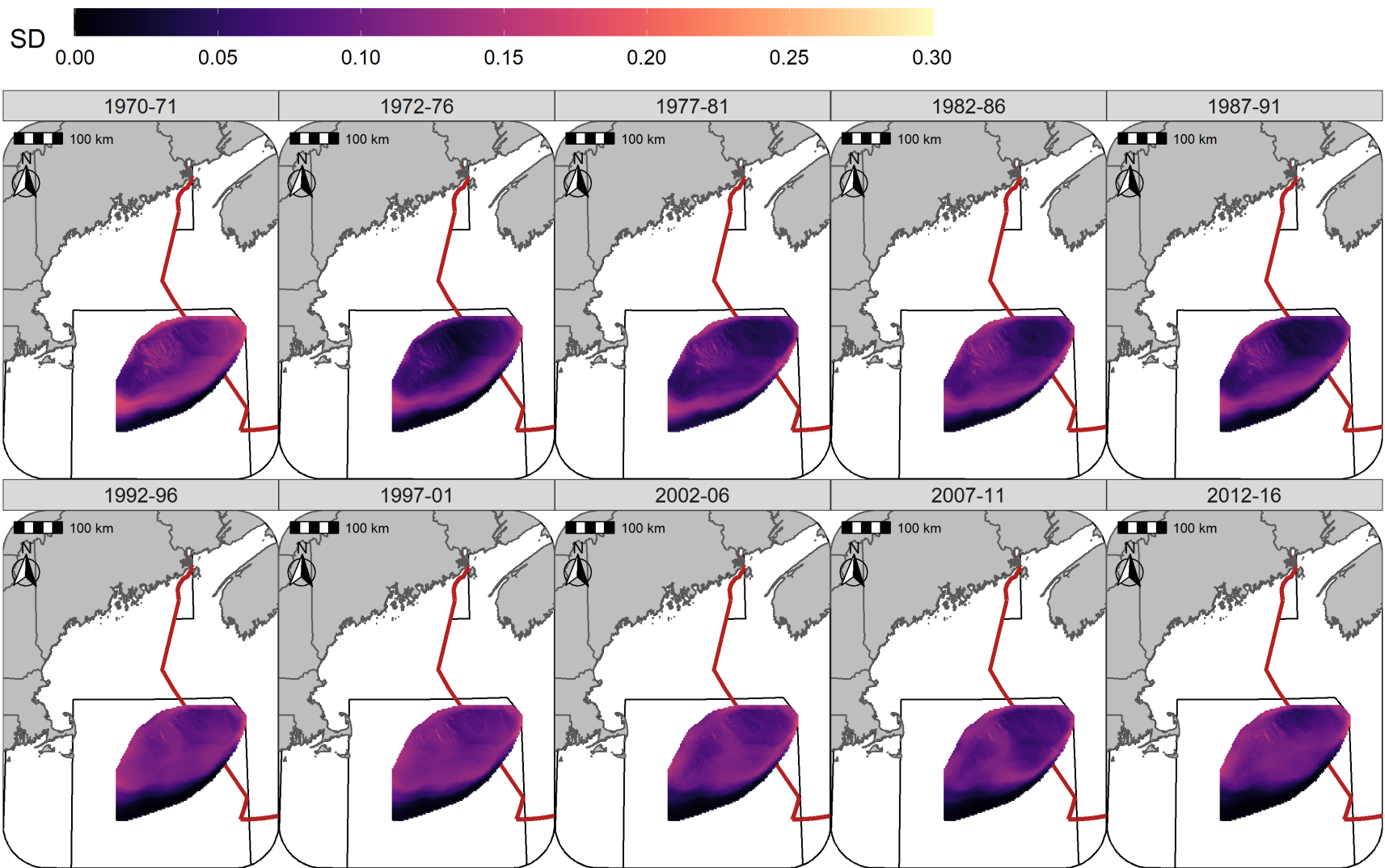


Figure S14: Standard deviation (logit scale) of predicted occurrence probability for Atlantic Cod in each era during the Spring (NMFS-spring survey) using the SST + Depth model and 5 year random field.

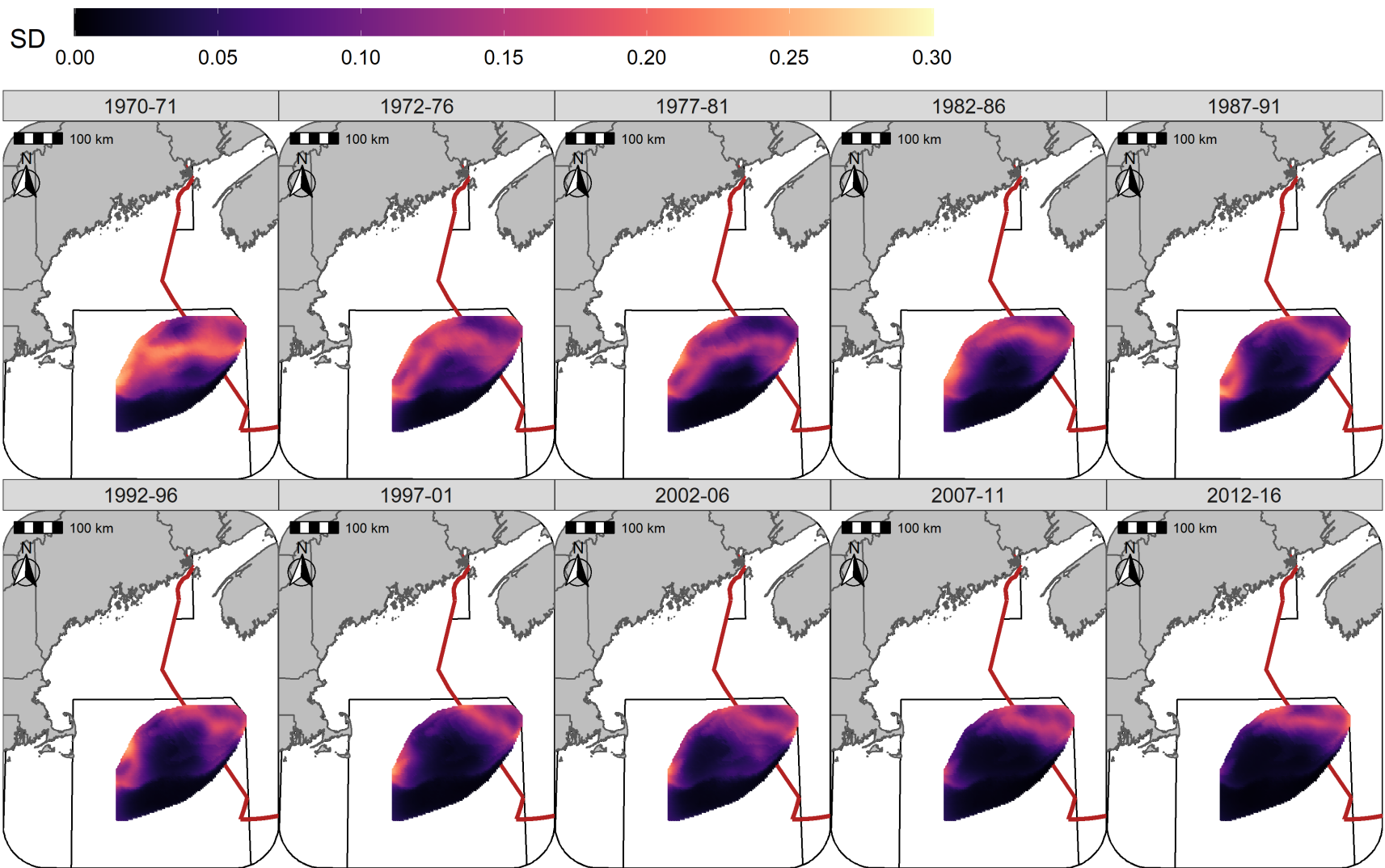


Figure S15: Standard deviation (logit scale) of predicted occurrence probability for Atlantic Cod in each era during the Fall (NMFS-fall survey) using the SST + Depth model and 5 year random field.

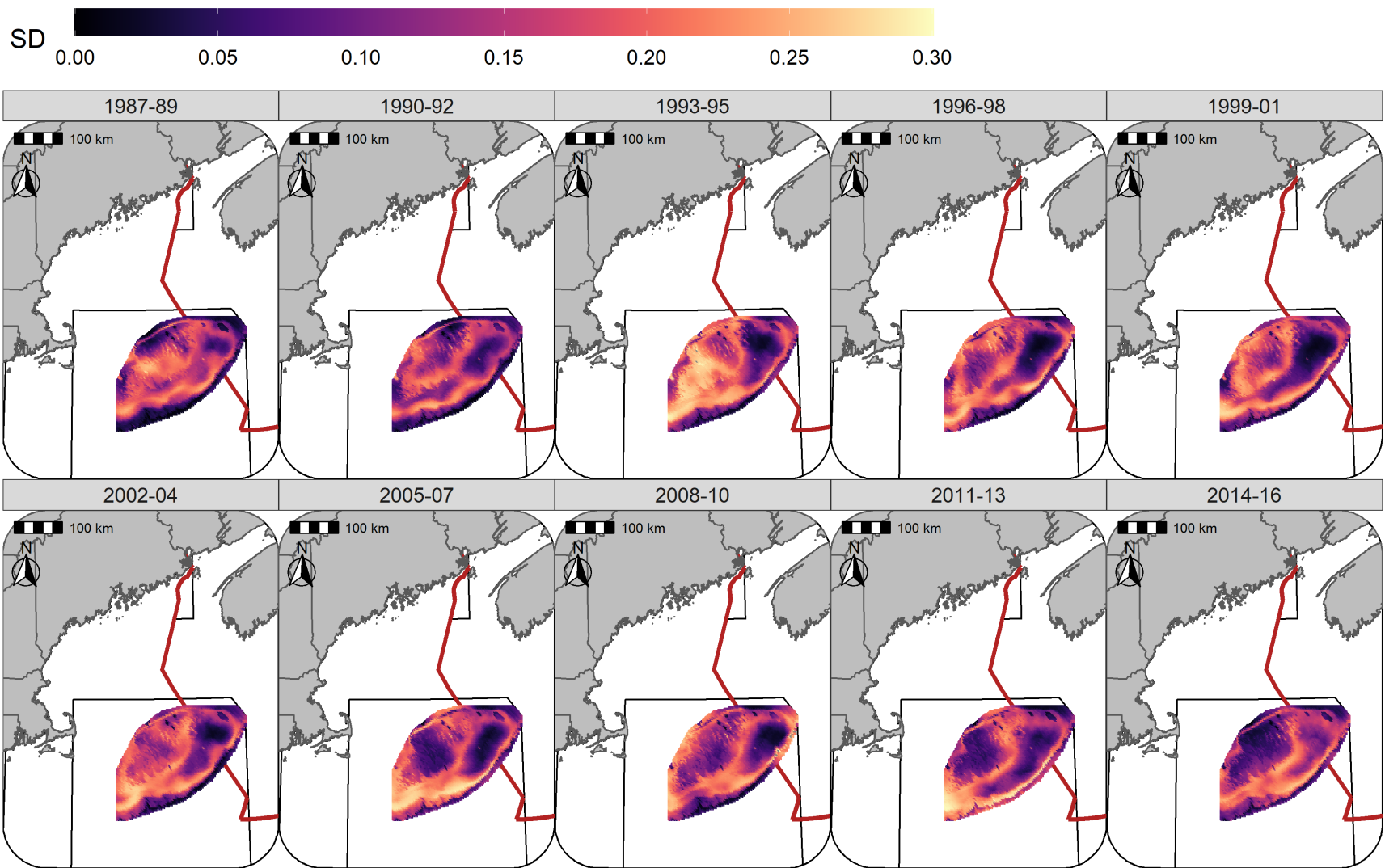


Figure S16: Standard deviation (logit scale) of predicted occurrence probability for Yellowtail Flounder in each era during the Winter (RV survey) using the SST + Depth + Sed model and 3 year random field.

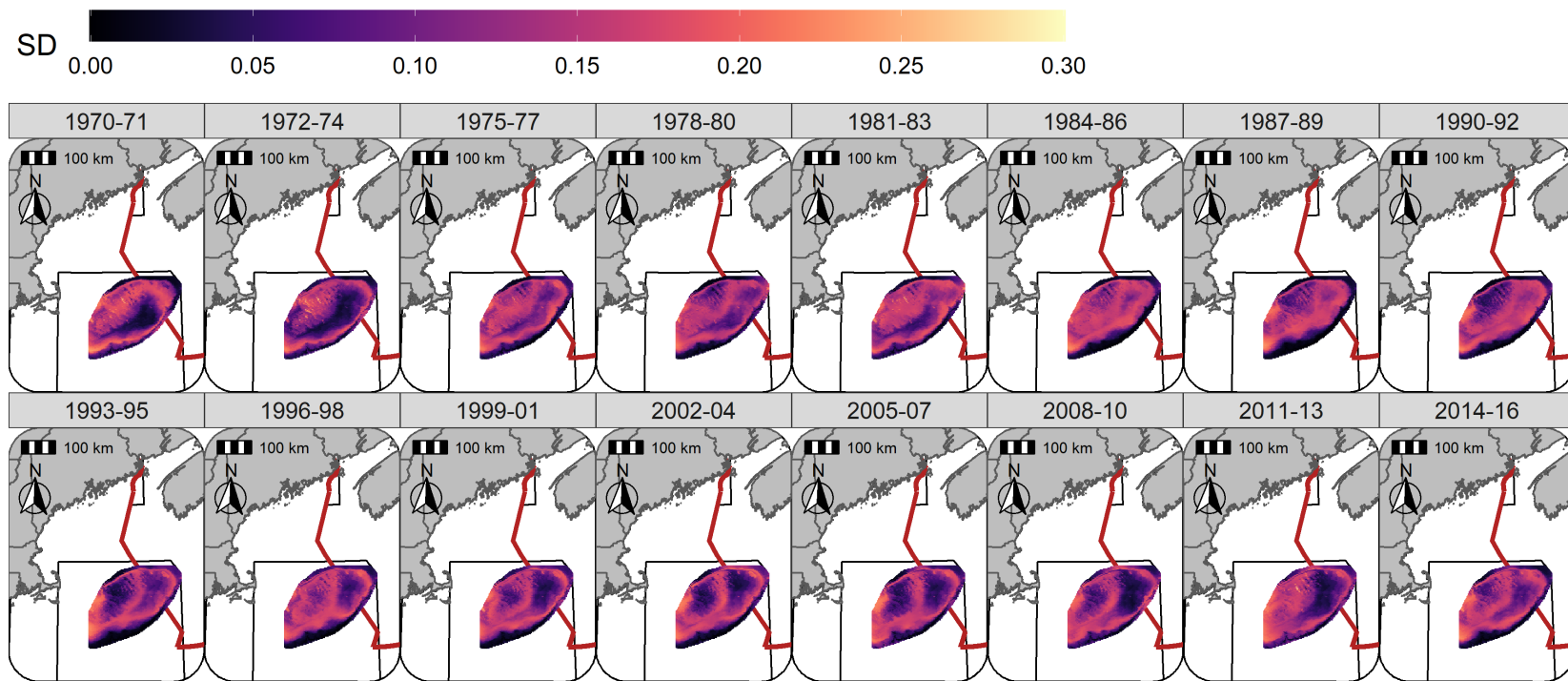


Figure S17: Standard deviation (logit scale) of predicted occurrence probability for Yellowtail Flounder in each era during the Spring (NMFS-spring survey) using the SST + Depth + Sed model and 3 year random field.

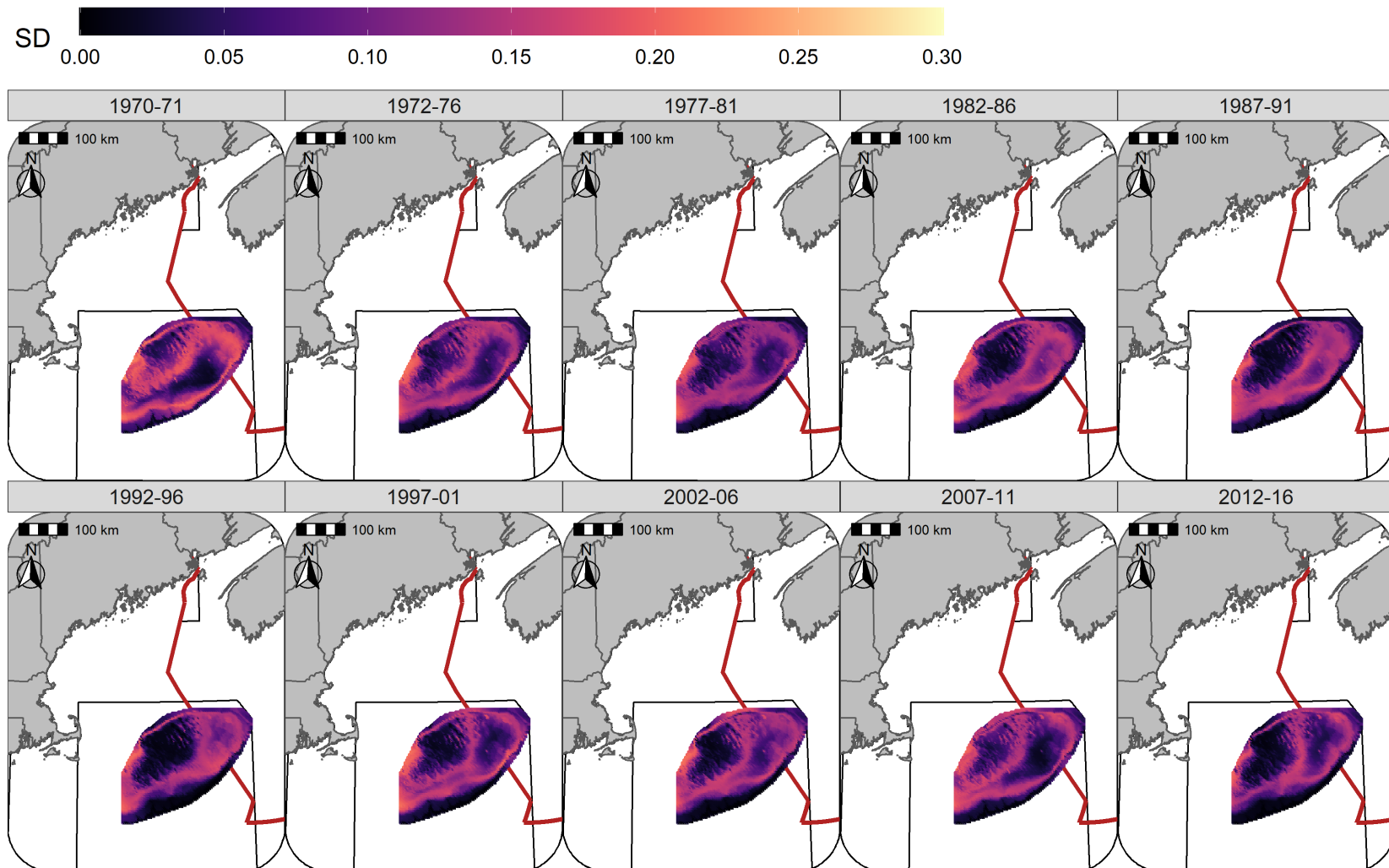


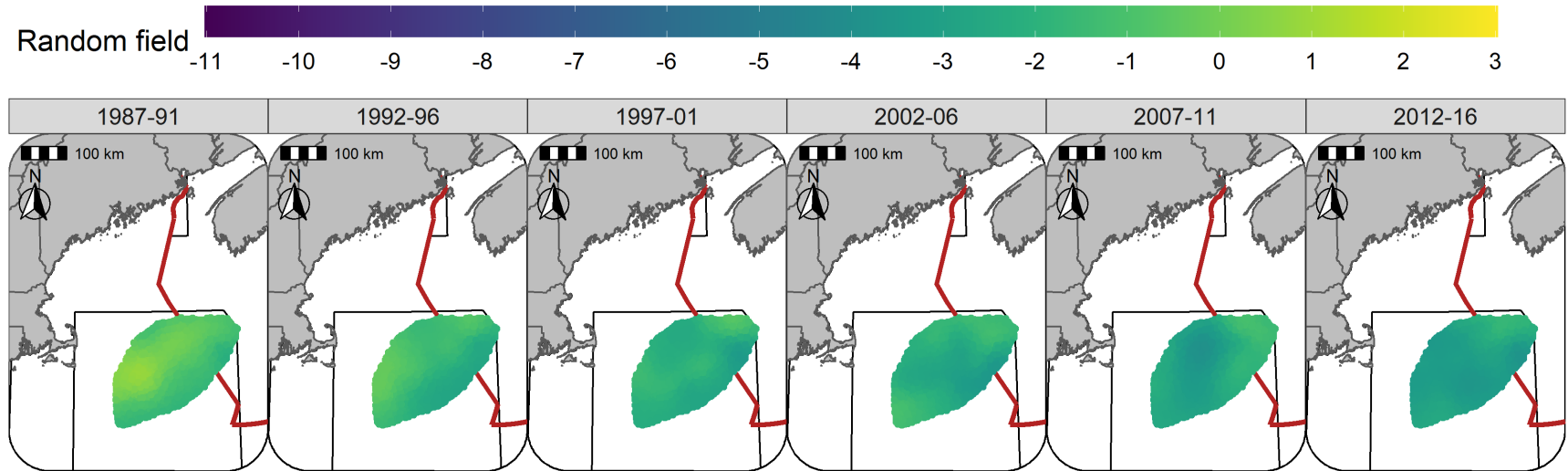
Figure S18: Standard deviation (logit scale) of predicted occurrence probability for Yellowtail Flounder in each era during the Fall (NMFS-fall survey) using the SST + Depth + Sed model and 5 year random field.

## **Random fields**

The 5-year random fields for Atlantic Cod in the Winter and Spring are seasonally consistent through time, with lower effect sizes observed in both seasons starting in 1992 and the largest declines in the effect size observed in the southern and western portions of GB (Figures S19 - S20). In the Fall the higher effect sizes were generally observed towards the north and in Canadian waters, with larger declines in the random field effect size towards the west over the study period (Figure S21).

The Yellowtail Flounder random field patterns were similar in the Winter and Spring while the random field effect sizes were somewhat smaller during the Fall (Figures S22 - S24). The effect size of the random fields, in all seasons, were lower throughout the later half of the 1980s and the early 1990s. The highest effect size of the random fields were observed in the 1970s and in the 2000s. Since the mid-1970s an area straddling the Canadian-U.S. border has been consistently identified as an area where the Yellowtail Flounder effect size of the random field is elevated (Figures S22 - S24).

The standard deviation (SD) of the random fields for Atlantic Cod were also similar between seasons with the lowest SD generally observed in the north and east and highest approaching the southern flank of GB. The SD was somewhat higher in the Fall throughout the central portion of GB (Figures S25 - S27). For Yellowtail Flounder, the SD was higher towards the southern portions of the bank with localized regions having elevated SD scattered throughout the bank in the Winter, Spring and Fall. (Figures S28 - S30).



51

Figure S19: Random fields (logit scale) for Atlantic Cod in each era during the Winter (RV survey) using the SST + Depth model and 5 year random field.

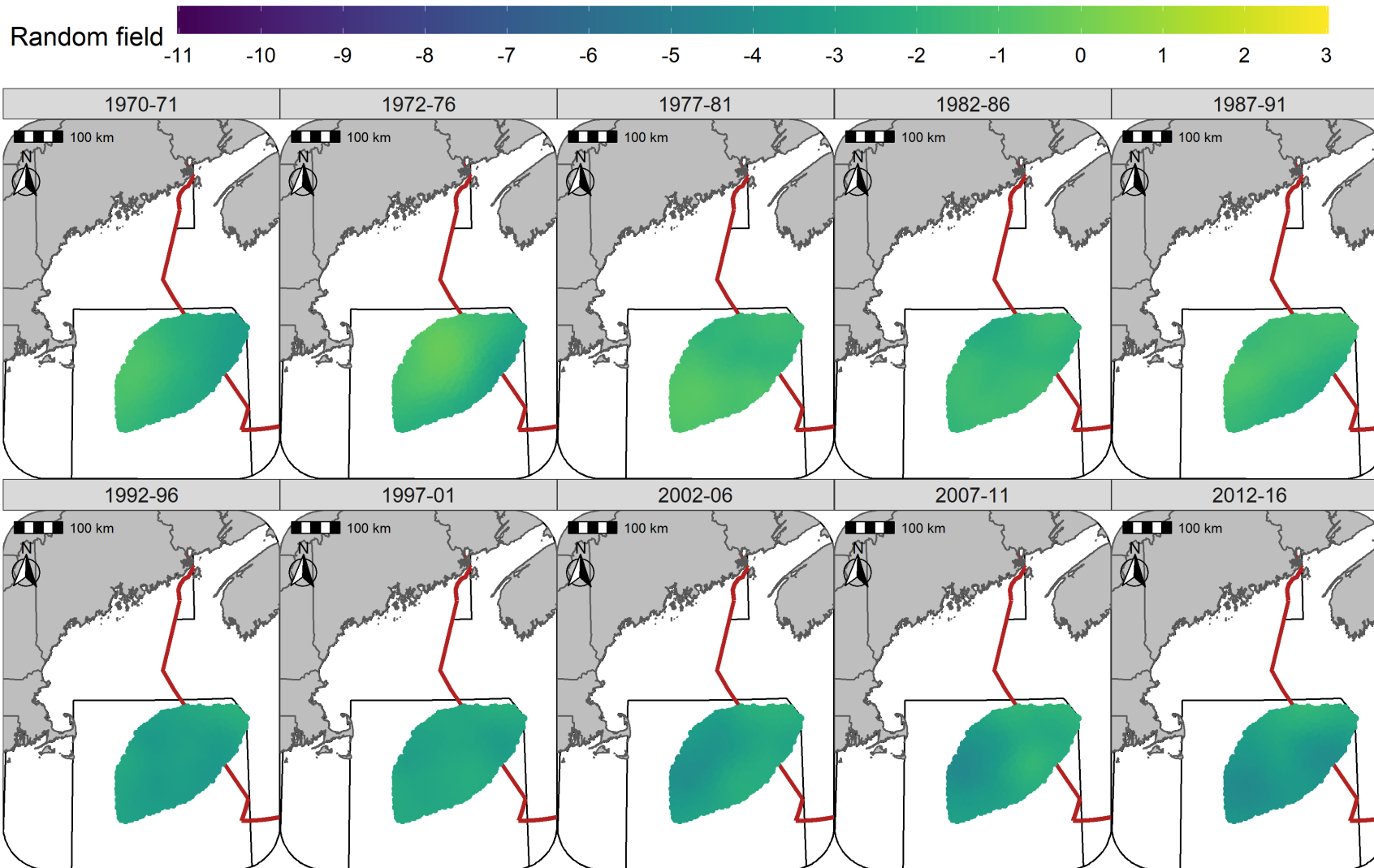


Figure S20: Random fields (logit scale) for Atlantic Cod in each era during the Spring (NMFS-spring survey) using the SST + Depth model and 5 year random field.

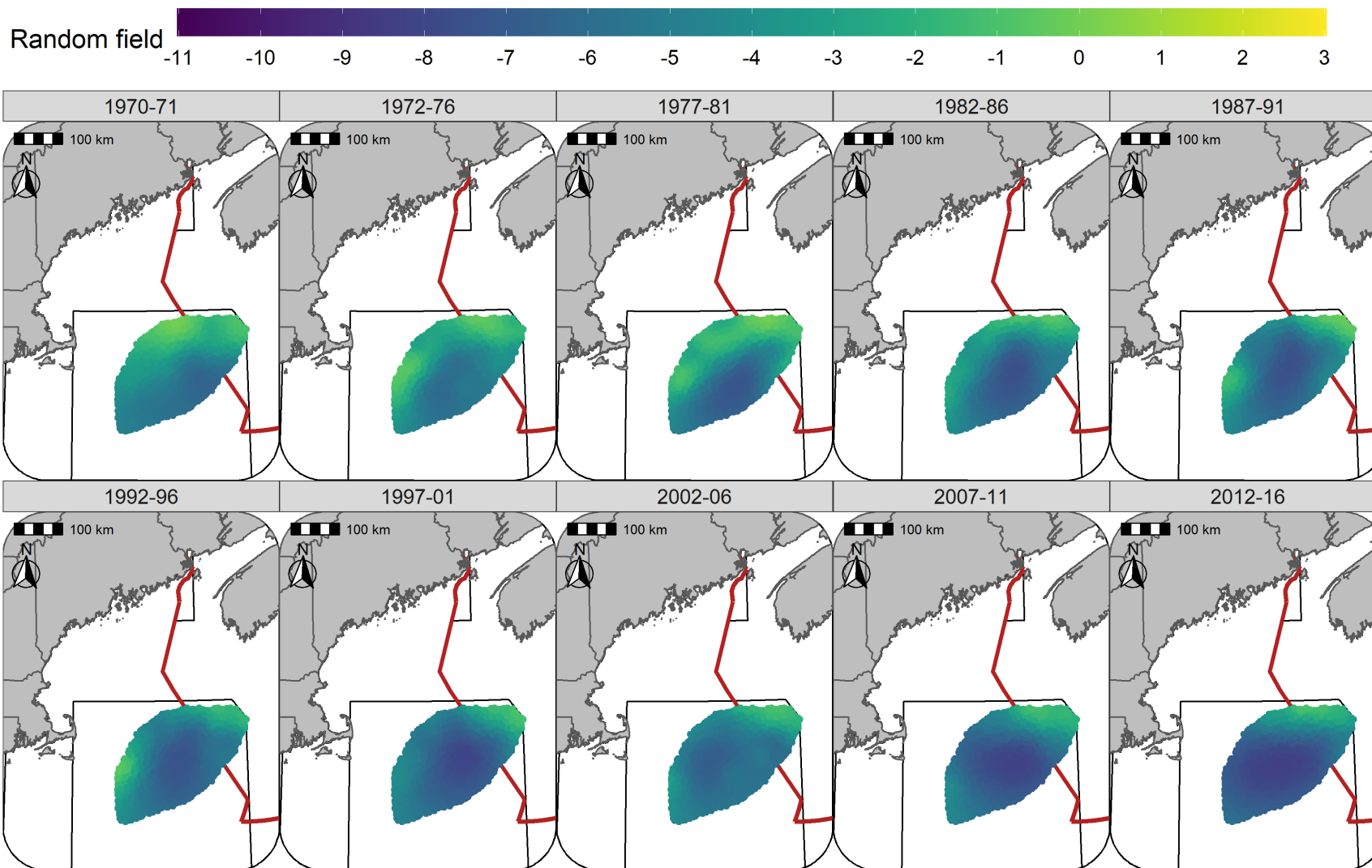


Figure S21: Random fields (logit scale) for Atlantic Cod in each era during the Fall (NMFS-fall survey) using the SST + Depth model and 5 year random field.

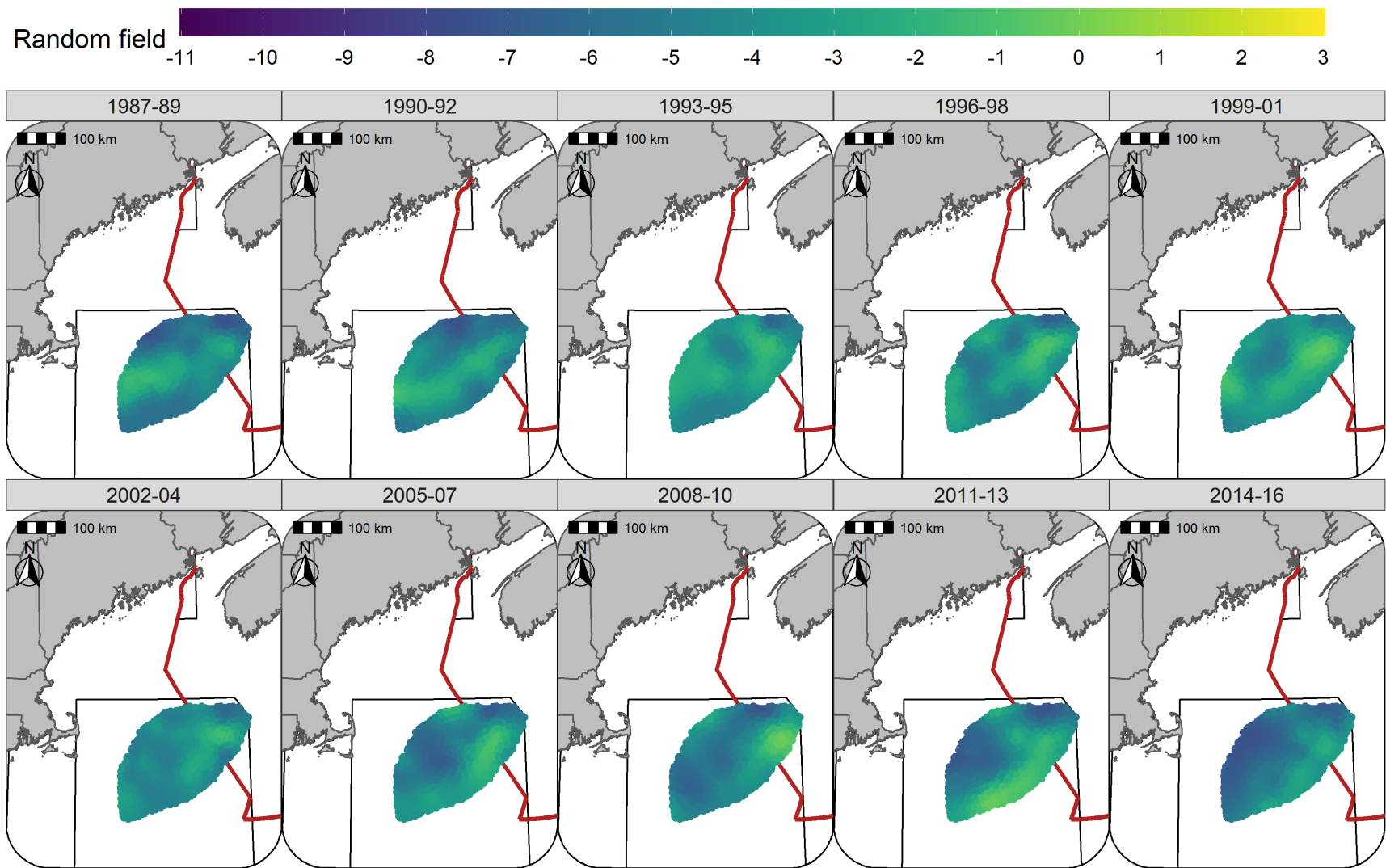


Figure S22: Random fields (logit scale) for Yellowtail Flounder in each era during the Winter (RV survey) using the SST + Depth + Sed model and 3 year random field.

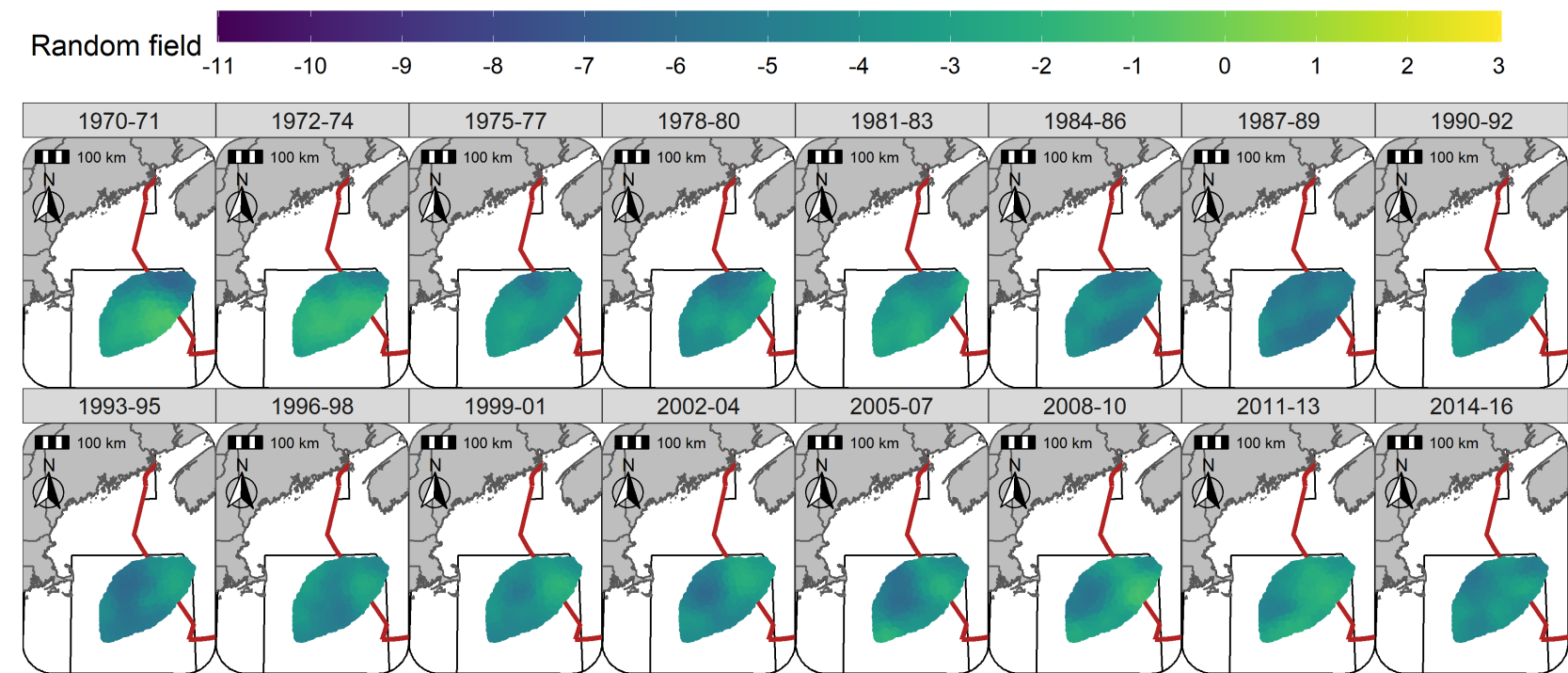


Figure S23: Random fields (logit scale) for Yellowtail Flounder in each era during the Spring (NMFS-spring survey) using the SST + Depth + Sed model and 3 year random field.

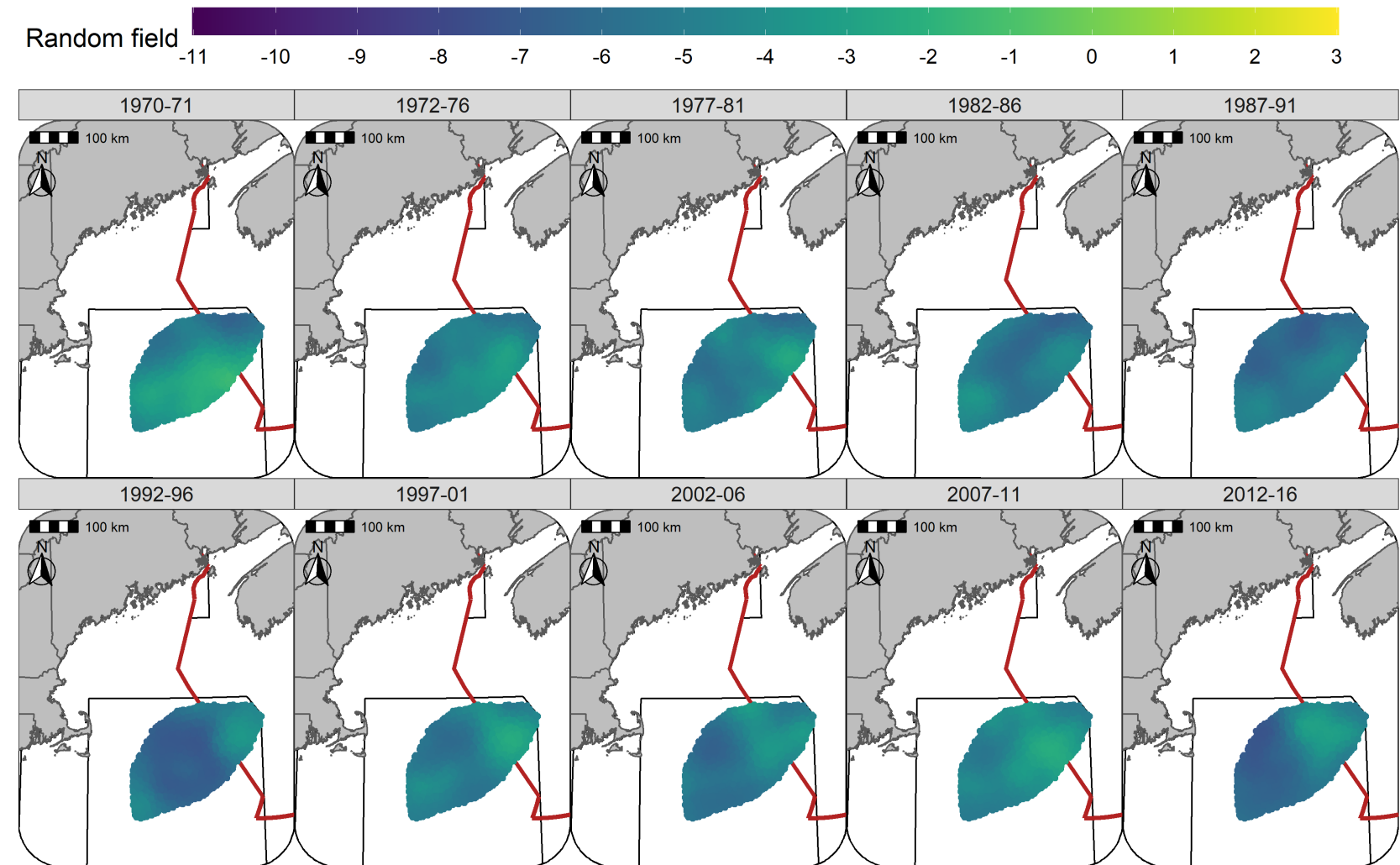


Figure S24: Random fields (logit scale) for Yellowtail Flounder in each era during the Fall (NMFS-fall survey) using the SST + Depth + Sed model and 5 year random field.

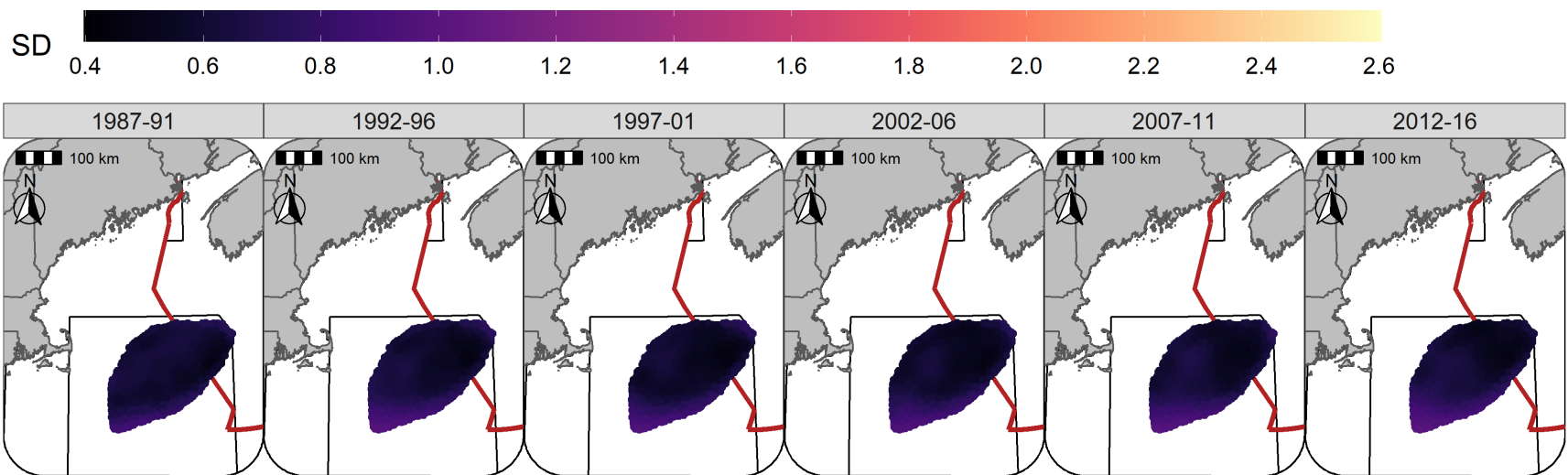


Figure S25: Standard deviation of random fields (logit scale) for Atlantic Cod in each era during the Winter (RV survey) using the SST + Depth model and 5 year random field.

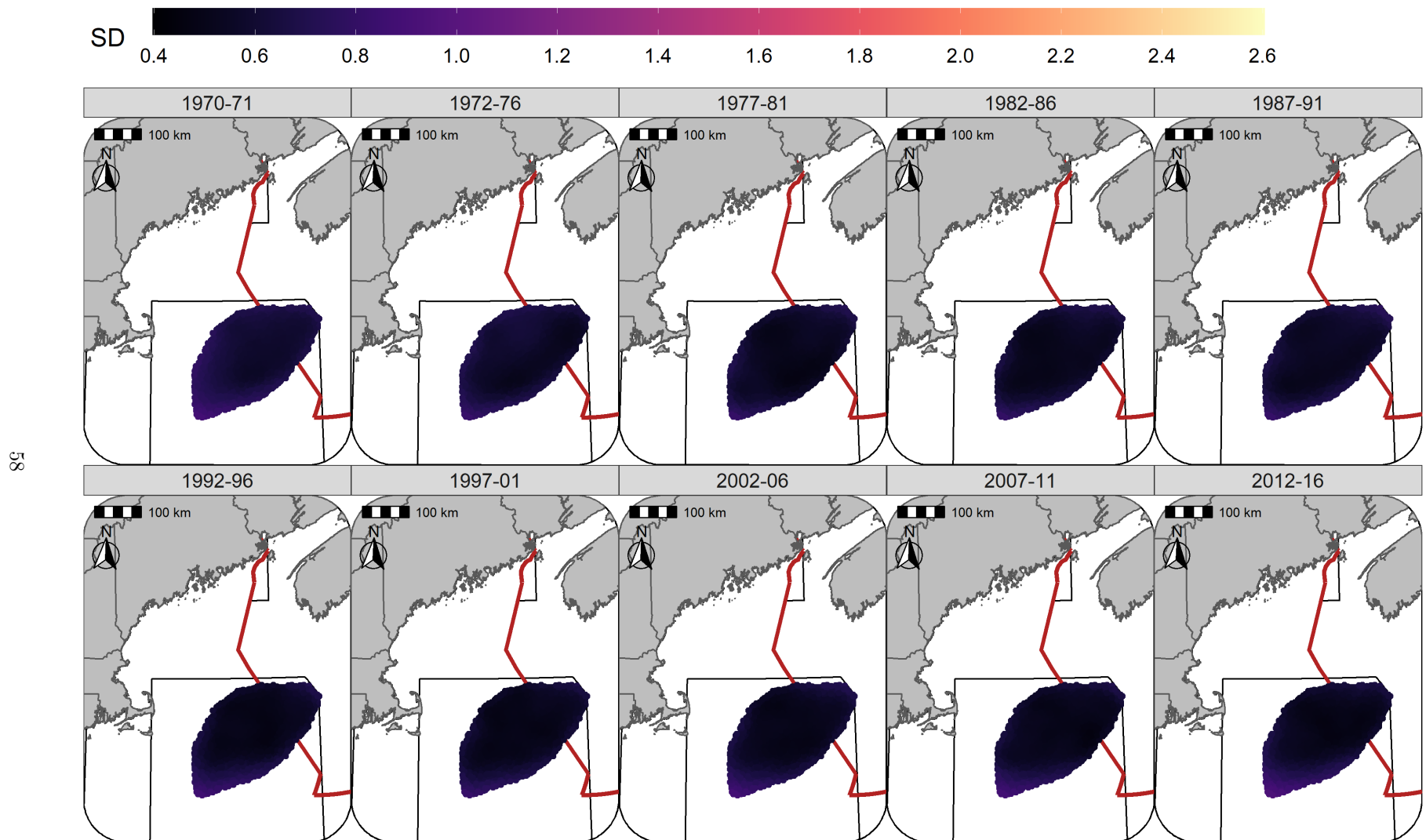


Figure S26: Standard deviation of random fields (logit scale) for Atlantic Cod in each era during the Spring (NMFS-spring survey) using the SST + Depth model and 5 year random field.

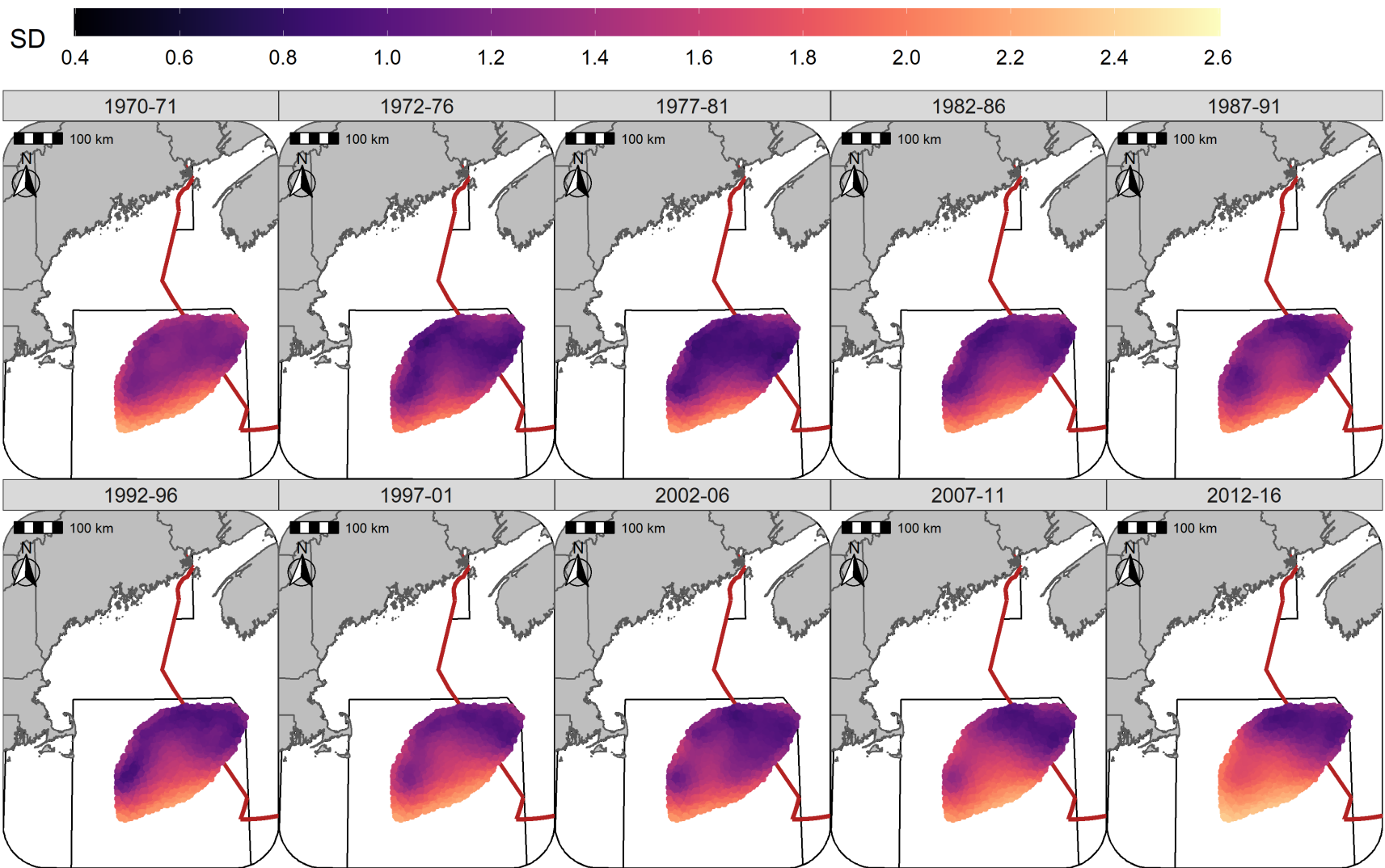


Figure S27: Standard deviation of random fields (logit scale) for Atlantic Cod in each era during the Fall (NMFS-fall survey) using the SST + Depth model and 5 year random field.

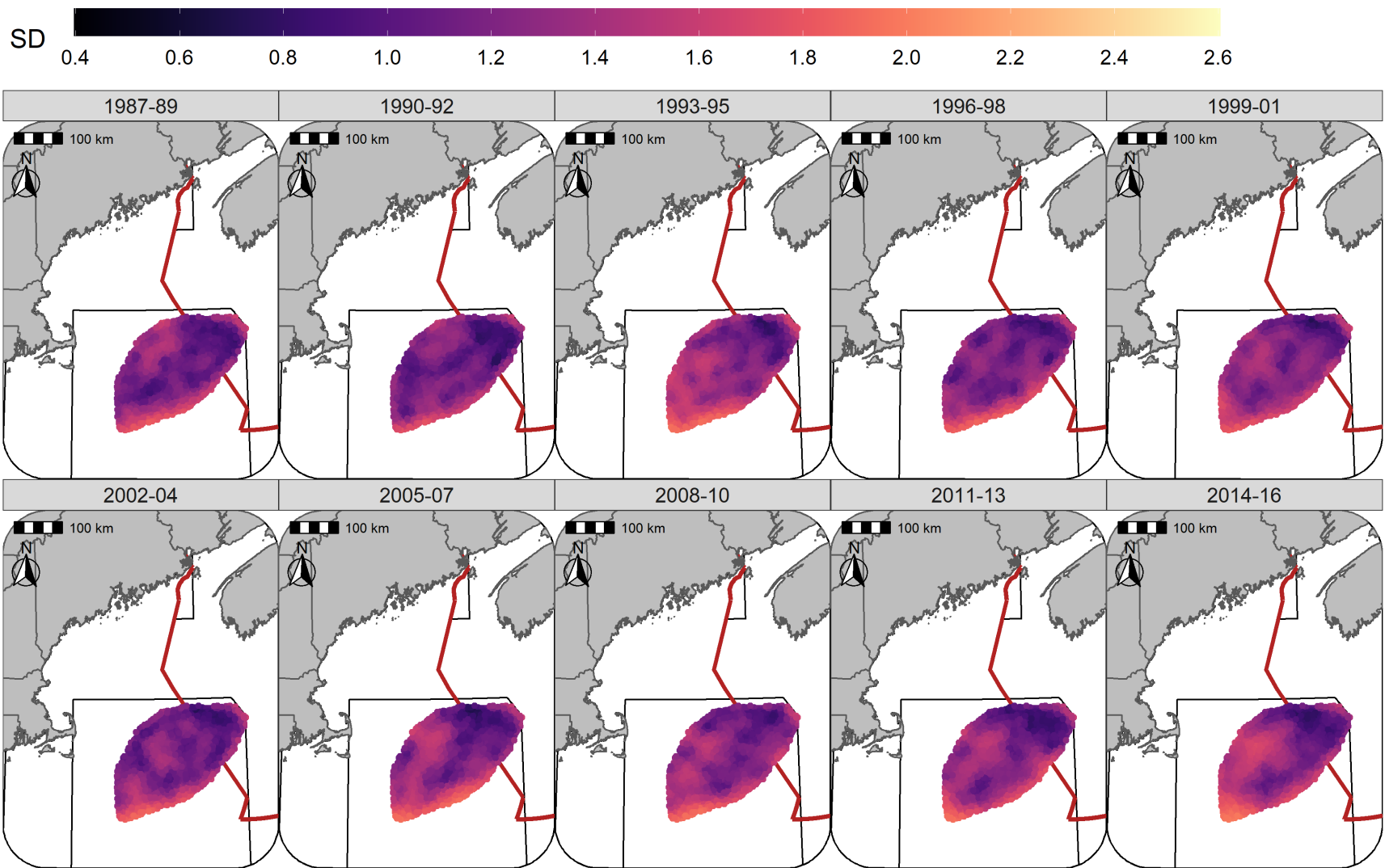


Figure S28: Standard deviation of random fields (logit scale) for Yellowtail Flounder in each era during the Winter (RV survey) using the SST + Depth + Sed model and 3 year random field.

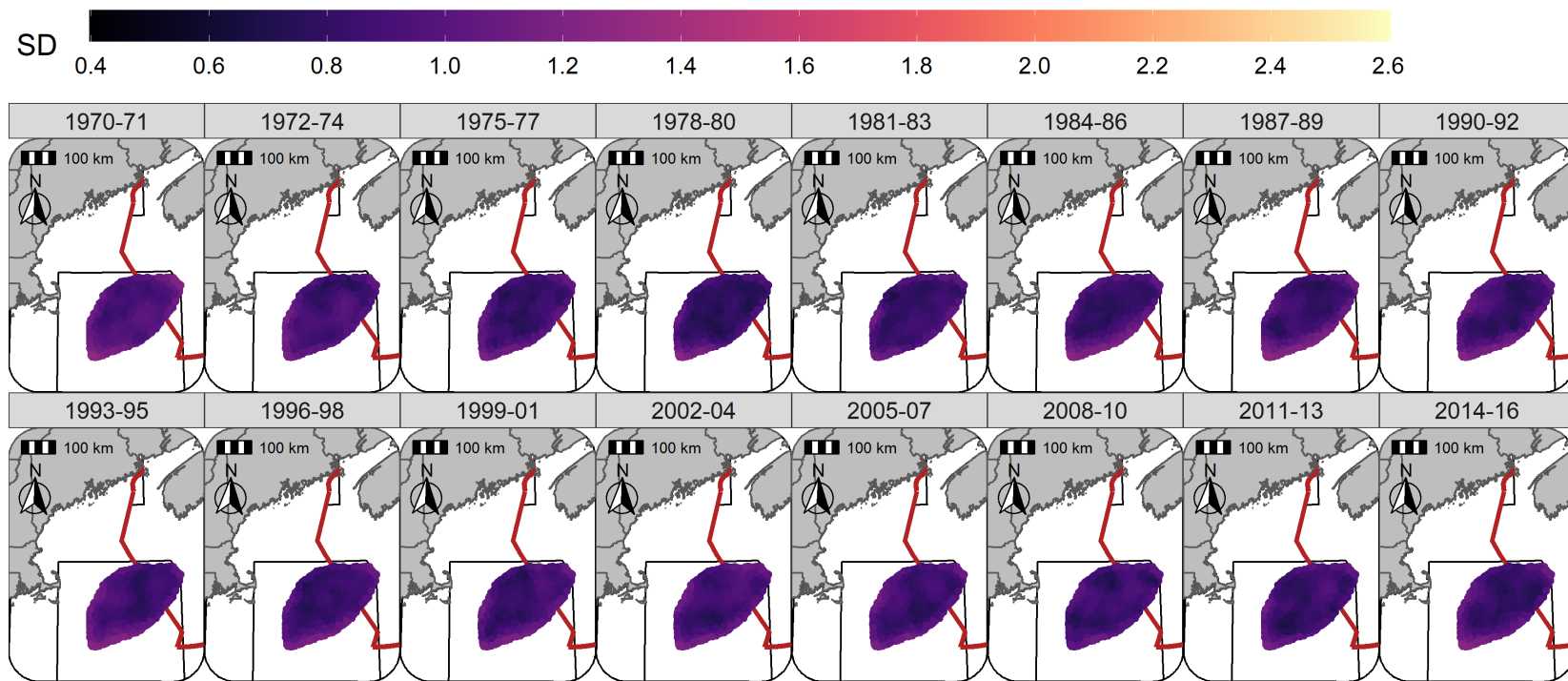


Figure S29: Standard deviation of random fields (logit scale) for Yellowtail Flounder in each era during the Spring (NMFS-spring survey) using the SST + Depth + Sed model and 3 year random field.

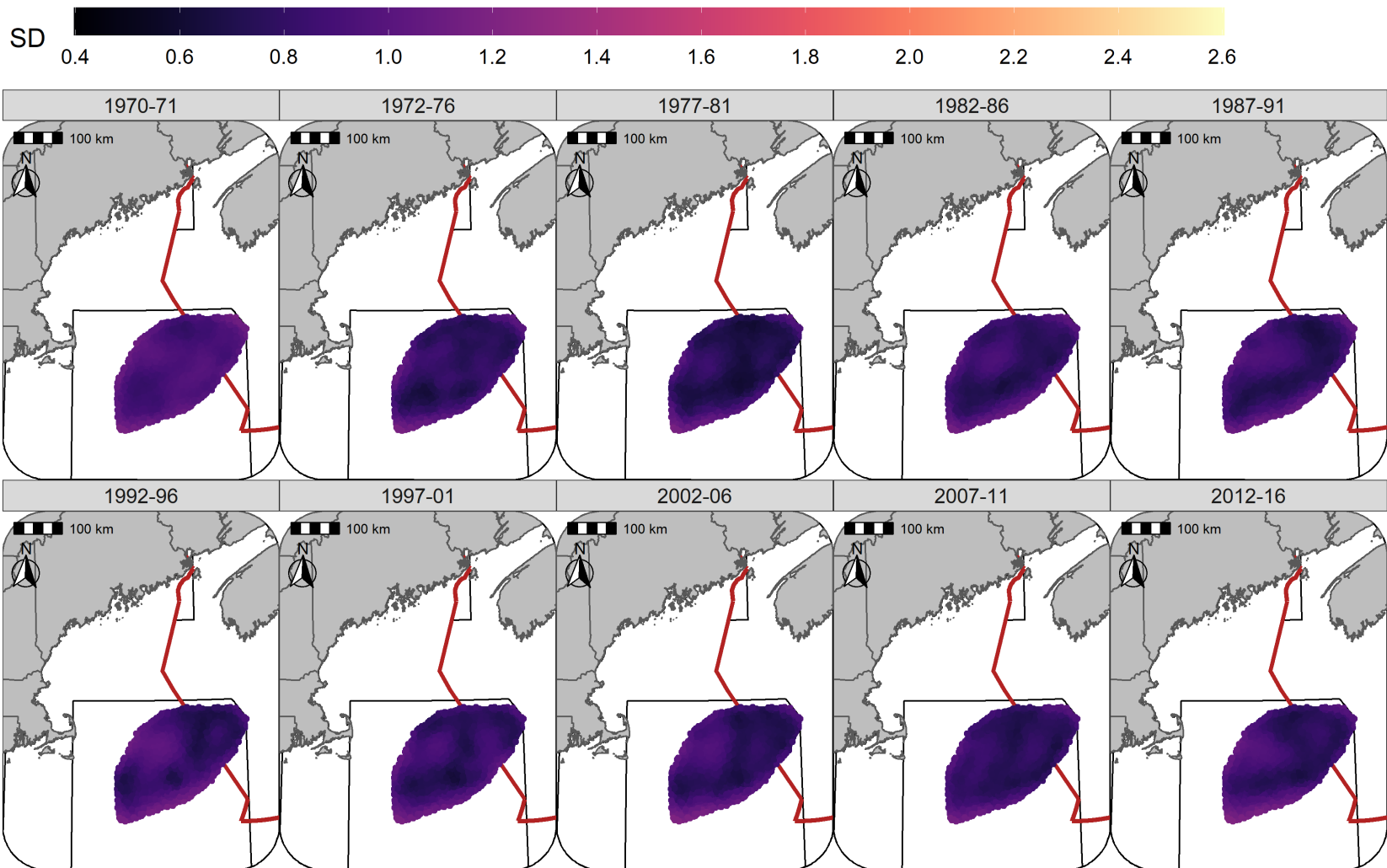


Figure S30: Standard deviation of random fields (logit scale) for Yellowtail Flounder in each era during the Fall (NMFS-fall survey) using the SST + Depth + Sed model and 5 year random field.

## Hyperparameters

For Atlantic Cod, the estimate for the variance of *Dep* variance hyperparameter was highest in Winter and declined through to the Fall, reflecting the decline in the influence of this covariate in the Fall (Figure S31). For Yellowtail Flounder, the variance of the *Dep* hyperparameter was higher than observed for Atlantic Cod throughout the year and reflected the relative stability in the effect size of this covariate throughout the year (Figure S31). The *SST* variance hyperparameter for Atlantic Cod was relatively stable throughout the year and reflects the consistent influence of the *SST* covariate on the distribution of cod. For Yellowtail Flounder, the *SST* variance hyperparameter was relatively low throughout the year and aligns with the consistent small effect of the *SST* covariate on the distribution of Yellowtail Flounder (Figure S32). The uncertainty of these estimates precludes any statistical differences being observed between the seasons.

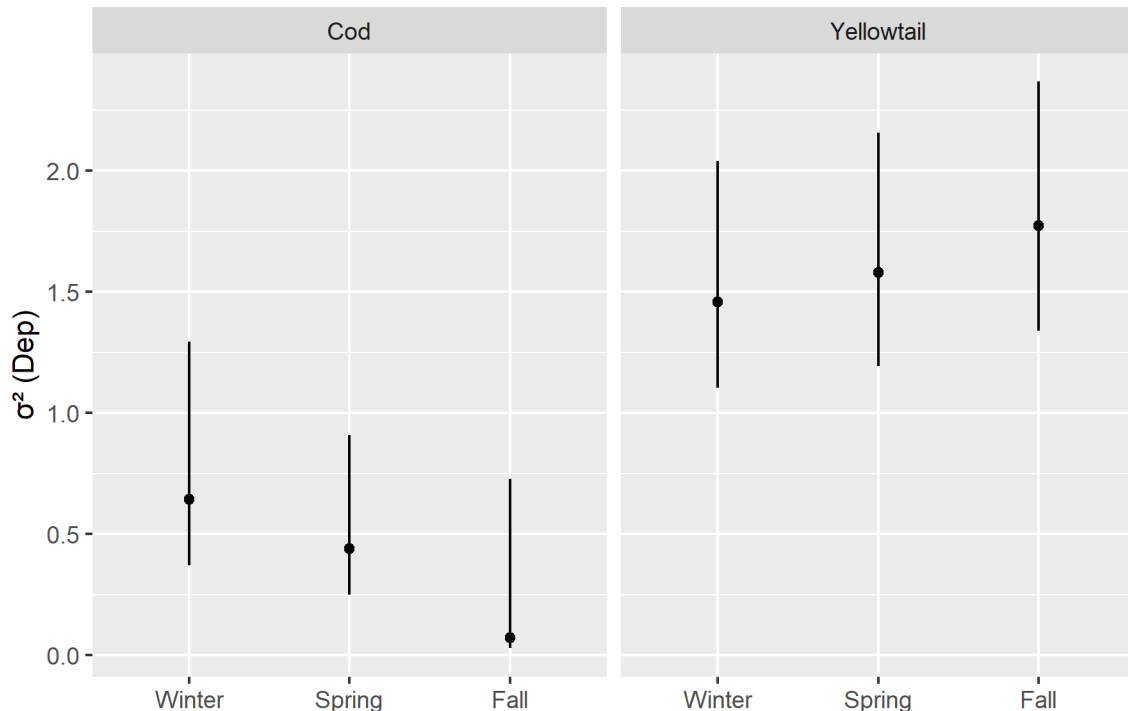


Figure S31: Depth variance hyperparameter estimate with 95%CI's for each stock in each season.

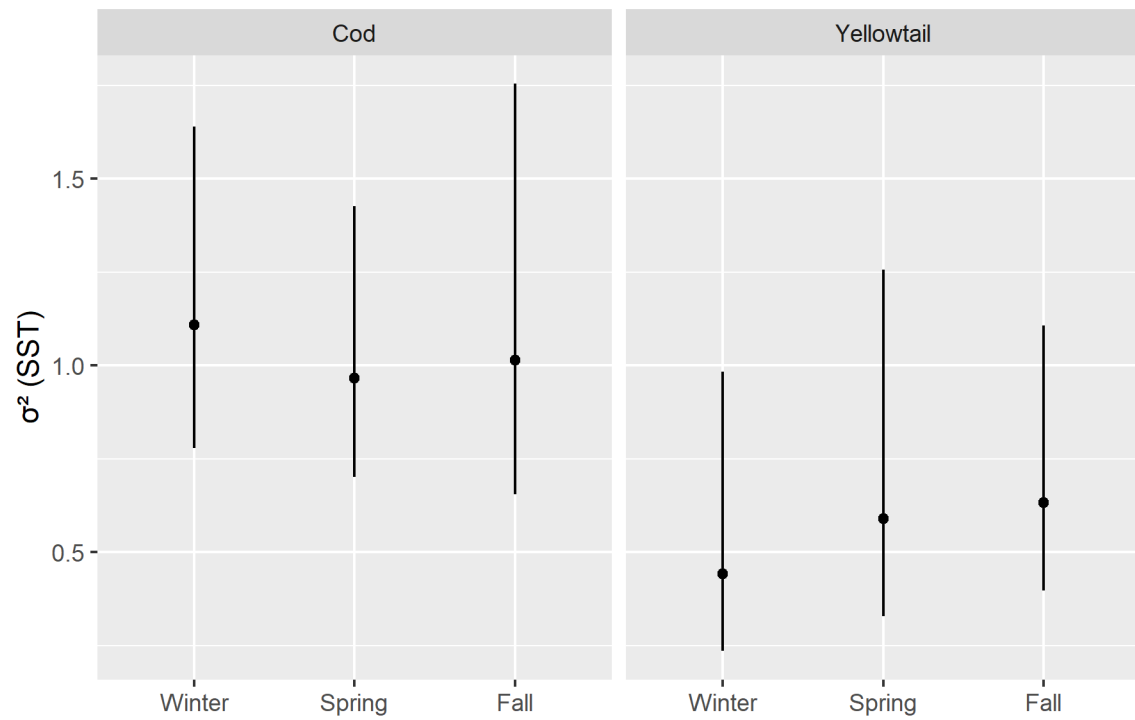


Figure S32: \*SST\* variance hyperparameter estimate with 95%CI's for each stock in each season.

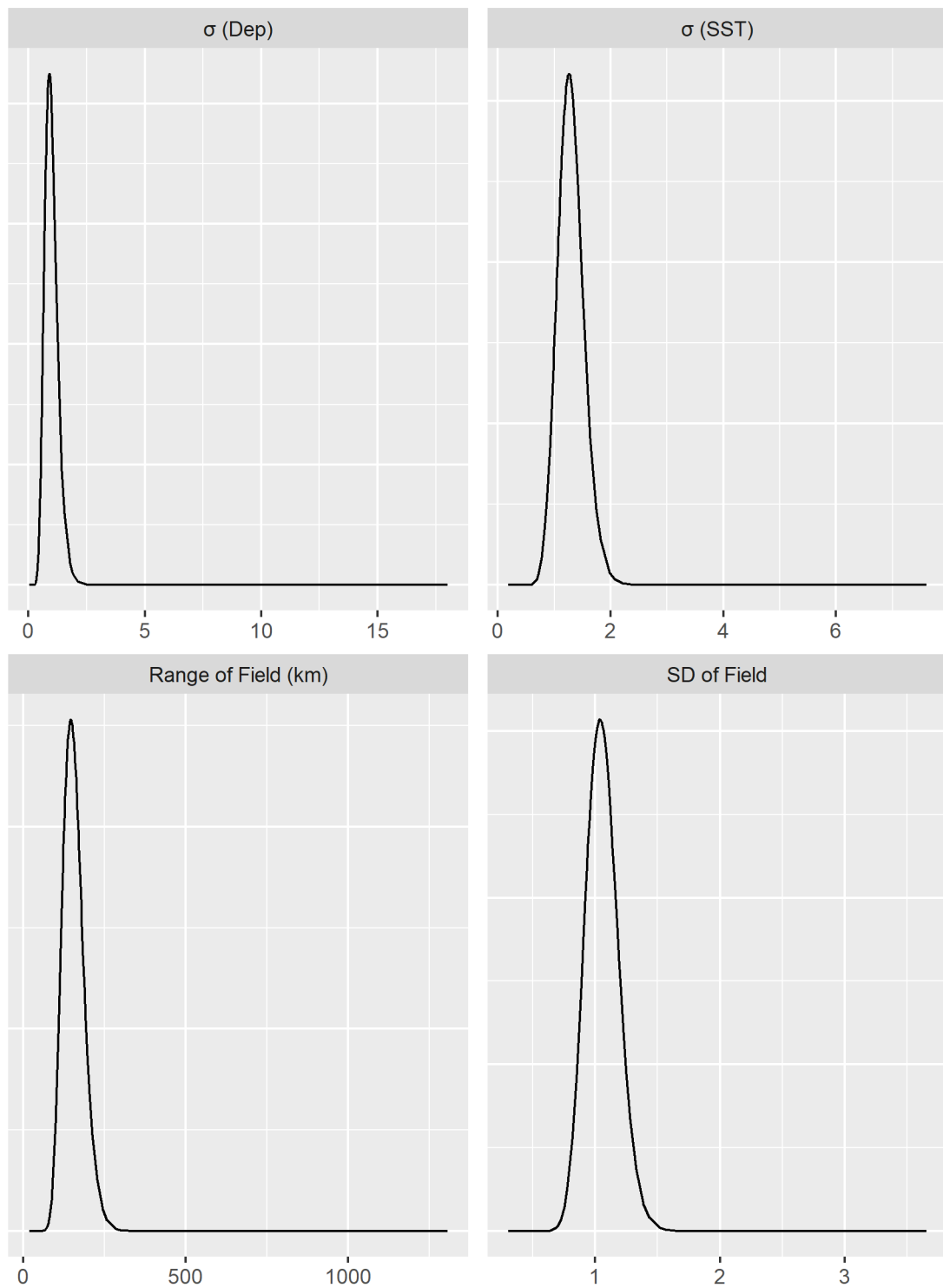


Figure S33: Posteriors distributions of the four model hyperparameters for Atlantic Cod in the Winter.

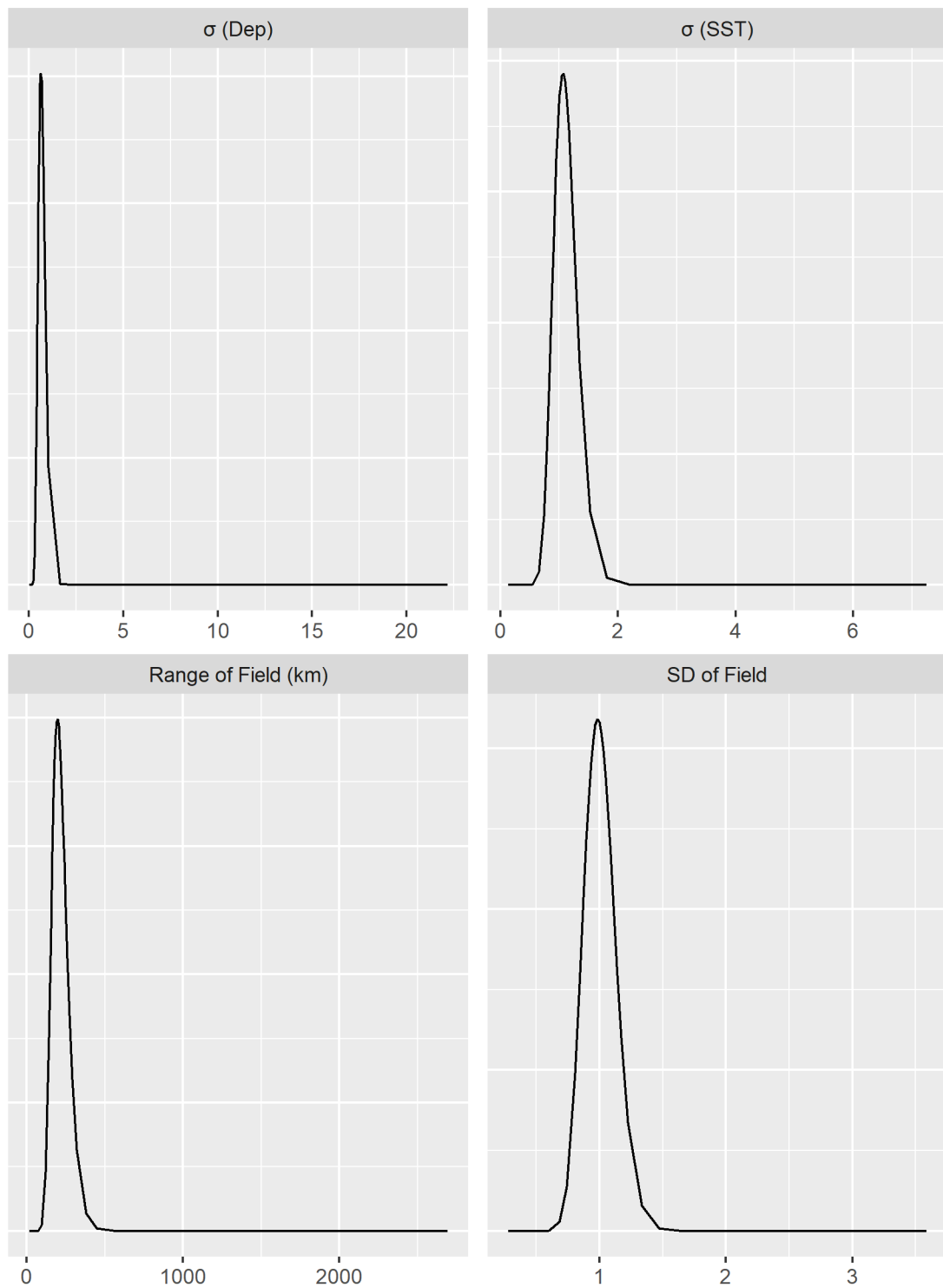


Figure S34: Posteriors distributions of the four model hyperparameters for Atlantic Cod in the Spring.

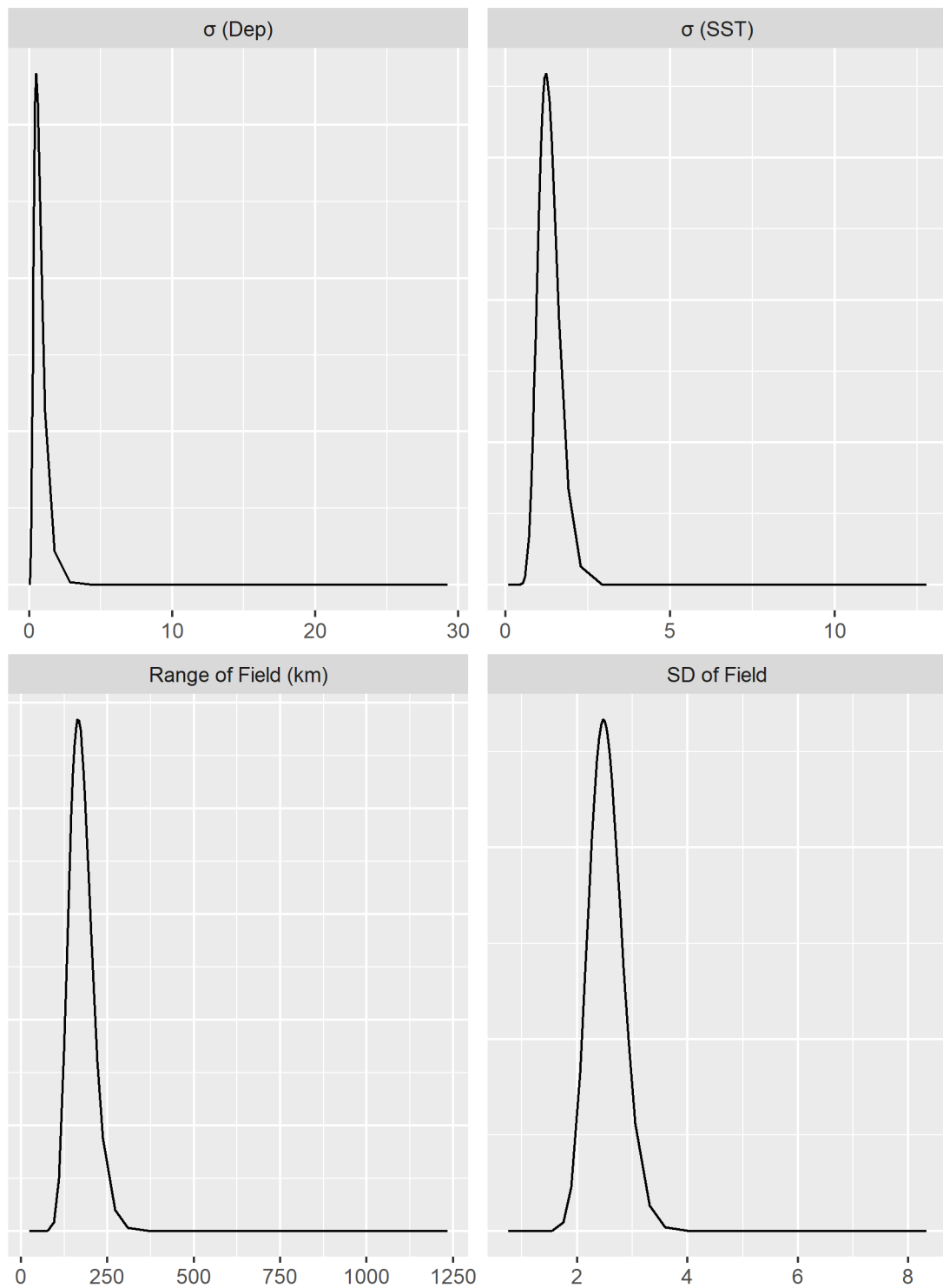


Figure S35: Posteriors distributions of the four model hyperparameters for Atlantic Cod in the Fall.

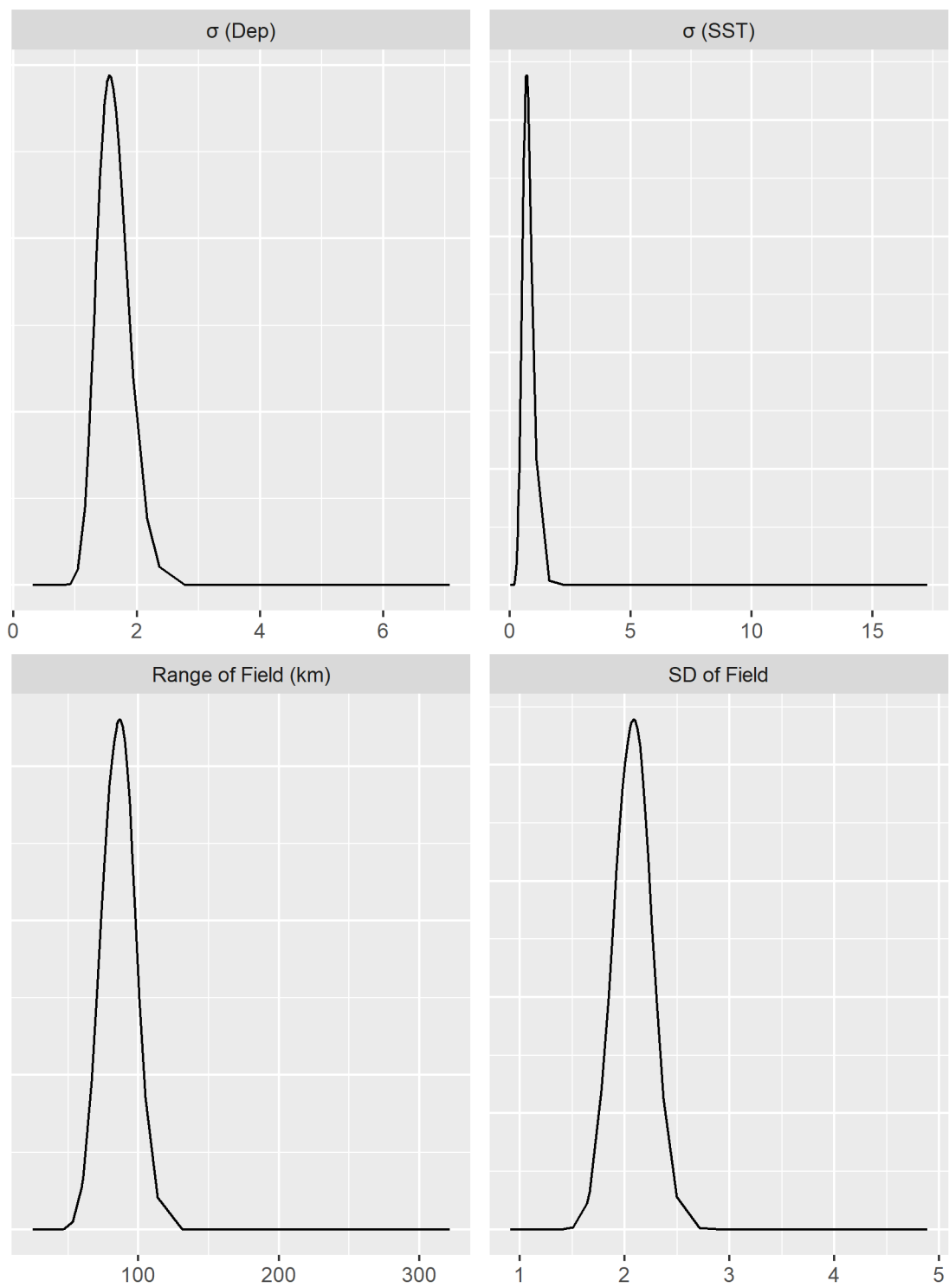


Figure S36: Posteriors distributions of the four model hyperparameters for Yellowtail Flounder in the Winter.

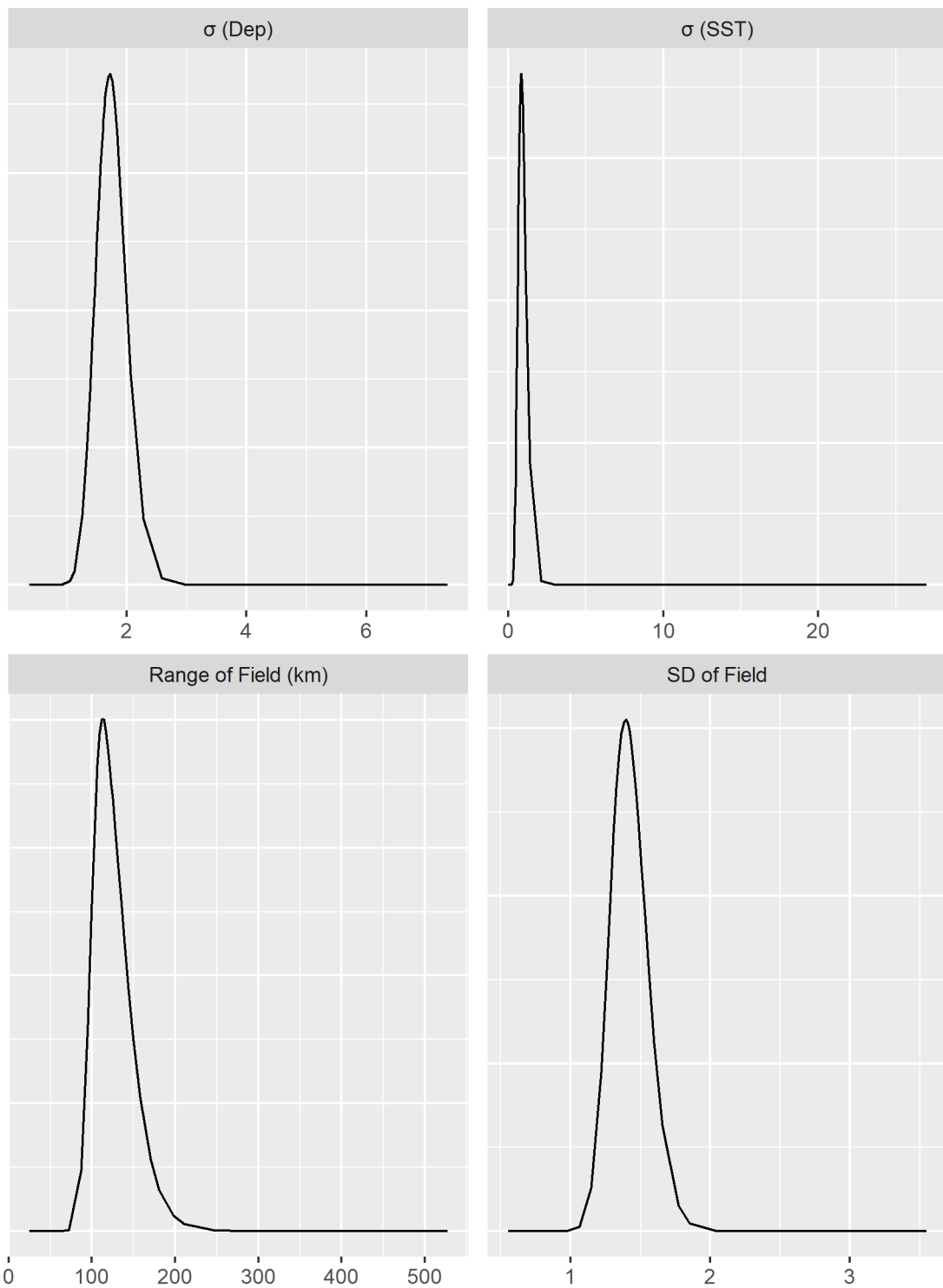


Figure S37: Posteriors distributions of the four model hyperparameters for Yellowtail Flounder in the Spring.

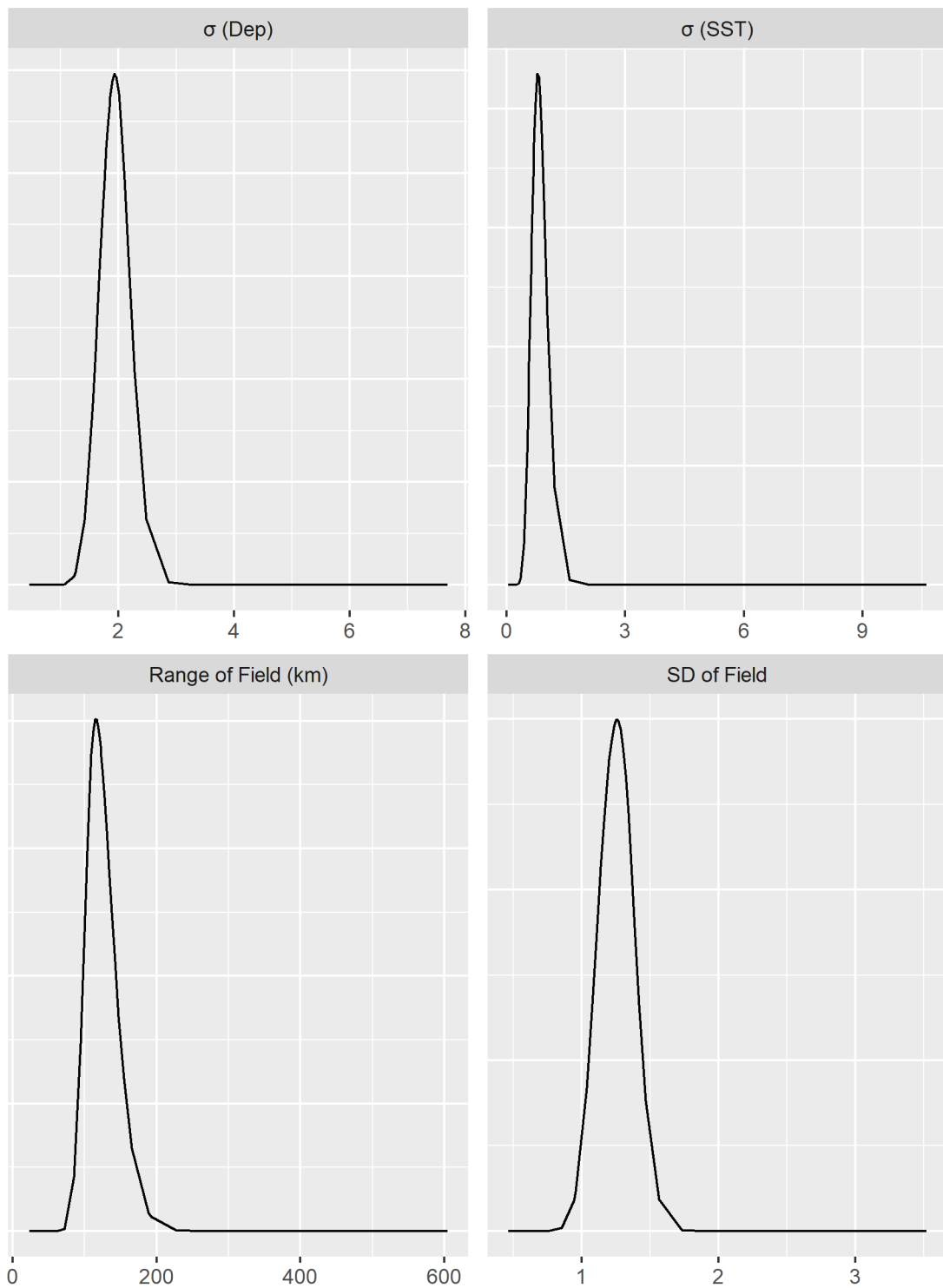


Figure S38: Posteriors distributions of the four model hyperparameters for Yellowtail Flounder in the Fall.